UNIVERSITY OF CALIFORNIA SAN DIEGO

Addressing applied fisheries ecology questions across species, fishery, and global scales.

A dissertation submitted in partial satisfaction of the requirements for the degree

Doctor of Philosophy

in

Marine Biology

by

Kayla Mackenzie Blincow

Committee in charge:

Professor Brice X. Semmens, Chair
Professor Jeff Bowman
Professor Phillip Hastings
Professor Carolyn Kurle
Professor Ed Parnell

2021

The dissertation of Kayla Mackenzie Blincow is approved, and it is acceptable in quality and form for publication on microfilm and electronically.

University of California San Diego

2021

DEDICATION

To the Blincows—Mike, Jeanie, Kelsey, and Kam.

Everything I am and everything I achieve is because of you.

EPIGRAPH

maggie and milly and molly and may
went down to the beach(to play one day)

and maggie discovered a shell that sang
so sweetly she couldn’t remember her troubles,and

milly befriended a stranded star
whose rays five languid fingers were;

and molly was chased by a horrible thing
which raced sideways while blowing bubbles:and

may came home with a smooth round stone
as small as a world and as large as alone.

For whatever we lose(like a you or a me)
it’s always ourselves we find in the sea

e.e. cummings

TABLE OF CONTENTS

LIST OF FIGURES

LIST OF TABLES

ACKNOWLEDGEMENTS

This dissertation is the culmination of five years of work, learning, and support, and it would not be in existence without the help of many, many people.

Thank you to my advisor, Dr. Brice Semmens, for taking me on despite the fact that I did not fit the bill for his ideal student. He showed patience in helping develop my coding and quantitative skills. He helped me become a true scientist, in all that the title entails. From analysis, to writing, to collaborating, Brice was always there to provide valuable guidance and insight. I will be forever grateful for the time I spent in his lab and for the lessons he taught me.

In addition to being my advisor, Brice is also responsible for bringing together an amazing group of people who helped give me moral and scientific support. The Semmens Lab is truly a wonderful place to learn, and I am so fortunate I got to be a part of such an amazing community. The original Semmens Lab crew, Lynn, Brian, Josh, Lyall, and Noah, each helped shape my trajectory as a scientist and made me feel welcomed and supported as a new lab member when I started this journey. The folks that came in along the way, Peter, Dan, Connor, Richie, and more, all also helped me succeed whether it was talking about coding or sharing their mad fishing skills. As for my ladies, Erica and Jordan, I cannot begin to express how grateful I am I got to meet them both and that they were there to support me through all of the ups and downs of graduate school. A lot of life has happened in the past five years, and they were there with me through it all to advise, commiserate, and celebrate.

Thank you to my committee members, Dr. Carolyn Kurle, Dr. Jeff Bowman, Dr. Phil Hastings, and Dr. Ed Parnell. You all provided valued guidance in completing this dissertation. Carolyn was my go to person for all things isotopes, but also shared helpful insight into the realities

of being a female and a mother in academia. Jeff was always available for a chat and brought a new perspective to the group that helped me get back to basics when discussing my work. I also deeply appreciated his advice when I was applying for postdoctoral opportunities and evaluating my future career aspirations. Phil shared his expansive knowledge of fish, was always quick to provide feedback on my drafts, and was a calming presence on my committee. As for Ed, I can only hope I will one day have a fraction of the natural history knowledge he has, and I thank him for bringing decades of experience working in San Diego's kelp forests to my committee. I really enjoyed our chats about Giant Sea Bass, and hearing all of his stories about how one of my favorite places in the world, the La Jolla Kelp Forest, has changed over the years.

In addition to my committee, I received guidance and aide from a number of other people. Dr. Rasmus Swalethorp lent his isotope expertise and was invaluable to developing my first chapter, particularly the compound specific stable isotope elements. Dr. Alan Haynie helped my ecologist-self wade into the waters of economics and trade relationships, and was instrumental in shaping the development of my last chapter from very different beginnings to the final product. Dr. Noah Ben-Aderet swept me into the world of acoustic tagging, and after a bit of a rocky start, developed into one my closest mentors and confidants. I would not have been able to complete this dissertation without the busiest people at SIO for some reason deciding I was worth their time to teach and guide through field work. Thank you Phil Zerofski, Rich Walsh, Brett Pickering, and Christian McDonald. SIO is incredibly fortunate to have these men leading their field programs, and teaching the next generation of field scientists. They are hands down the best teachers I had the privilege of learning from at SIO. Each in their own way has perfected the art of stressing the seriousness of safety while still empowering their students to feel confident handling boats, diving, and organizing field operations.

I would also be remiss if I did not thank the *many* volunteers who helped with receiver diving and fishing for Giant Sea Bass. I will not name them all here, but you know who you are. Taking sole ownership of the field work involved in this dissertation was a massive undertaking, but it was made much easier by the enthusiastic support of my volunteer divers and boat crews. Thank you, thank you, thank you.

I received funding from a number of different sources that helped support my research as well as my time spent as a student at UC San Diego. I would like to thank the Center for Marine Biodiversity and Conservation (CMBC) Program for Interdisciplinary Environmental Research for supporting my first year of graduate school via the San Diego Fellowship and the Mary M. Yang Graduate Fellowship for Environmental Stewardship, and introducing me to an amazing community of scientists, academics, and passionate conservation minded folks. I would also like to acknowledge the NMFS QUEST/CIMEC funds for supporting myself and the Semmens Lab more broadly. Through their dedication to training quantitative scientists they provided me the freedom to explore many different quantitative techniques at SIO and the University of Washington. Thank you to the Los Angeles Rod and Reel Club Foundation Maxwell J. Fenmore Memorial Fellowship for their support as well. And finally thank you to the grants and fellowships that supported my research activities, including the Mia Tegner Memorial Fellowship, The Women Divers of Hall of Fame Marine Conservation Scholarship sponsored by the Rachel Morrison Memorial Fund, the Link Family Foundation (via Dr. Phil Hastings), and the Edna Bailey Sussman Fund Graduate Environmental Internship.

Finally, I need to thank my family, birth and chosen. My parents successfully convinced me that I can do and be whatever I want in this life by constantly telling me they are proud of me and that I am amazing. Thank you to them for never leaving room to doubt my ability to succeed

and being my lifelong cheerleaders in all that I decide to commit myself to. Thank you to my brother and sister, Kam and Kelsey, for being lifelong best friends and for not letting me slack on developing my social skills while I have been nerding out for the past 30 years. Thank you to all of the friends I made at SIO and beyond over the past five years, they not only made my PhD experience bearable, they made it enjoyable. And last but certainly not least, thank you to Alex. I told him recently I didn't think I could do this without him, and he told me I definitely could. I think he was probably right, but I know for certain it would have been a whole lot harder. Thank you for helping me clean pigeon poop off the boat, dumpster diving for dead Giant Sea Bass (literally), deriving macroeconomics equations before I was able to find them in the literature, and picking me up and setting me straight whenever I stumbled.

Chapter 1, in full, is currently being prepared for submission for publication and is printed here with the permission of co-authors Rasmus Swalethorp, Arturo Ramirez-Valdez, and Brice X. Semmens. The dissertation author is the primary investigator and author of this paper.

Chapter 2, in full, is currently being prepared for submission for publication and is printed here with the permission of co-author Brice X. Semmens. The dissertation author is the primary investigator and author of this paper.

Chapter 3, in full, has been submitted for publication and is printed here with the permission of co-author Brice X. Semmens. The dissertation author is the primary investigator and author of this paper.

Chapter 4, in full, is currently being prepared for submission for publication and is printed here with the permission of co-authors Alan C. Haynie and Brice X. Semmens. The dissertation author is the primary investigator and author of this paper.

VITA

2012	B.S. Ecology, Behavior, Evolution Biology, University of California San Diego
2014	Master of Conservation Biology, University of Queensland
2021	Doctor of Philosophy Marine Biology, Scripps Institution of Oceanography, University of California San Diego

PUBLICATIONS

Nosal AP, Cartamil DC, Ammann AJ, Bellquist LF, Ben-Aderet NJ, **Blincow KM**, Burns ES, Chapman ED, Freedman RM, Klimley AP, Logan RK, Lowe CG, Semmens BX, White CF, Hastings PA. Triennial migration and philopatry in the Critically Endangered Soupfin Shark (*Galeorhinus galeus*). *Journal of Applied Ecology*. 2021; 00: 1-13.

Blincow KM, Bush PG, Heppell SA, McCoy CM, Johnson BC, Pattengill-Semmens CV, Heppell SS, Stevens-McGeever SJ, Whaylen L, Luke K, Semmens BX. Spatial ecology of Nassau Grouper at home reef sites: using acoustic telemetry to track a large, long-lived epinephelid across multiple years (2005-2008). *Marine Ecology Progress Series.* 2020; 655: 199-214.

Hanna G, **Blincow KM**, Hein E. Species abundance and sex ratios of *Drosophila melanogaster* and *Zaprionus indianus* in two different habitats of the Tropical Dry Forest of Alamos, Mexico (Diptera: Drosophilidae). *Drosophila Information Service*. 2010; 93: 106-109.

ABSTRACT OF THE DISSERTATION

Addressing applied fisheries ecology questions across species, fishery, and global scales.

by

Kayla Makenzie Blincow

Doctor of Philosophy in Marine Biology

University of California San Diego, 2021

Professor Brice X. Semmens, Chair

Fisheries are economically and culturally important features of coastal communities around the globe. Ranging from recreational fishing to commercial harvest, fisheries represent the final large-scale vestige of humans hunting for food. While terrestrial food systems shifted almost entirely toward agriculture and cultivation, aquatic and marine food systems are still remarkably reliant on wild capture for their supply. As a result, fisheries and the species they target are inextricably linked to human behavior. Ecologists wishing to better understand fisheries and how

to make them more sustainable must account not only for variables in the natural environment, but also variables associated with the anthropogenic use of fisheries resources. My dissertation explores this notion by addressing applied fisheries ecology questions across species, fishery, and global scales. At the species scale, chapters one and two investigate the trophic and movement ecology of Giant Sea Bass (*Stereolepis gigas*), a species nearly extirpated from United States waters by fishing activities. At the fishery scale, chapter three explores the interdependencies between species harvested by a multispecies fishery and how those relationships change as a function of sea surface temperature. And finally at the global scale, chapter four looks at the nature of global seafood trade and characterizes the management intensity associated with production versus consumption of seafood across countries. Each chapter and scale of fisheries ecology investigated contributes a different type of information to the broader knowledge base of fisheries science, and combined they present a valuable contribution to the field.

Chapter 1:

Giant Appetites: Exploring the trophic ecology of the kelp forest's largest predator, the Giant Sea Bass (*Stereolepis gigas*).

Kayla M. Blincow, Rasmus Swalethorp, Arturo Ramirez-Valdez, Brice X. Semmens

Abstract

After suffering severe population declines due to fishing pressure, Giant Sea Bass (*Stereolepis gigas*) in southern California are showing signs of recovery. As large-bodied predators often associated with the kelp forest and rocky reef environments of southern California and Baja California, Mexico, the local recovery of this species could influence trophic dynamics in these systems. Here we leverage stable isotope and gut content analysis to produce the first study describing the trophic ecology of adult Giant Sea Bass. We found that Giant Sea Bass are generalist predators, feeding on a wide array of different prey. We also found that Giant Sea Bass feeding habits change as they grow, with larger individuals relying more heavily on macroalgae-derived carbon, expanding their diets to include other and larger prey taxa, and obtaining higher trophic positions. Using these results, we speculate about the relationship between Giant Sea Bass and kelp forest ecosystems, a vulnerable yet key habitat, including the impact of the return of these predators, as well as how contemporary threats to kelp forests might mediate the continued recovery of Giant Sea Bass.

1.1 Introduction

Giant Sea Bass (*Stereolepis gigas*) are Critically Endangered (International Union for Conservation of Nature) large-bodied predators that were once abundant in the kelp forests and rocky reefs of southern California and Baja California, Mexico (Dayton et al. 1998, Domeier 2001, Hawk and Allen 2014, Erauskin-Extramiana et al. 2017). Historically a sought after recreational and commercial fisheries species, Giant Sea Bass experienced severe population declines due to overfishing in the early 20th century (Baldwin and Keiser 2008, Allen 2017). By the 1970s Giant Sea Bass were nearing extirpation in California; however, recent reports suggest that they are recovering after implementation of fishing regulations that decreased intentional and incidental catch of the species in the United States (Pondella and Allen 2008, Allen and Andrews 2012, House et al. 2016). Few studies currently exist on the ecology of Giant Sea Bass, due in part to the rarity of this species over the last half century.

With the exception of one study that focused on the young-of-the-year age class (Benseman 2018), we were unable to find any published records of studies explicitly researching the trophic and feeding dynamics of this species. However, there are natural history reports on the species that provide a baseline for what to expect regarding their trophic ecology (Young 1969, Feder et al. 1974, Domeier 2001). Giant Sea Bass are assumed to be generalist, high trophic level predators that feed on a wide array of primarily benthic nearshore rocky reef and kelp forest species, ranging from stingrays and small sharks to lobsters and octopuses (Domeier 2001, Allen and Andrews 2012, House et al. 2016). They are suction feeders, rapidly expanding their jaws to create a flow of water into their mouths that carries their prey along with it (Bishop et al. 2008). Beyond this feeding mechanism and long lists of anecdotal reports of prey items, little else is known about Giant Sea Bass feeding ecology. For instance, there is not an understanding of the influence of

ontogeny, different primary producers, or individual prey species on Giant Sea Bass trophic dynamics.

Understanding how Giant Sea Bass rely on different primary producers in their environment can help determine the extent to which shifts in production dynamics, whether from natural or anthropogenic drivers, might mediate Giant Sea Bass recovery. Kelp forests are a key habitat for Giant Sea Bass (Domeier 2001, House et al. 2016). Kelp supports complex trophic systems by serving as an ecosystem engineer, creating structure and habitat in nearshore environments for diverse communities of organisms (Teagle et al. 2017, Layton et al. 2019). Primary production in kelp forest systems is derived chiefly from macroalgae (e.g., kelp) and phytoplankton (Duggins et al. 1989, Fredriksen 2003, von Biela et al. 2016). Fluctuations in these producers can propagate throughout the food web, influencing the growth and production of higher trophic level species, including fishes (Koenigs et al. 2015; von Biela et al. 2016). Kelp forests globally are declining in patch size and kelp density, likely due to anthropogenic drivers of global change (Johnson et al. 2011, Steneck and Johnson 2014, Layton et al. 2019). While previous studies demonstrate that, generally, higher trophic level fish tend to rely more on macroalgae-derived primary production in kelp forest ecosystems (Koenigs et al. 2015, von Biela et al. 2016), no studies have assessed the link between primary producers and Giant Sea Bass trophic ecology.

As high-level predators, fluctuations in the population size of Giant Sea Bass have the potential to influence food web structure and ecosystem function (Hamilton et al. 2014, Spiers et al. 2016, Donohue et al. 2017, Ho et al. 2019). Understanding the extent to which this is the case is hampered by a lack of knowledge of Giant Sea Bass trophic ecology. It is not uncommon for other generalist fish predators to undergo size-dependent diet shifts (Werner and Gilliam 1984,

Hamilton et al. 2014). However, once settled in rocky reef and kelp forest environments, we do not know if or how the role of Giant Sea Bass in the food web changes ontogenetically.

In this study we leveraged bulk and compound specific stable isotope analyses along with gut content data to better understand the trophic role of Giant Sea Bass in kelp forest and rocky reef systems throughout their range. In particular, we set out to determine: (1) what Giant Sea Bass eat, and how that changes as a function of size/ontogeny; (2) which primary production sources Giant Sea Bass are most reliant on and if/how that relationship changes throughout their life history; (3) the relative trophic position of Giant Sea Bass; and, (4) what insight this information can give us about the role of Giant Sea Bass in one of their key habitats, the kelp forest ecosystem.

1.2 Methods

Using a combination of field campaigns and opportunistic collection, we collected tissue samples from regions within the core range of Giant Sea Bass from northern San Diego County, USA, to central Baja California and Gulf of California, Mexico (Figure 1.1). We analyzed our tissue samples using bulk and compound-specific stable isotope analysis to gather information on the trophic ecology of Giant Sea Bass. To link our isotope data with observed diets, we collated gut content information from the literature, unpublished data, and physical samples associated with our sample collection effort.

Sample Collection

We collected fin clip samples, approximately 1-2 cm of tissue clipped from the anal fin, to perform stable isotope analyses (n = 63). Our sampling effort took place from 2017 to 2020, and spanned the core range of Giant Sea Bass, which is south of Pt. Conception, California, USA to

Punta Abreojos, Baja California, Mexico and the upper Gulf of California (Domeier 2001) (Figure 1.1). We collected the majority of our samples (n = 56) from individuals caught by fishing cooperatives involved in the finfish fishery in Baja California, Mexico, through a collaboration with the biological monitoring program, Proyecto Mero Gigante, and the non-profit Comunidad y Biodiversidad A.C. (COBI). Additionally, we collected samples from La Jolla, California, as part of a separate effort permitted by the California Department of Fish and Wildlife (CDFW) that involved tagging and releasing Giant Sea Bass (n = 5). We opportunistically collected two samples from deceased individuals that washed up in Solana Beach and Carlsbad, California. Due to limited availability of freezer facilities for our samples from Mexico, we preserved all the fin clip samples in a 95% ethanol solution. In addition to fin clips, we gathered morphometric information on all the fish sampled, including total length (TL), head length (HL), and in some cases standard length (SL).

We gathered information on the isotopic signatures of potential primary producers (macroalgae vs. phytoplankton) through two methods. First, we collected samples of the dominant macroalgae (*Macrocystis pyrifera*) from a kelp forest in La Jolla, California (the same location where we collected fin clip samples) in the fall of 2019 (n = 8). We also collected samples of pyrosomes (*Pyrosoma atlanticum*), which have previously been used as a primary consumer proxy for phytoplankton production (Richards et al. 2020), from the offshore waters of San Diego, California during Scripps Institution of Oceanography research cruises in the fall of 2019 (n =10). We preserved these samples by freezing them. Second, we conducted a literature review and recorded *M. pyrifera* and particulate organic matter (a proxy for phytoplankton; POM) isotope values from studies that previously measured primary producers in our study region (Table A1.1)

(Page et al. 2008, Hamilton et al. 2011, Vega-García et al. 2015, Piñón-Gimate et al. 2016, Kurle and McWhorter 2017, Gabara 2020).

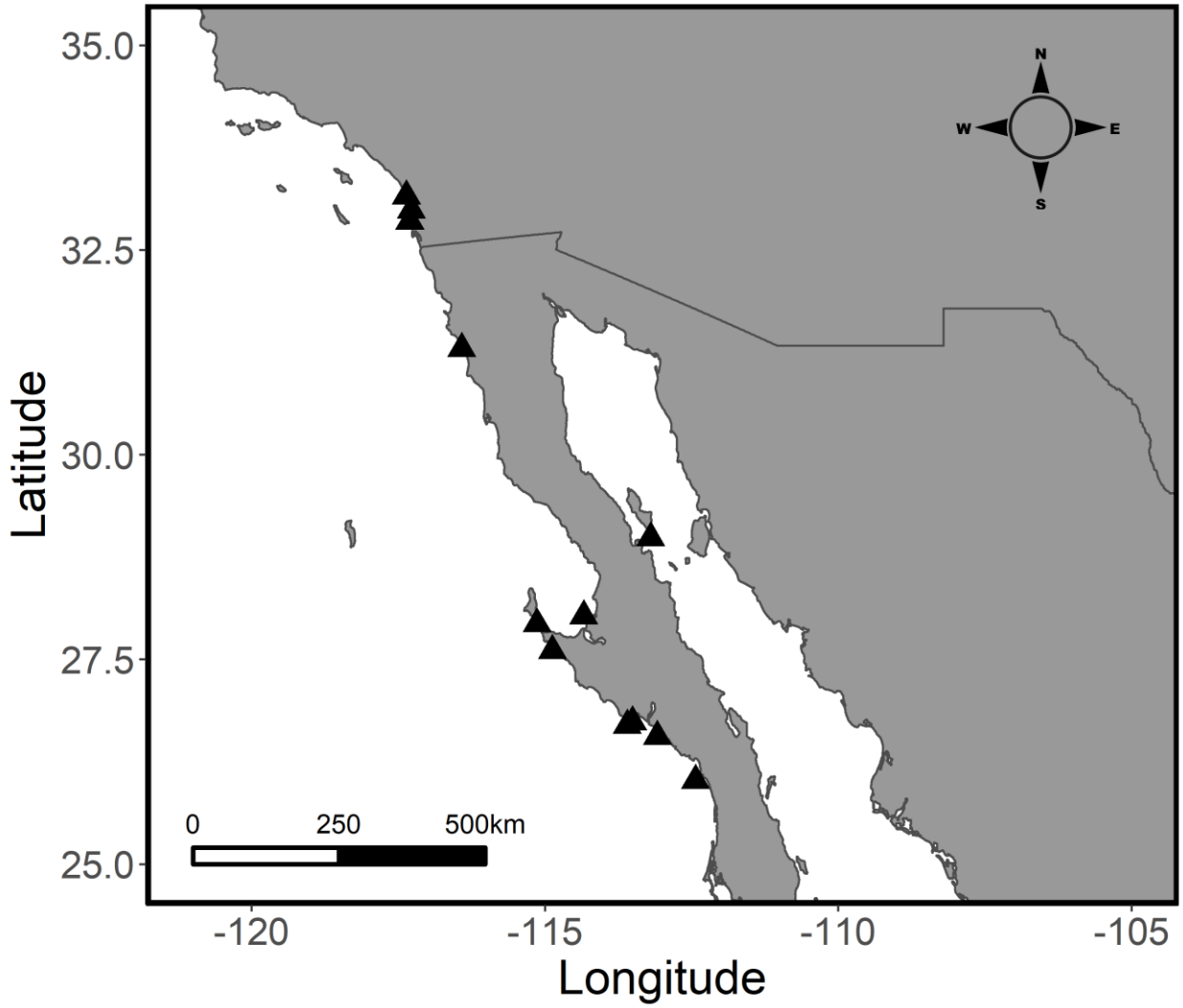

Figure 1.1. Map depicting the sampling locations (triangles) for Giant Sea Bass fin clips.

Gut Content Data

Gut content data are difficult to collect for Giant Sea Bass, because they are largely protected from harvest in the United States and those that are caught in fisheries are generally gutted at sea. To overcome this challenge and gather information on the diet of Giant Sea Bass we

drew from multiple data sources. First, we conducted a literature review, recording all prey taxa mentioned and whether the observations were from live feeding events, from inspecting gut contents, or uncredited anecdotal reports. Second, the Hubbs-SeaWorld Research Institute (HSWRI) shared information recorded on the stomach contents of Giant Sea Bass caught incidentally during their juvenile White Seabass (*Atractoscion nobilis*) gill net surveys. Third, we conducted gut content analysis on an individual that washed up in Solana Beach, CA, as well as 10 individuals from Isla Natividad, Baja California, Mexico, that had their gut contents retained by fishing cooperative members on our request. And finally, we reached out to fellow researchers for any unpublished records of gut content analysis or observations of feeding interactions in the field. Most notably, Dr. Larry Allen provided information on an individual from La Jolla, CA that he performed a necropsy and gut content analysis on in 2015.

Bulk Stable Isotope Analysis

Unlike gut contents, which provide information on what an organism was eating just before being sampled, stable isotopes constitute a representation of trophic interactions that is integrated through space and time. Ratios of nitrogen isotopes ($^{15}N/^{14}N$) can help determine the relative trophic position (TP) of an organism, because they enrich at a predictable rate with each increasing trophic level (Finlay et al. 2002, Post 2002). Ratios of carbon isotopes ($^{13}C/^{12}C$) tend to reflect sources of primary productivity, because carbon isotopic signatures are generally well-conserved through trophic transfer (Hobson 2005, Kurle et al. 2011). Typically, stable isotope analyses of fish use muscle tissue; however previous studies demonstrate that fin clips can be good analogs for muscle tissue when the latter is not available, as was the case in this study (Suzuki et al. 2005, Sanderson et al. 2009, Hanisch et al. 2010, Jardine et al. 2011).

We prepared fin clip and primary producer samples for bulk stable isotope analysis in accordance with previously published works (Hanisch et al. 2010, Jardine et al. 2011, Hetherington et al. 2019). We removed each sample from its ethanol preservative (for fin clips) or the freezer (for primary producers), rinsed it with de-ionized water for at least one minute, and freeze-dried the samples for 48 hours. Once dried, we homogenized the samples using a mortar and pestle and/or a scalpel, and placed approximately 1 mg ± 0.2 mg (for fin clips) or 5 mg ± 0.2 mg (for primary producers) of material into pre-weighed tin capsules. The Isotope Biogeochemistry facility at Scripps Institution of Oceanography analyzed all samples to determine the bulk carbon and nitrogen isotope values. We expressed all results as δ values (parts per thousand differences from a standard or per mil (‰)) using the following equation:

(1) $$\delta X = \left(\frac{R_{sample}}{R_{standard}} - 1\right) * 1000$$

where X is either ^{13}C or ^{15}N, R is the ratio $^{13}C/^{12}C$ or $^{15}N/^{14}N$using acetanilide standards (Baker A068-03, Lot A15467).

Compound Specific Stable Isotope Analysis

We performed compound specific stable isotope analysis of amino acid (CSIA-AA) nitrogen on a subsample of 20 fin clips. Selected samples came from fish captured in Guerrero Negro, Mexico that represented a wide size range of fish (TL: 51 cm – 197 cm). We split a single fin clip from one individual into three subsamples that we processed separately to produce procedural reproducibility errors for each of four target AAs: Alanine (Ala), Glutamic acid (Glu), Glycine (Gly) and Phenylalanine (Phe). $\delta^{15}N$ of the selected AAs is not significantly altered by ethanol and thus preservation effects on TP estimation are negligible (Swalethorp et al. 2020).

We removed each sample from the ethanol preservative, rinsed with de-ionized water for at least one minute, and then freeze-dried for 48 hours. We employed a relatively new high precision method using high-pressure liquid chromatography and offline elemental analysis - IRMS (HPLC/EA-IRMS) (Broek and McCarthy 2014, Swalethorp et al. 2020). All specifics of this method can be found in Swalethorp et al. (2020). Briefly, we hydrolyzed a minimum of 6 mg (dry weight) of each sample in 1 mL of 6 mol L^{-1} HCl in capped glass tubes for 24 hours at 90°C. We then dried the samples on a centrifugal evaporator under vacuum at 60°C, re-dissolved them in 0.5 mL 0.1 mol L^{-1} HCl, and filtered them through an IC Nillix—LG 0.2-μm hydrophilic polytetrafluoroethylene (PTFE) filter to remove particulates. Finally, we re-dried the samples before re-dissolving them in 100 μL of 0.1% trifluoroacetic acid (TFA) in Milli-Q water and transferring them to glass inserts in glass vials. We stored all samples at -80°C for 1-4 weeks prior to AA purification. For each sample we purified and collected the trophic AAs Ala and Glu, and the source amino acids Gly and Phe. We dried these AAs in a centrifugal evaporator at 60°C, re-dissolved them in 40 μL 0.1 mol L^{-1} HCl, then transferred them into small tin capsules and dried them under vacuum. We used the Stable Isotope Laboratory facility at the University of California, Santa Cruz to carry out analyses on a Nano-EA-IRMS designed for high precision analysis of low mass samples (≥0.6 μg N).

Data Analysis

We performed all analyses using R statistical software, version 3.6.1 (R Core Team 2019). The code for our analyses can be found at https://github.com/kmblincow/GSBIsotopeAnalysis.

We analyzed the bulk stable isotope data for relationships with fish body size using Bayesian linear models coded in R and JAGS software (Plummer 2003) with the package R2jags (Su and Yajima 2020). In order to account for possible influences of year and sample location, we

tested multiple models incorporating different combinations of these variables (Table 1.1). We treated year, sample site, and a derived categorical variable of year and sample site combined as random effects, and the TL of each fish sampled as a fixed effect. We ran each model using 3 parallel Monte Carlo Markov Chain (MCMC) chains, each obtaining 350,000 samples, the first 25,000 of which were discarded as burn-in. We retained every 25th iteration to reduce autocorrelation, resulting in an output of 39,000 samples of the posterior distribution for each chain. We confirmed model convergence by evaluating trace plots and the potential scale reduction factor (R hat) (Gelman and Rubin 1992). We used leave-one-out cross-validation (LOO) to determine which models best predicted the data using the package loo (Vehtari et al. 2017, 2020).

We incorporated our bulk isotope results into a Bayesian isotope mixing model to determine what proportion of Giant Sea Bass diets are derived from either phytoplankton or macroalgae primary production sources using the MixSIAR package (Stock et al. 2018). MixSIAR requires the input of source isotope values (i.e. macroalgae and phytoplankton primary production), mixture isotope values (i.e. Giant Sea Bass), estimates of the trophic discrimination factors (TDF) between the source and mixture for each isotope, and data on relevant covariates (i.e. TL). We ran our model using 3 parallel MCMC chains, each obtaining 100,000 samples, the first 50,000 of which were discarded as burn-in. We retained every 50^{th} iteration. We used the same convergence criteria as in the prior analysis.

To determine our source isotopic signatures, we collected the mean estimated bulk isotope values from multiple studies (including our own), and then calculated the mean and variance of these values. We subsequently used these means and variances as fixed source values (not estimated based on sample data) in our mixing model (Stock et al. 2018). We estimated the relative proportion of macroalgae-derived carbon by relying on isotopic estimates of the dominant Pacific

coastal macroalgae species in our sample locations, *M. pyrifera* (Edwards and Hernández-Carmona 2005). However, we had one fin clip sample from the upper Gulf of California, which does not encompass the range *M. pyrifera*. Despite the fact that other coastal macroalgae present in the upper Gulf of California likely have similar values to *M. pyrifera*, we chose to exclude this sample from the mixing model analysis because it was unreasonable to assume *M. pyrifera* would be contributing to its isotopic signature. In order to convert pyrosome isotope values into phytoplankton primary production (under the assumption that pyrosomes rely exclusively on a phytoplankton-derived food web), we corrected our pyrosome-derived $\delta^{15}N$ estimates by -2 ‰ and our $\delta^{13}C$ estimates by 0.5 ‰ based on previously published estimates of the trophic position of pelagic tunicates (Hetherington et al. 2018, Décima et al. 2019, Schram et al. 2020).

To our knowledge, there are no experimental estimates of TDF for Giant Sea Bass. We chose to use mean TDF values of 0.9 ‰ (SD = 0.5) and 3.4 ‰ (SD = 0.5) for $\delta^{13}C$ and $\delta^{15}N$, respectively, based on previously published isotope research for similar species (Artero et al. 2015) and broad TDF estimates for carnivorous species (DeNiro and Epstein 1978, Post 2002). Since our source and mixture populations were multiple trophic steps apart, it was necessary to correct our TDF values based on that difference (Phillips et al. 2014). To do so we used the trophic position estimates from our CSIA-AA analysis (described below) to calculate a mean trophic position for Giant Sea Bass and multiplied our TDF values by that value minus 1.

We evaluated the isotopic niche of different age classes of Giant Sea Bass using the SIBER package (Stable Isotope Bayesian Ellipses in R) (Jackson et al. 2011). Giant Sea Bass are thought to mature between the ages of 7 and 13 (Domeier 2001, Hawk and Allen 2014). Using the age-growth equation derived by Hawk and Allen (2014), we calculated the expected age associated with each of our samples, and classified them as either “immature” (< 7, n = 18), “transition” (7-

12, n = 23), or "mature" (>12, n = 22). We calculated the standard ellipse area (SEAc), which is a representation of bivariate standard deviation, for each of these groups. Additionally, we performed Bayesian estimation of the standard ellipses and compared across groups. SEAc is robust to small sample sizes, unlike other isotopic niche metrics such as convex hulls (Jackson et al. 2011). We ran our SIBER model using 3 parallel MCMC chains, each obtaining 50,000 samples, the first 25,000 of which were discarded as burn-in. We retained every 5th iteration. We confirmed model convergence by evaluating trace plots and the potential scale reduction factor (R hat).

We used the two trophic (Trp) and two source (Scr) AAs δ^{15}N values to calculate the trophic position of Giant Sea Bass using β and TDF values from Bradley et al. (2015) and the following equation:

(2) $$FCL = \frac{\delta^{15}\mathrm{N}_{Trp} - \delta^{15}\mathrm{N}_{Scr} - \beta}{TDF_{AA}} + 1$$

Where β is the δ^{15}N offset between Trp and Scr AAs in primary producers while TDF_{AA} is the average δ^{15}N enrichment of Trp relative to Scr AAs in consumers for each increasing trophic step. To generate more robust trophic position estimates we used weighted means of both Ala and Glu, and Gly and Phe (Nielsen et al. 2015) using the following equation:

(3) $$\delta^{15}N_{\bar{x}_W} = \frac{\Sigma\frac{\delta^{15}N_x}{\sigma_x^2}}{\Sigma\frac{1}{\sigma_x^2}}$$

Where $\delta^{15}N_x$ is the value of a specific Trp or Scr AA and σ_x is the procedural reproducibility error reported here as the standard deviation (SD) from replicate analysis of the three subsamples of one of the fin clips. These SD values were 0.24, 0.68, 0.17, 1.57 for Ala, Glu, Gly and Phe, respectively.

We also calculated weighted means for the β and TDF values and associated SDs (Bradley et al. 2015).

After calculating the trophic position associated with our samples, we performed a simple Bayesian linear regression to look for a relationship with fish size (TL) using the same model specifications described for the linear models above. For the fin clip sample that was split into three and run separately, we calculated the mean of the associated results so as not to triple count them.

After compiling the disparate records of stomach contents, we generated a list of potential prey items and grouped each based on our confidence in the source of the information. For the data that encompassed enumeration of prey types definitively associated with visual inspection of stomach contents (HSWRI, Larry Allen's necropsy, and our own stomach content analyses), we generated a species accumulation curve to determine whether we had sampled the full range of prey using the vegan package (Oksanen et al. 2020).

1.3 Results

Bulk Stable Isotopes

We gathered a total of 63 tissue samples from fish with TLs ranging from 44 to 197 cm (94.57 ± 42.08; Mean ± SD). $\delta^{13}C$ values ranged from -16.50 to -12.39 ‰ (-14.53 ± 1.10), and $\delta^{15}N$ values ranged from 15.95 to 19.54 ‰ (17.91 ± 0.90) (Figure 1.2). Due to our opportunistic sampling strategy, the sample sites are not evenly represented (Table A1.2), with the majority of samples coming from Baja California, Mexico (n = 56), in particular Guerrero Negro (n = 31). Our Bayesian linear models indicated a strong positive relationship between TL and $\delta^{13}C$ (Figure 1.3a).

LOO model comparison found that sample site and TL were the most important variables for predicting $\delta^{13}C$ (Table 1.1). While LOO identified year and TL as the best predictors of $\delta^{15}N$ out of the variables we tested (Table 1.1), the relationship between TL and $\delta^{15}N$ was weak (Figure 1.3b). We should note that some of the models we evaluated using LOO had a small number of Pareto *k* values that exceeded 0.5. We evaluated each of these points individually, and found that they rarely exceeded 0.7, the recommended cutoff for the utility of LOO methods in model comparison (Vehtari et al. 2017). Based on the guidance of Vehtari et al. (2017), we decided our models were robust for LOO comparison.

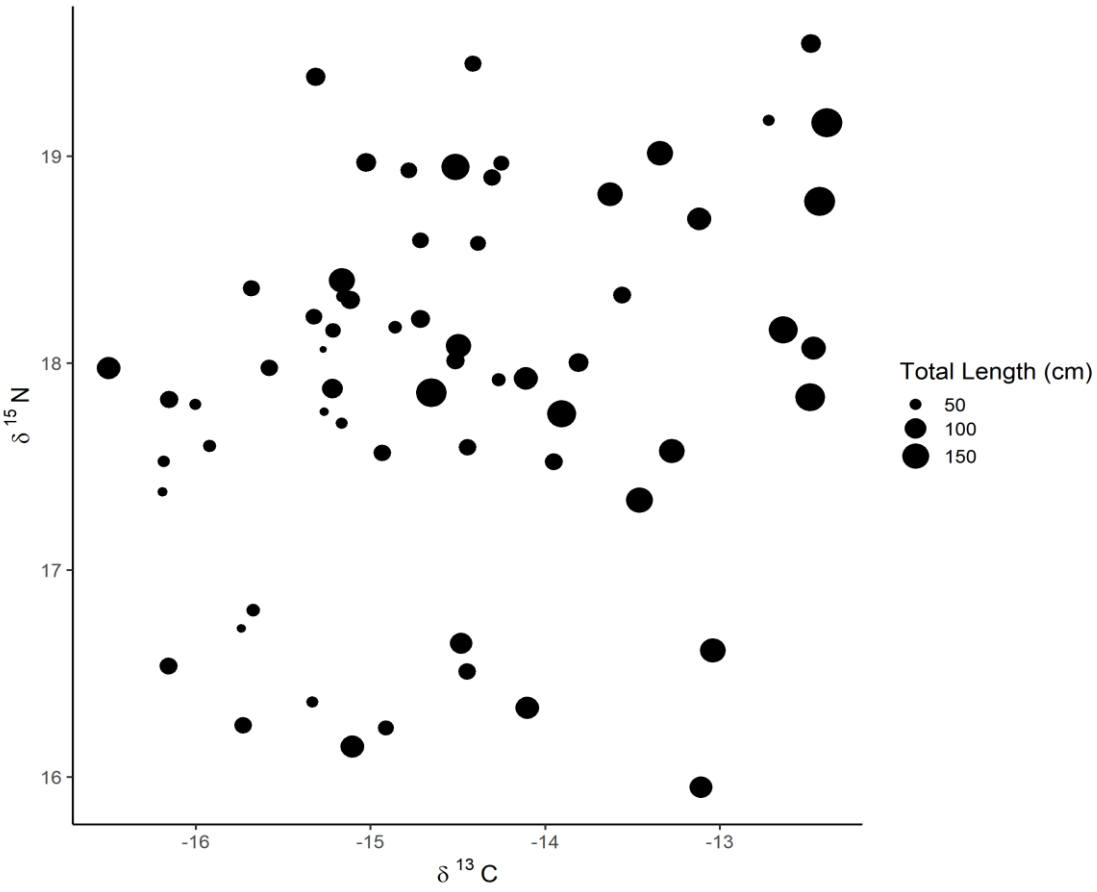

Figure 1.2. $\delta^{13}C$- $\delta^{15}N$ biplot for all bulk stable isotope samples. The size of the points denotes the total length of the fish the sample is derived from.

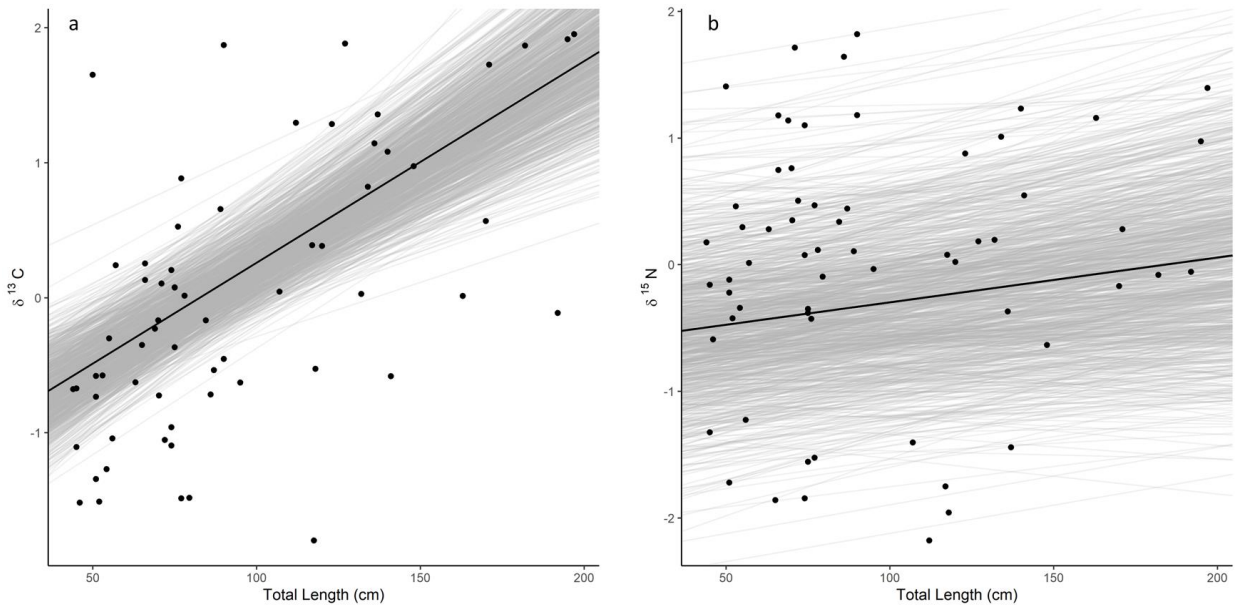

Figure 1.3. Bayesian estimates of the linear relationships between the bulk isotope results and total length. Note that the y axis displays the scaled bulk isotope values, which have a mean of 0 and standard deviation of 1. The black lines denote the mean posterior hyperparameter estimates for the slope and intercept. The gray lines depict 1,000 random draws from the hyperparameter posterior estimates for the slope and intercept. a) $\delta^{13}C$ and total length (cm) using the model which incorporated total length as a fixed effect and sample site as a random effect. b) $\delta^{15}N$ and total length (cm) using the model which incorporated total length as a fixed effect and year as a random effect.

The mixing model showed that Giant Sea Bass are chiefly reliant on macroalgae as a basal carbon source and that this trend increases with size (Figure 1.4). The median proportion of the diet associated with macroalgae was 0.61 (95% Credible Interval (CI): 0.55 – 0.66) at the smallest end of the size range and 0.91 (95% CI: 0.83 – 0.95) at the largest end of the size range.

By plotting the SEAc derived from the SIBER analysis, we found overlap in the isotopic niches of the three different age groups (Figure 1.5a). We found that the mature age class had the highest Bayesian SEAc estimate, followed by the transition, then the immature age classes (Figure 1.5b).

Table 1.1. Leave-one-out cross-validation model comparison testing the relationship between bulk isotope estimates and total length (fixed effect), sample site (random effect), year (random effect), and year/site (random effect). Expected log pointwise predictive accuracy (elpd_loo) is a measure of the predictive accuracy of the model which can be compared across models using the same data. The difference between these values for different models is given by the elpd_diff column, and the standard error of component-wise differences of the elpd_loo between models is shown in the se_diff column.

Model	elpd_loo	elpd_diff	se_diff
δ13C			
δ13C ~ TL + Site	-77.8	0	0
δ13C ~ TL + YearSite	-77.9	-0.1	0.4
δ13C ~ TL	-77.9	-0.1	1.5
δ13C ~ TL + Year	-78.5	-0.7	1.6
δ13C ~ Year	-91.1	-13.3	5.8
δ13C ~ Site	-91.5	-13.7	5.8
δ13C ~ YearSite	-91.5	-13.7	5.8
δ15N			
δ15N ~ TL + Year	-86	0	0
δ15N ~ Year	-86.3	-0.3	1.1
δ15N ~ TL + YearSite	-89.4	-3.4	2.6
δ15N ~ TL + Site	-89.6	-3.6	3.3
δ15N ~ YearSite	-90.1	-4.2	2.7
δ15N ~ Site	-90.6	-4.6	3.6
δ15N ~ TL	-91.1	-5.2	4.1

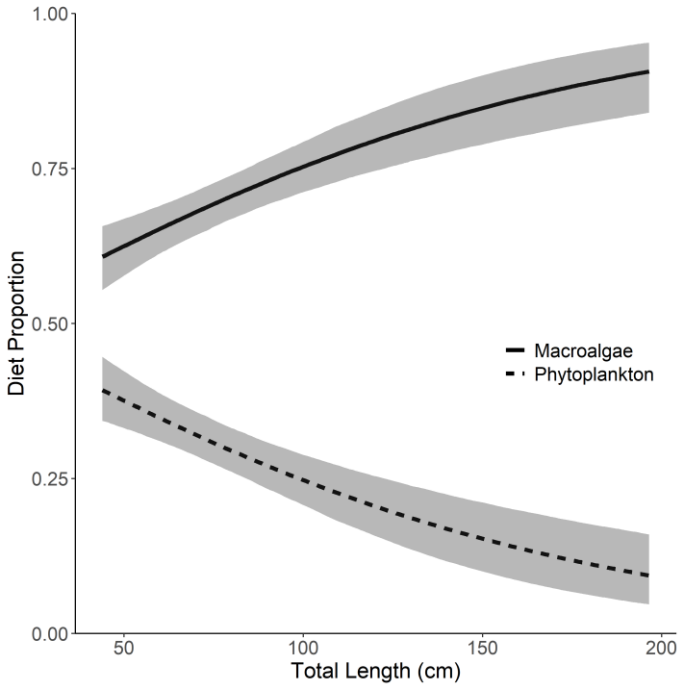

Figure 1.4. Mixing model results showing the relative proportion of different primary producers in Giant Sea Bass diets as a function of total length.

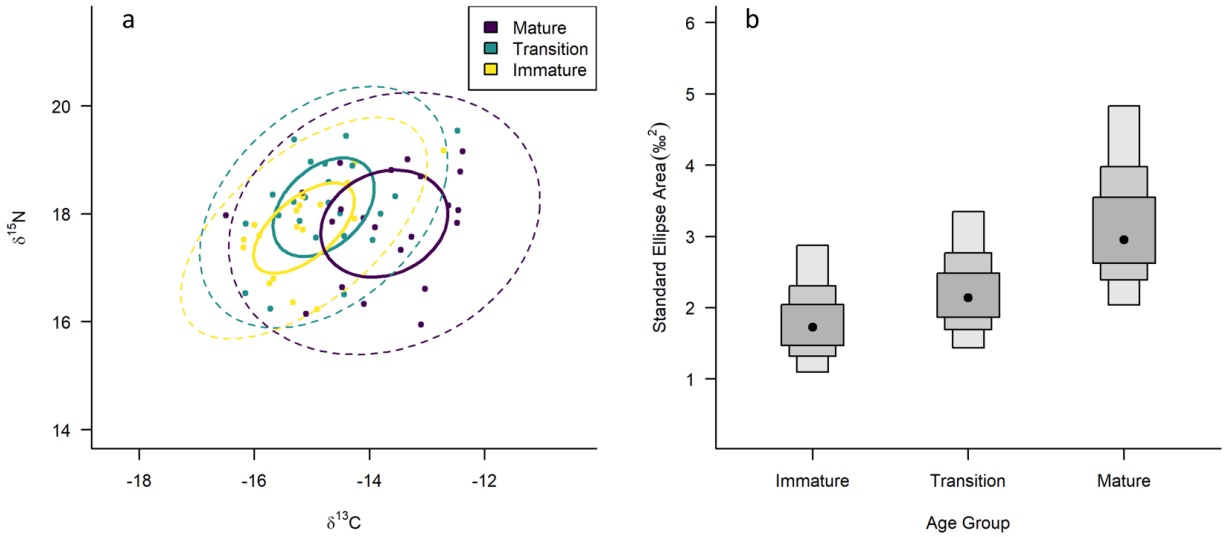

Figure 1.5. Results of the SIBER analysis. a) Bulk stable isotope biplot with standard ellipse areas (SEAc) for each age class shown by the solid ellipses, and ellipses encompassing 95% of the data shown by the dotted lines. b) Bayesian estimates of the SEAc where the black dot represents the mode and the boxes indicate the 50%, 75%, and 95% credible intervals.

CSIA-AA

Of the 20 samples we used for CSIA-AA, we found that three had unreasonably high Phe $\delta^{15}N$ values that lead to very low trophic position estimates, and neither was supported by the associated bulk $\delta^{15}N$ data. These samples had possibly degraded and were classified as outliers and subsequently removed from further analyses (Figure A1.1**)**. Additionally, we were unable to determine the Gly value for one sample, so we did not include that sample in our trophic position estimates. Ala values ranged from 25.65 to 30.06 ‰ (28.04 +/- 1.45), Glu acid values ranged from 26.65 to 32.11 ‰ (29.81 +/- 1.72), Gly values ranged from 7.15 to 11.51 ‰ (9.42 +/- 1.00), and Phe ranged from 10.01 to 13.16 ‰ (11.67 +/- 0.90) (Figure 1.6a**)**. The trophic position estimates ranged from 2.7 to 4.1 (3.39 +/- 0.35). We found a strong positive linear relationship between trophic position and TL (Figure 1.6b).

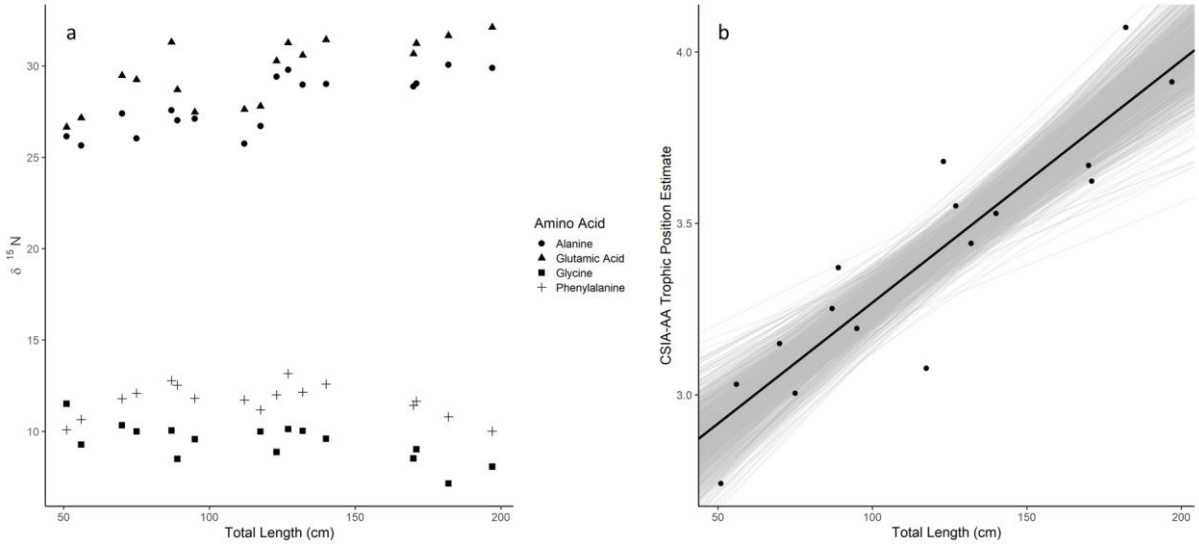

Figure 1.6. Compound specific stable isotope analysis of amino acids (CSIA-AA) results. a) The $\delta^{15}N$ values for the AAs we tested. Glutamic acid and alanine are trophic AAs which enrich with trophic level increases, while glycine and phenylalanine are source AAs which do not enrich with increasing trophic levels. We used the differences between the source and trophic AAs to estimate the trophic position for each fish tested using CSIA-AA. b) The Bayesian estimate of the linear relationship between the trophic position and total length of samples analyzed using CSIA-AA. The black line denotes the line associated with the mean posterior estimates of slope and intercept. The gray lines denote 1,000 random draws from the posterior estimates for slope and intercept.

Gut Contents

Synthesizing information from the compiled gut content data and literature reports, we found a total of 35 prey items, 24 of which were associated with direct observations from Giant Sea Bass ranging in size from 43.7-141.3 cm TL (60.90 ± 27.58, n = 22) (Table 1.2). Most of our gut content data did not include records of prey size, though where it was recorded we found that the largest prey items tended to be associated with larger Giant Sea Bass (Table 1.2). We should note that this relationship was not reciprocal, and larger Giant Sea Bass also had smaller prey items in their stomachs, such as the Solana Beach individual (137.0 cm TL) which had 20 individual crabs in its stomach ranging in size from 4.2 to 9.0 cm in carapace length (Table 1.2). Prey items included both fish and invertebrates, and most were associated with benthic habitats, with the largest proportion (44.8%) associated primarily with sandy bottom habitats (Figure 1.7). Three other habitats were equally represented (18.4% each), including rocky or sandy bottom habitats, rocky bottom habitats, and pelagic habitats (Figure 1.7). By plotting the species accumulation curve associated with the stomach content data, we found that the curve did not reach an asymptote (Figure 1.8).

Table 1.2. Prey types gathered from direct and anecdotal observations. The size of the Giant Sea Bass and associated prey items are given where available, along with the habitat associated with the prey type, and the source of the observation. Lengths of prey items are recorded in total length for fish and octopus, and carapace length for crustaceans.

Count	Type	Common Name	Scientific Name	Habitat	Prey Length (cm)	GSB Total Length (cm)	Source
Direct Observation							
1	Fish	Spotted Cusk Eel	*Chilara taylori*	Sandy	21.3	60.9	HSWRI
2	Fish	Plainfin Midshipman	*Porichthys notatus*	Sandy	18	63.0	Isla Natividad Stomach
3	Fish	Hornyhead Turbot	*Pleuronichthys verticalis*	Sandy	15.1; 15.9	63.3	HSWRI

Table 1.2. Prey Types, Continued.

Count	Type	Common Name	Scientific Name	Habitat	Prey Length (cm)	GSB Total Length (cm)	Source
Direct Observation							
6	Fish	Scorpionfish	*Scorpaenidae spp.*	Rocky	17.8	69.1	HSWRI
5	Fish	Sardine	*Sardinops sagax*	Open Water	NA	76.5	HSWRI; Feder et al. (1974); Baldwin and Keiser (2008)
6	Fish	Cabezon	*Scorpaenichthys marmoratus*	Rocky/ Sandy	21.6, 27.0	78.8	HSWRI
7	Fish	Barracuda	*Sphryaena argentea*	Open Water	NA	79.0	HSWRI
8	Fish	Specklefin Midshipman	*Porichthys myriaster*	Rocky/ Sandy	NA	79.1	HSWRI; Young (1969); Baldwin and Keiser (2008)
9	Fish	Turbot	*Unspecified*	Sandy	NA	79.1	HSWRI
10	Fish	Queenfish	*Seriphus politus*	Sandy	21.3	88.8	HSWRI
11	Fish	Shovelnose Guitarfish	*Rhinobatis productus*	Sandy	30.0, 60.0	141.3	Allen Necropsy
12	Fish	White Croaker	*Genyonemus lineatus*	Sandy	18.3; NA	53.7; 86.7	HSWRI; Young (1969); Baldwin and Keiser (2008)
13	Fish	Smooth stargazer	*Kathetostoma averruncus*	Sandy	22	NA	SIO Vertebrate Collection
14	Fish	Bat Ray	*Myliobaus californica*	Rocky/ Sandy	NA	NA	Diver Video
15	Invertebrate	Ghost Shrimp	*Neotrypaea spp.*	Sandy	NA	42.1	HSWRI
16	Invertebrate	California Two-Spot Octopus	*Octopus bimaculoides*	Rocky	18	63.0	Isla Natividad Stomach
17	Invertebrate	Razor Clam	*Tagelus spp.*	Sandy	NA	79.1	HSWRI
18	Invertebrate	Spiny Lobster	*Panulirus interruptus*	Rocky	NA	113.5	HSWRI; Diver Observation; Feder et al. (1974); Domeier (2001)

Table 1.2. Prey Types, Continued.

Count	Type	Common Name	Scientific Name	Habitat	Prey Length (cm)	GSB Total Length (cm)	Source
Direct Observation							
19	Invertebrate	Graceful Crab	*Metacarcinus gracilis*	Sandy	8.0; 8.4; 9.0	137.0	Solana Beach Stomach
20	Invertebrate	Armed Box Crab	*Platymera gaudichaudii*	Sandy	4.2; 5.4; 6.3; 6.5; 6.6; 7.0; 7.0; 7.1; 7.2; 7.3; 7.4; 7.6; 7.7	137.0	Solana Beach Stomach
21	Invertebrate	Swimming Crab	*Portunus xantusii*	Sandy	6.1; 6.2; 6.3; 6.8	137.0	Solana Beach Stomach
22	Invertebrate	Octopus	*Unspecified*	Rocky	NA	43.7; 46.6; 51.8; 61.5	HSWRI; Domeier (2001)
23	Invertebrate	Red Crab	*Pleuroncodes planipes*	Rocky/ Sandy/ Open Water	NA	85.0; 110.0	Isla Natividad Stomach; Domeier (2001); Baldwin and Keiser (2008)
24	Invertebrate	California Mantis Shrimp	*Hemisquilla californiensis*	Sandy	7.0; NA	90.0; 141.3	Isla Natividad Stomach; Allen Necropsy
Anecdotal Observation							
25	Fish	Sargo	*Anisotremus davidsonii*	Rocky/ Sandy	NA	NA	Domeier (2001)
26	Fish	Ocean Whitefish	*Caulolatilus princeps*	Rocky	NA	NA	Young (1969); Domeier (2001); Baldwin and Keiser (2008)
27	Fish	Blacksmith	*Chromis punctipinnis*	Rocky	NA	NA	Domeier (2001)
28	Fish	Anchovies	*Engraulis mordax*	Open Water	NA	NA	Young (1969); Baldwin and Keiser (2008)

Table 1.2. Prey Types, Continued.

Count	Type	Common Name	Scientific Name	Habitat	Prey Length (cm)	GSB Total Length (cm)	Source
Anecdotal Observation							
29	Fish	Kelp Bass	*Paralabrax clathratus*	Rocky/Sandy	NA	NA	Feder et al. (1974); Domeier (2001)
30	Fish	Barred Sand Bass	*Paralabrax nebulifer*	Sandy	NA	NA	Young (1969); Domeier (2001); Baldwin and Keiser (2008)
31	Fish	Pacific Bonito	*Sarda chiliensis lineolata*	Open Water	NA	NA	Feder et al. (1974); Baldwin and Keiser (2008)
32	Fish	Pacific Mackerel	*Scomber japonicus*	Open Water	NA	NA	Baldwin and Keiser (2008)
33	Fish	California Sheephead	*Semicossyphus pulcher*	Rocky	NA	NA	Young (1969); Domeier (2001); Baldwin and Keiser (2008)
34	Fish	Pacific Jack Mackerel	*Trachurus symmetricus*	Open Water	NA	NA	Young (1969); Baldwin and Keiser (2008)
35	Fish	Sting Ray	*Unspecified*	Sandy	NA	NA	Domeier (2001); Baldwin and Keiser (2008)

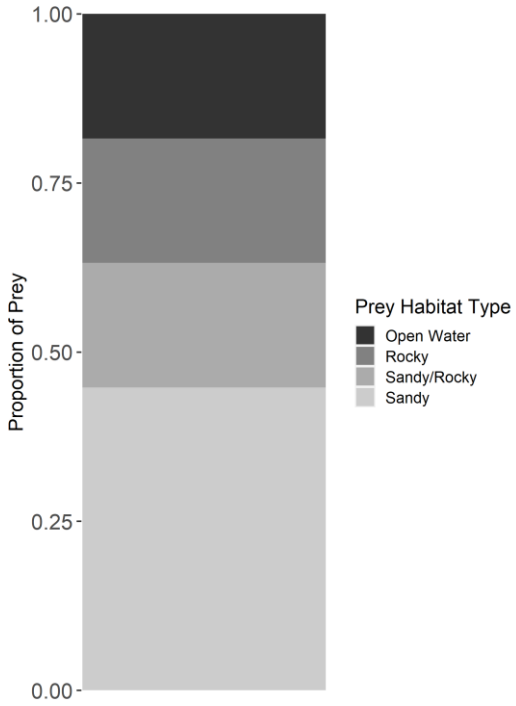

Figure 1.7. Relative proportion of prey from all stomach content observations (direct and anecdotal) associated with different habitat types.

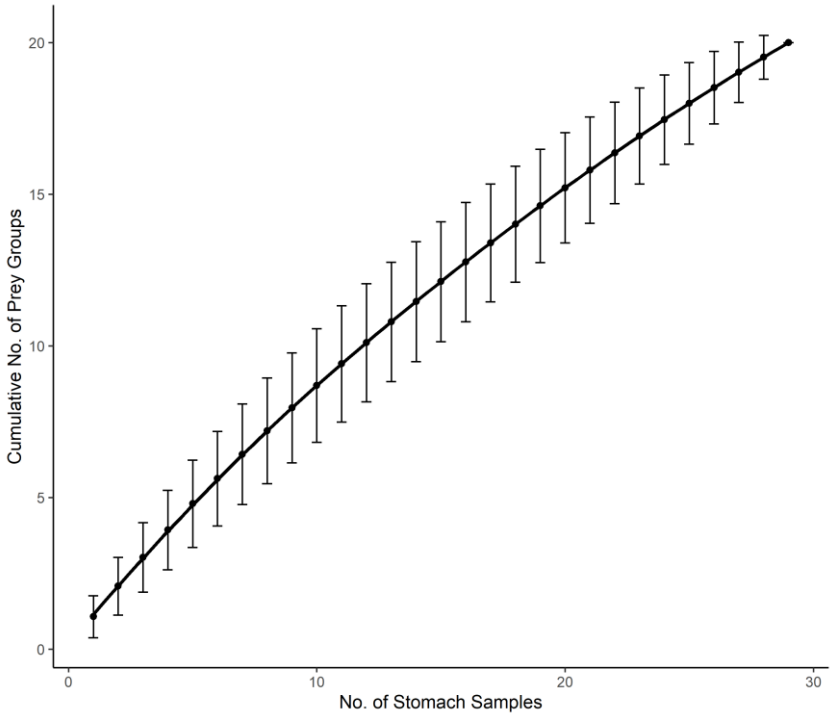

Figure 1.8. Species accumulation curve associated with prey observations from stomach samples.

1.4 Discussion

The analysis we present here constitutes the first documented study of the trophic ecology of adult Giant Sea Bass. The wide array of observed prey items and the fact that our stomach content species accumulation curve did not reach an asymptote support the previous characterization of Giant Sea Bass as generalist predators (Domeier 2001, Allen and Andrews 2012, House et al. 2016), at least at the population level. It is also clear that Giant Sea Bass alter their feeding habits as they grow. The increase in $\delta^{13}C$, estimated trophic position, and trophic niche width with increasing size are indicative of shifts in their diet with size. The overlap of trophic niche width among age classes and an increase in SEAc among the mature age class suggests that Giant Sea Bass are likely consuming similar prey across size ranges, but that they expand their diet to include new types of prey as they grow. It is possible the expansion of trophic niche width is due to size limitation, with larger Giant Sea Bass expanding their diets to include larger, higher trophic level species that were inaccessible at smaller sizes. This relationship could also account for the increased trophic position we found in larger individuals. A widening trophic niche in the mature population also suggests increased specialization at the individual level. For the gut content samples where prey size information was available, it was the case that larger prey items tended to be found in stomachs of larger individuals. For example, the largest Giant Sea Bass sampled, measuring 141 cm in TL, had two Shovelnose Guitarfish (*Rhinobatus productus*) measuring 60 cm and 30 cm in TL inside its stomach. It is unlikely Giant Sea Bass at the smaller end of those analyzed in this study (~40-60 cm) would be able to consume these prey. Anecdotal reports cited in Baldwin and Keiser (2008) also support the idea that Giant Sea Bass alter their feeding ecology as they grow, and that smaller Giant Sea Bass are associated with small transient species such as anchovies and sardines.

Our mixing model results indicated that Giant Sea Bass feed chiefly in macroalgae-based food chains, and that this becomes increasingly true as they grow. Anecdotal reports of smaller Giant Sea Bass relying more heavily on pelagic species such as anchovies and sardines (Baldwin and Keiser 2008) provide an explanation for the shifts we see in the relative proportion of primary producer sources in their diets. These prey could serve as links between offshore and nearshore environments, increasing the relative proportion of phytoplankton-derived carbon in the tissue of smaller Giant Sea Bass. As Giant Sea Bass grow and transition to a diet consisting of predominantly benthic organisms, there is an increase in the proportion of macroalgae-derived carbon in their diets. Previous studies tracing primary producer contributions to fish diets in nearshore environments in the eastern Pacific also document high proportions of macroalgae-derived carbon (Duggins et al. 1989, Koenigs et al. 2015, von Biela et al. 2016). The vast majority of the prey items we documented lived in benthic habitats, and most of those benthic prey were associated with sandy bottom habitats in particular. Initially, this might seem to contradict the mixing model results; however, it is likely that Giant Sea Bass are feeding in sandy bottom habitats that rely on macroalgae from adjacent rocky reefs to subsidize their carbon supply (Polis et al. 1997, Harroschold et al. 1998, KR et al. 2009, Filbee-Dexter et al. 2018).

It is unclear how current threats to kelp forest systems, such as climate change, will influence the trophic ecology of Giant Sea Bass and by extension their continued recovery, but we can make some speculations based on the results of this study. While the individuals in our analysis showed that a large portion of their diet is derived from macroalgae-based food chains, their prey are not necessarily obligate kelp forest inhabitants and neither are the Giant Sea Bass themselves. Assuming that the ecosystem can still support an adequate prey supply, there does not seem to be a reason Giant Sea Bass need kelp. One study that looked at the impact of *M. pyrifera* deforestation

caused by urchin grazing on kelp forest food web structure found that the negative impacts of deforestation were not as strong at higher trophic levels (similar to those occupied by Giant Sea Bass) (Graham 2004). Furthermore, a portion of the geographic range of Giant Sea Bass does not coincide with the range of kelp, and there are anecdotal reports of the local extirpation of kelp from rocky reefs in the Channel Islands having no apparent influence on the presence of Giant Sea Bass (Domeier 2001). These findings suggest that threats to kelp forests do not necessarily equate to threats to Giant Sea Bass.

It is likely that the reason Giant Sea Bass are often associated with kelp forest environments is the ability of these systems to support a high biomass of diverse prey groups both in the immediate rocky reef environment and in adjacent sandy bottom habitats (Polis et al. 1997, Graham 2004). As such, the impact of the potential loss of kelp forests on Giant Sea Bass will depend, at least in part, on the extent of the impacts on Giant Sea Bass prey. Generally, resource-limited conditions, like those brought on by the loss of kelp, lead to increased diet specialization among predator populations because there is an increased need for efficient resource exploitation (Bolnick et al. 2003, Matich et al. 2011). For example, sea otters in Central California, a relatively resource-limited environment experiencing ongoing declines in kelp biomass, have more specialized diets when compared to sea otters in Washington, a more resource-rich environment (Laidre and Jameson 2006, Tinker et al. 2008, Matich et al. 2011). It is possible that we could see a similar shift in Giant Sea Bass trophic ecology with the reduction of kelp. Overall, their ability to exploit a diverse array of prey items suggests that Giant Sea Bass populations would be able to adapt relatively well to changing conditions when compared to other more specialist predators.

Giant Sea Bass have been essentially absent from kelp forests in their southern California range for over 50 years making it difficult to predict how their recovery will influence these

ecosystems. It is very possible that ecosystem conditions have changed since the last time Giant Sea Bass were a regular feature of kelp forest environments in the region. Previous work has found that fluctuations in generalist predator populations can be associated with intense ecosystem impacts (Clavel et al. 2011, Layman and Allgeier 2012). For example, *Pisaster ochraceus* is a generalist predatory sea star that is the subject of many foundational studies in trophic ecology, informing our understanding of keystone predators, trophic cascades, and indirect effects of predation (Paine 1966, 1969, 1974). The recent decline of *P. ochraceus* populations as a result of sea star wasting disease resulted in a release of prey communities, shifts in abundance of predator communities, and an alteration of the structure of rocky intertidal ecosystems throughout the Pacific coast of North America (Menge et al. 2016, Miner et al. 2018, Kay et al. 2019). The ongoing recovery of *P. ochraceus* seems to influence and be influenced by trophic dynamics, with increased recruitment of juveniles in areas with high prey availability and drastic impacts on prey community structure (especially in regard to mussel abundance) where sea star densities have recovered (Blanchette et al. 2005, Menge et al. 2016). As generalists, the impact of the Giant Sea Bass population is spread across a wide variety of prey, but our finding that they primarily feed on benthic species, especially as large adults, suggests their recovery is likely to influence the structure of benthic communities in particular. Furthermore, the observed increase in trophic position with size suggests that these impacts are not limited to lower trophic level species, but can influence intermediate benthic predator populations as well.

While Giant Sea Bass are remarkably generalist predators at the population level, our results show an increase in isotopic niche space with growth suggesting that adults have increasingly specialized diets at the individual level. Individual specialization in predators can influence the magnitude of their trophic-related impacts, including their effect on the stability of

prey populations and inter- and intra-species competition for prey resources (Bolnick et al. 2003, 2011, Araújo et al. 2011, Layman and Allgeier 2012). Individual specialization can serve to diversify the prey communities impacted by a predator population, reducing intra-specific competition and promoting the stability of both predator and prey populations (Bolnick et al. 2011, Araújo et al. 2011). However, depending on its energy demands, a single predatory individual with a specialized diet can have large impacts on the prey communities it targets, especially if those communities are already experiencing stress from other sources, such as fishing pressure or climate change. While we determined that individual specialization is likely a factor in Giant Sea Bass trophic ecology, further work is needed to determine the extent to which it influences the trophic structure of the ecosystems Giant Sea Bass inhabit.

In this study we confirmed that Giant Sea Bass are generalist predators, occupying a relatively high trophic position overall, though they feed on a wide array of different prey items throughout the food web. We found that they occupy similar trophic niche space throughout their life history, but that they expand their diets to include new prey as they grow. These diet shifts contribute to individuals occupying increasingly higher trophic positions as they grow, and are likely associated with increased individual specialization. We determined that Giant Sea Bass are chiefly feeding in macroalgae-based food webs, especially as adults. Despite the importance of macroalgae as a major carbon source for Giant Sea Bass diets, they do not appear to be directly reliant on kelp forests for survival. When combined, our findings suggest that Giant Sea Bass likely have broad, top down effects on kelp forest ecosystems, particularly among benthic communities, that will strengthen through time as populations continue to recover. The extent to which these impacts will influence prey communities, competition with other predators, and kelp forest ecosystem dynamics overall is still unclear. Future work should be directed toward monitoring

shifts in kelp forest community structure as Giant Sea Bass populations continue to increase, especially in regard to benthic prey communities and potential inter-species competitors.

Acknowledgements

We would like to acknowledge the funding sources that contributed to this work: the Mia Tegner Memorial Fellowship, the SIO Center for Marine Biodiversity and Conservation Mentorship Program, the Women Divers Hall of Fame Marine Conservation Scholarship sponsored by the Rachel Morrison Memorial Fund, and the Link Family Foundation (via Dr. Phil Hastings). We would like to acknowledge Youssef Doss, the undergraduate REU intern who helped prepare fin clip samples for bulk isotope analysis. We would also like to acknowledge everyone who contributed to the data collection for this project, including the fishing cooperatives who allowed us to use samples from their catch, HSWRI, Dr. Larry Allen, the SIO Vertebrate Collection, Dr. Peter Kuriyama and the Solana Beach lifeguards who notified us when a Giant Sea Bass washed up on their beach, and all the researchers who shared their experiences of Giant Sea Bass feeding behavior.

Chapter 1, in full, is currently being prepared for submission for publication and is printed here with the permission of co-authors Rasmus Swalethorp, Arturo Ramirez-Valdez, and Brice X. Semmens. The dissertation author is the primary investigator and author of this paper.

Appendix

Table A1.1 Primary producer isotope values derived from the literature.

	Sample Site	Mean δ13C	Mean δ15N	Source
Kelp				
Macrocystis pyrifera (drift)	Santa Catalina Island, California	-15.33	10.25	Gabara (2020)
Macrycystis pyrifera (fresh)	Santa Catalina Island, California	-16.49	10.36	Gabara (2020)
Macrocystis pyrifera	Santa Cruz Island, California	-13.48	7.27	Hamilton et al. (2011)
Macrocystis pyrifera	Bahia Tortugas, Baja California Sur	-15.20	10.90	Pinon-Gimate et al. (2016)
Macrocystis pyrifera	Bahia Tortugas, Baja California Sur	-15.90	10.40	Vega-Garcia et al. (2015)
Macrocystis pyrifera	La Bocana, Baja California Sur	-22.10	11.60	Vega-Garcia et al. (2015)
Macrocystis pyrifera (new growth)	Arroyo Quemado, California	-12.20	9.70	Page et al. (2008)
Macrocystis pyrifera (new growth)	Naples, California	-13.00	9.50	Page et al. (2008)
Macrocystis pyrifera (new growth)	Carpinteria, California	-12.40	9.70	Page et al. (2008)
Macrocystis pyrifera (old growth)	Arroyo Quemado, California	-12.70	8.60	Page et al. (2008)
Macrocystis pyrifera (old growth)	Naples, California	-13.80	8.50	Page et al. (2008)
Macrocystis pyrifera (old growth)	Carpinteria, California	-13.20	9.70	Page et al. (2008)
Phytoplankton				
POM	Santa Catalina Island, California	-23.02	7.39	Gabara (2020)
POM	Santa Cruz Island, California	-20.11	5.49	Hamilton et al. (2011)
POM	Santa Barbara Channel, California	-21.00	6.80	Page et al. (2008)
POM	Southern California Bight, California	-22.70	8.00	Kurle and McWhorter (2017)

Table A1.2 Table showing number of fin clip samples from each sample site.

Sample Site	n
GuerreroNegro	31
ElDatil	6
LagunaSanIgnacio	5
LaJolla	5
BahiaTortugas	4
SanJuanico	3
AjuscoErendira	2
PuntaAbreojos	2
BahiaDeLosAngeles	1
Carlsbad	1
ElRosario	1
IslaNatividad	1
SolanaBeach	1

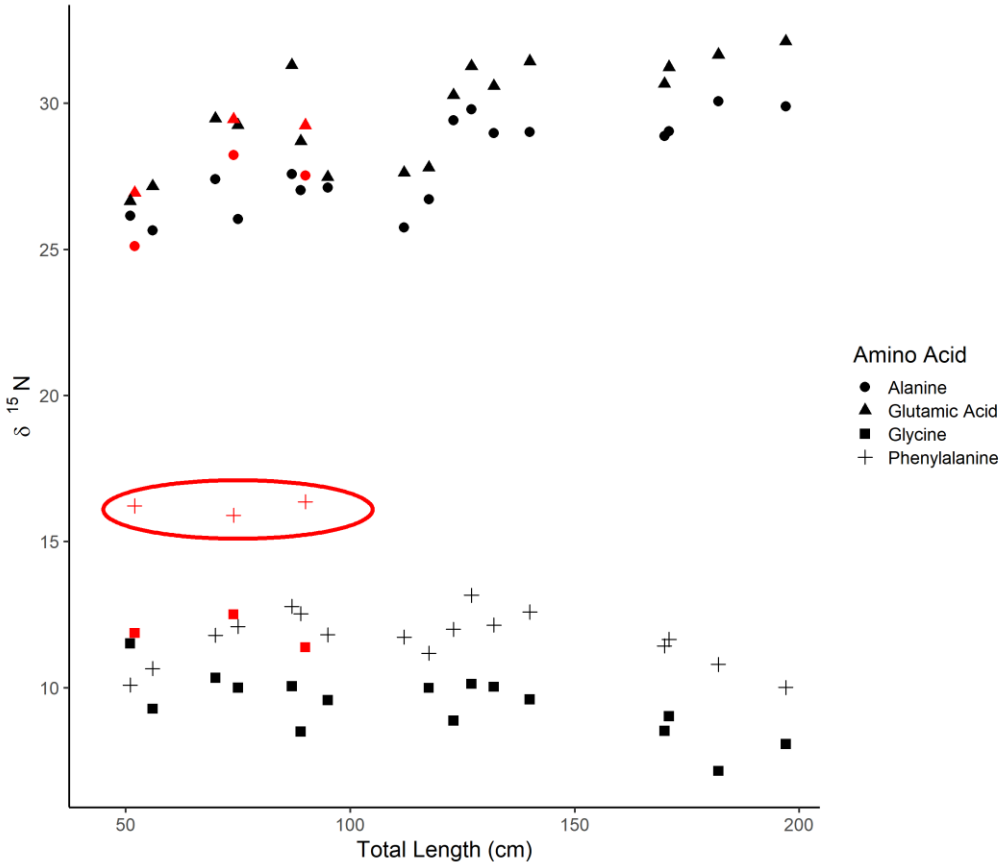

Figure A1.1. While we ran CSIA-AA on 20 samples, we only calculated the trophic position for 16 samples. Three samples had unreasonable phenylalanine results which indicated that there was an error during sample processing so they were removed from all data analysis. There was one additional sample we were unable to determine the glycine value for, so it was not included in the trophic position estimates either. This figure shows the unreasonable phenylalanine samples (circled). The other AA values associated with those samples are also shown in red.

Works Cited

Allen, L. G. 2017. GIANTS! Or… The Return of the Kelp Forest King. Copeia 105:10–13.

Allen, L. G., and A. H. Andrews. 2012. Bomb radiocarbon dating and estimated longevity of Giant Sea Bass (*Stereolepis gigas*). Bulletin, Southern California Academy of Sciences 111:1–14.

Araújo, M. S., D. I. Bolnick, and C. A. Layman. 2011, September 1. The ecological causes of individual specialisation. John Wiley & Sons, Ltd.

Artero, C., C. C. Koenig, P. Richard, R. Berzins, G. Guillou, C. Bouchon, and L. Lampert. 2015. Ontogenetic dietary and habitat shifts in goliath grouper *Epinephelus itajara* from French Guiana. Endangered Species Research 27:155–168.

Baldwin, D. S., and A. Keiser. 2008. Giant sea bass, *Stereolepis gigas*. Status of the Fisheries Report, Cal. Dept. Fish Game.

Benseman, S. 2018. Recruitment, growth rates, planktonic larval duration, and behavior of the young-of-the-year of giant sea bass, *Stereolepis gigas*, off southern California. Masters of Science Thesis. California State University, Northridge.

von Biela, V. R., S. D. Newsome, J. L. Bodkin, G. H. Kruse, and C. E. Zimmerman. 2016. Widespread kelp-derived carbon in pelagic and benthic nearshore fishes suggested by stable isotope analysis. Estuarine, Coastal and Shelf Science 181:364–374.

Bishop, K. L., P. C. Wainwright, and R. Holzman. 2008. Anterior-to-posterior wave of buccal expansion in suction feeding fishes is critical for optimizing fluid flow velocity profile. Journal of The Royal Society Interface 5:1309–1316.

Blanchette, C. A., D. V Richards, J. M. Engle, B. R. Broitman, and S. D. Gaines. 2005. Regime shifts, community change and population booms of keystone predators at the Channel Islands. Pages 435–441 Proceedings of the California Islands Symposium.

Bolnick, D. I., P. Amarasekare, M. S. Araújo, R. Bürger, J. M. Levine, M. Novak, V. H. W. Rudolf, S. J. Schreiber, M. C. Urban, and D. A. Vasseur. 2011, April 1. Why intraspecific trait

variation matters in community ecology. Elsevier Current Trends.

Bolnick, D. I., R. Svanbäck, J. A. Fordyce, L. H. Yang, J. M. Davis, C. D. Hulsey, and M. L. Forister. 2003. The ecology of individuals: Incidence and implications of individual specialization. American Naturalist 161:1–28.

Bradley, C. J., N. J. Wallsgrove, C. A. Choy, J. C. Drazen, E. D. Hetherington, D. K. Hoen, and B. N. Popp. 2015. Trophic position estimates of marine teleosts using amino acid compound specific isotopic analysis. Limnology and Oceanography: Methods 13:476–493.

Broek, T. A. B., and M. D. McCarthy. 2014. A new approach to δ15N compound-specific amino acid trophic position measurements: Preparative high pressure liquid chromatography technique for purifying underivatized amino acids for stable isotope analysis. Limnology and Oceanography: Methods 12:840–852.

Clavel, J., R. Julliard, and V. Devictor. 2011. Worldwide decline of specialist species: toward a global functional homogenization? Frontiers in Ecology and the Environment 9:222–228.

Crawley, K., G. Hyndes, M. Vanderklift, and A. Revill. 2009. Allochthonous brown algae are the primary food source for consumers in a temperate, coastal environment. Marine Ecology Progress Series 376:33–44.

Dayton, P. K., M. J. Tegner, P. B. Edwards, and K. L. Riser. 1998. Sliding baselines, ghosts, and reduced expectations in kelp forest communities. Ecological Applications 8:309–322.

Décima, M., M. R. Stukel, L. López-López, and M. R. Landry. 2019. The unique ecological role of pyrosomes in the Eastern Tropical Pacific. Limnology and Oceanography 64:728–743.

DeNiro, M. J., and S. Epstein. 1978. Influence of diet on the distribution of carbon isotopes in animals. Geochimica et cosmochimica acta 42:495–506.

Domeier, M. L. 2001. Giant sea bass. California's living marine resources: a status report. Calif Fish Game, Sacramento:209–211.

Donohue, I., O. L. Petchey, S. Kéfi, A. Génin, A. L. Jackson, Q. Yang, and N. E. O'Connor. 2017.

Loss of predator species, not intermediate consumers, triggers rapid and dramatic extinction cascades. Global Change Biology 23:2962–2972.

Duggins, D. O., C. A. Simenstad, and J. A. Estes. 1989. Magnification of secondary production by kelp detritus in coastal marine ecosystems. Science 245:170–173.

Edwards, M. S., and G. Hernández-Carmona. 2005. Delayed recovery of giant kelp near its southern range limit in the North Pacific following El Niño. Marine Biology 2005 147:1 147:273–279.

Erauskin-Extramiana, M., S. Z. Herzka, G. Hinojosa-Arango, and O. Aburto-Oropeza. 2017. An interdisciplinary approach to evaluate the status of large-bodied Serranid fisheries: The case of Magdalena-Almejas Bay lagoon complex, Baja California Sur, Mexico. Ocean & Coastal Management 145:21–34.

Feder, H. M., C. H. Turner, and C. Limbaugh. 1974. Observation on fishes associated with kelp beds in Southern California. Page State of California The Resources Angency Deaprment of Fish and Game Fish Bulletin 160.

Filbee-Dexter, K., T. Wernberg, K. M. Norderhaug, E. Ramirez-Llodra, and M. F. Pedersen. 2018. Movement of pulsed resource subsidies from kelp forests to deep fjords. Oecologia 187:291–304.

Finlay, J. C., S. Khandwala, and M. E. Power. 2002. Spatial scales of carbon flow in a river food web. Ecology 83:1845–1859.

Fredriksen, S. 2003. Food web studies in a Norwegian kelp forest based on stable isotope (δ13C and δ15N) analysis. Marine Ecology Progress Series 260:71–81.

Gabara, S. S. 2020. Trophic structure and potential carbon and nitrogen flow of a rhodolith bed at Santa Catalina Island inferred from stable isotopes. Marine Biology 167:1–14.

Gelman, A., and D. B. Rubin. 1992. A single series from the Gibbs sampler provides a false sense of security. Bayesian statistics 4:625–631.

Graham, M. H. 2004, April 27. Effects of local deforestation on the diversity and structure of southern California giant kelp forest food webs. Springer New York.

Hamilton, S. L., J. E. Caselle, C. A. Lantz, T. L. Egloff, E. Kondo, S. D. Newsome, K. Loke-Smith, D. J. Pondella II, K. A. Young, and C. G. Lowe. 2011. Extensive geographic and ontogenetic variation characterizes the trophic ecology of a temperate reef fish on southern California (USA) rocky reefs. Marine Ecology Progress Series 429:227–244.

Hamilton, S. L., S. D. Newsome, and J. E. Caselle. 2014. Dietary niche expansion of a kelp forest predator recovering from intense commercial exploitation. Ecology 95:164–172.

Hanisch, J. R., W. M. Tonn, C. A. Paszkowski, and G. J. Scrimgeour. 2010. δ13C and δ15N signatures in muscle and fin tissues: nonlethal sampling methods for stable isotope analysis of salmonids. North American Journal of Fisheries Management 30:1–11.

Harrold, C., K. Light, and S. Lisin. 1998. Organic enrichment of submarine-canyon and continental-shelf benthic communities by macroalgal drift imported from nearshore kelp forests. Limnology and Oceanography 43:669–678.

Hawk, H. A., and L. G. Allen. 2014. Age and growth of the giant sea bass, *Stereolepis gigas*. CalCOFI Report 55:128–134.

Hetherington, E. D., C. M. Kurle, M. D. Ohman, and B. N. Popp. 2019. Effects of chemical preservation on bulk and amino acid isotope ratios of zooplankton, fish, and squid tissues. Rapid communications in mass spectrometry 33:935–945.

Hetherington, E. D., J. A. Seminoff, P. H. Dutton, L. C. Robison, B. N. Popp, and C. M. Kurle. 2018. Long-term trends in the foraging ecology and habitat use of an endangered species: an isotopic perspective. Oecologia 188:1273–1285.

Ho, H., J. M. Tylianakis, J. X. Zheng, and S. Pawar. 2019. Predation risk influences food-web structure by constraining species diet choice. Ecology letters 22:1734–1745.

Hobson, K. A. 2005. Stable isotopes and the determination of avian migratory connectivity and seasonal interactions. The Auk 122:1037–1048.

House, P. H., B. L. F. Clark, and L. G. Allen. 2016. The return of the king of the kelp forest: Distribution, abundance, and biomass of Giant sea bass (*Stereolepis gigas*) off Santa Catalina Island, California, 2014-2015. Bulletin, Southern California Academy of Sciences 115:1–14.

Jackson, A. L., R. Inger, A. C. Parnell, and S. Bearhop. 2011. Comparing isotopic niche widths among and within communities: SIBER - Stable Isotope Bayesian Ellipses in R. Journal of Animal Ecology 80:595–602.

Jardine, T. D., R. J. Hunt, B. J. Pusey, and S. E. Bunn. 2011. A non-lethal sampling method for stable carbon and nitrogen isotope studies of tropical fishes. Marine and Freshwater Research 62:83–90.

Johnson, C. R., S. C. Banks, N. S. Barrett, F. Cazassus, P. K. Dunstan, G. J. Edgar, S. D. Frusher, C. Gardner, M. Haddon, and F. Helidoniotis. 2011. Climate change cascades: Shifts in oceanography, species' ranges and subtidal marine community dynamics in eastern Tasmania. Journal of Experimental Marine Biology and Ecology 400:17–32.

Kay, S. W. C., A. L. M. Gehman, and C. D. G. Harley. 2019. Reciprocal abundance shifts of the intertidal sea stars, *Evasterias troschelii* and *Pisaster ochraceus*, following sea star wasting disease. Proceedings of the Royal Society B: Biological Sciences 286.

Koenigs, C., R. J. Miller, and H. M. Page. 2015. Top predators rely on carbon derived from giant kelp *Macrocystis pyrifera*. Marine Ecology Progress Series 537:1–8.

Kurle, C. M., and J. K. McWhorter. 2017. Spatial and temporal variability within marine isoscapes: implications for interpreting stable isotope data from marine systems. Marine Ecology Progress Series 568:31–45.

Kurle, C. M., E. H. Sinclair, A. E. Edwards, and C. J. Gudmundson. 2011. Temporal and spatial variation in the δ 15 N and δ 13 C values of fish and squid from Alaskan waters. Marine Biology 158:2389–2404.

Laidre, K. L., and R. J. Jameson. 2006. Foraging patterns and prey selection in an increasing and explanding sea otter population. Journal of Mammalogy 87:799–807.

Layman, C., and J. Allgeier. 2012. Characterizing trophic ecology of generalist consumers: a case study of the invasive lionfish in The Bahamas. Marine Ecology Progress Series 448:131–141.

Layton, C., V. Shelamoff, M. J. Cameron, M. Tatsumi, J. T. Wright, and C. R. Johnson. 2019. Resilience and stability of kelp forests: The importance of patch dynamics and environment-engineer feedbacks. PloS one 14:e0210220.

Matich, P., M. R. Heithaus, and C. A. Layman. 2011. Contrasting patterns of individual specialization and trophic coupling in two marine apex predators. Journal of Animal Ecology 80:294–305.

Menge, B. A., E. B. Cerny-Chipman, A. Johnson, J. Sullivan, S. Gravem, and F. Chan. 2016. Sea Star Wasting Disease in the Keystone Predator Pisaster ochraceus in Oregon: Insights into differential population impacts, recovery, predation rate, and temperature effects from long-term research. PLoS ONE 11:e0153994.

Miner, C. M., J. L. Burnaford, R. F. Ambrose, L. Antrim, H. Bohlmann, C. A. Blanchette, J. M. Engle, S. C. Fradkin, R. Gaddam, C. D. G. Harley, B. G. Miner, S. N. Murray, J. R. Smith, S. G. Whitaker, and P. T. Raimondi. 2018. Large-scale impacts of sea star wasting disease (SSWD) on intertidal sea stars and implications for recovery. PLoS ONE 13:e0192870.

Nielsen, J. M., B. N. Popp, and M. Winder. 2015. Meta-analysis of amino acid stable nitrogen isotope ratios for estimating trophic position in marine organisms. Oecologia 178:631–642.

Oksanen, J., F. G. Blanchet, M. Friendly, R. Kindt, P. Legendre, D. McGlinn, P. R. Minchin, R. B. O'Hara, G. L. Simpson, P. Solymos, H. Stevens, E. Szoecs, and H. Wagner. 2020. vegan: Community Ecology Package. CRAN.

Page, H. M., D. C. Reed, M. A. Brzezinski, J. M. Melack, and J. E. Dugan. 2008. Assessing the importance of land and marine sources of organic matter to kelp forest food webs. Marine Ecology Progress Series 360:47–62.

Paine, R. T. 1966. Food web complexity and species diversity. The American Naturalist 100:65–75.

Paine, R. T. 1969. A note on trophic complexity and community stability. The American Naturalist

103:91–93.

Paine, R. T. 1974. Intertidal community structure. Oecologia 15:93–120.

Phillips, D. L., R. Inger, S. Bearhop, A. L. Jackson, J. W. Moore, A. C. Parnell, B. X. Semmens, and E. J. Ward. 2014. Best practices for use of stable isotope mixing models in food-web studies. Canadian Journal of Zoology 92:823–835.

Piñón-Gimate, A., M. M. Gómez-Valdez, A. Mazariegos-Villarreal, and E. Serviere-Zaragoza. 2016. Trophic relationships between two gastropods and seaweeds in subtropical rocky reefs based on stable isotope analyses. Journal of Shellfish Research 35:191–197.

Plummer, M. 2003. JAGS: A program for analysis of Bayesian graphical models using Gibbs sampling.

Polis, G. A., W. B. Anderson, and R. D. Holt. 1997. Toward an integration of landscape and food web ecology:The dynamics of spatially subsidized food webs. Annual Review of Ecology and Systematics 28:289–316.

Pondella, D. J., and L. G. Allen. 2008. The decline and recovery of four predatory fishes from the Southern California Bight. Marine Biology 154:307–313.

Post, D. M. 2002. Using stable isotopes to estimate trophic position: models, methods, and assumptions. Ecology 83:703–718.

R Core Team. 2019. R: A language and environment for statistical computing. R Foundation for Statistical Computing, Vienna, Austria.

Richards, T. M., T. T. Sutton, and R. J. D. Wells. 2020. Trophic Structure and Sources of Variation Influencing the Stable Isotope Signatures of Meso- and Bathypelagic Micronekton Fishes. Frontiers in Marine Science 7:876.

Sanderson, B. L., C. D. Tran, H. J. Coe, V. Pelekis, E. A. Steel, and W. L. Reichert. 2009. Nonlethal sampling of fish caudal fins yields valuable stable isotope data for threatened and endangered fishes. Transactions of the American Fisheries Society 138:1166–1177.

Schram, J. B., H. L. Sorensen, R. D. Brodeur, A. W. E. Galloway, and K. R. Sutherland. 2020. Abundance, distribution, and feeding ecology of Pyrosoma atlanticum in the Northern California Current. Marine Ecology Progress Series 651:97–110.

Spiers, E. K. A., R. Stafford, M. Ramirez, D. F. V. Izurieta, M. Cornejo, and J. Chavarria. 2016. Potential role of predators on carbon dynamics of marine ecosystems as assessed by a Bayesian belief network. Ecological informatics 36:77–83.

Steneck, R. S., and C. R. Johnson. 2014. Kelp forests: dynamic patterns, processes and feedbacks In: Burtness MD, Bruno J, Silliman BR, Stachowicz JJ, editors. Marine commmunity ecology. Sinauer Associates, Inc.

Stock, B. C., A. L. Jackson, E. J. Ward, A. C. Parnell, D. L. Phillips, and B. X. Semmens. 2018. Analyzing mixing systems using a new generation of Bayesian tracer mixing models. PeerJ 6:e5096.

Su, Y.-S., and M. Yajima. 2020. R2jags: Using R to Run "JAGS." CRAN.

Suzuki, K. W., A. Kasai, K. Nakayama, and M. Tanaka. 2005. Differential isotopic enrichment and half-life among tissues in Japanese temperate bass (*Lateolabrax japonicus*) juveniles: implications for analyzing migration. Canadian Journal of Fisheries and Aquatic Sciences 62:671–678.

Swalethorp, R., L. Aluwihare, A. R. Thompson, M. D. Ohman, and M. R. Landry. 2020. Errors associated with compound-specific δ15N analysis of amino acids in preserved fish samples purified by high-pressure liquid chromatography. Limnology and Oceanography: Methods 18:259–270.

Teagle, H., S. J. Hawkins, P. J. Moore, and D. A. Smale. 2017. The role of kelp species as biogenic habitat formers in coastal marine ecosystems. Journal of Experimental Marine Biology and Ecology 492:81–98.

Tinker, M. T., G. Bentall, and J. A. Estes. 2008. Food limitation leads to behavioral diversification and dietary specialization in sea otters. Proceedings of the National Academy of Sciences of the United States of America 105:560–565.

Vega-García, P. D., A. Piñón-Gimate, N. Vélez-Arellano, and S. E. Lluch-Cota. 2015. Differences in diet of green (*Haliotis fulgens*) and pink (*Haliotis corrugata*) wild abalone along the Pacific coast of the Baja California Peninsula, using stable isotope analyses. Journal of Shellfish Research 34:879–884.

Vehtari, A., J. Gabry, M. Magnusson, Y. Yao, P. Bürkner, T. Paananen, and A. Gelman. 2020. loo: Efficient leave-one-out cross-validation and WAIC for Bayesian models. CRAN.

Vehtari, A., A. Gelman, and J. Gabry. 2017. Practical Bayesian model evaluation using leave-one-out cross-validation and WAIC. Statistics and Computing 27:1413–1432.

Werner, E. E., and J. F. Gilliam. 1984. The ontogenetic niche and species interactions in size-structured populations. Annual review of ecology and systematics 15:393–425.

Young, P. H. 1969. The California Partyboat Fishery 1947-1967. State of California, The Resources Agency, Department of Fish and Game Fish Bulletin 145.

Chapter 2:

Investigating the spatial ecology of Giant Sea Bass (*Stereolepis gigas*) using acoustic telemetry in the La Jolla kelp forest.

Kayla M. Blincow, Brice X. Semmens

Abstract

The history of Giant Sea Bass fisheries is closely linked to their spatial ecology. Overharvest of the species is directly associated with their formation of spatially distinct spawning aggregations during summer months, while their subsequent population growth appears to be the result of spatially-explicit gear restrictions. It stands to reason that understanding the spatial ecology of Giant Sea Bass is a key part of efforts to assess interactions with contemporary commercial harvest and incidental catch by recreational fisheries. In this study, we used acoustic telemetry to characterize Giant Sea Bass space use in the La Jolla kelp forest by tracking acoustically tagged individuals with a passive hydrophone network that encompasses two marine protected areas (MPAs) and proximal, heavily trafficked recreational fishing grounds (where all of our fish were tagged). Five of the seven fish we tagged remained in the La Jolla array for at least six months following tagging, while two were resident throughout the three year study. Only one of the fish that left the La Jolla array was detected in the broader network of regional acoustic receivers, moving north to Del Mar. Fish tagged outside MPAs tended to spend most of their time outside MPAs, exhibiting strong site fidelity that likely benefits those individuals with fidelity to habitat inside MPAs. However, increased movements between non-proximal receivers and increased detections in unprotected habitat on the northwest corner of the La Jolla kelp forest suggest that spawning behaviors are increasing individual exposure to incidental catch. Thus, during spawning season, recreational anglers should take extra care to avoid incidental catch, and should be well prepared to safely and quickly release these fish.

2.1 Introduction

Reaching close to three meters in length, Giant Sea Bass, *Stereolepis gigas* (Polyprionidae), are the largest bony fish found in the kelp forests and rocky reefs of Southern California and the Baja California Peninsula (Hawk and Allen 2014). They are top predators that were once plentiful in coastal rocky reef habitats south of Point Conception (Dayton et al. 1998, Domeier 2001, Erauskin-Extramiana et al. 2017). Historically, Giant Sea Bass were a sought after fisheries species (Domeier 2001, Baldwin and Keiser 2008, Allen 2017). Commercial landings peaked in 1932 at approximately 115 metric tons in the United States of America (US) and approximately 367 metric tons in Mexico (Domeier 2001, Baldwin and Keiser 2008). Both sides of the US-Mexico border experienced declines in commercial landings following these peaks (Domeier 2001). The peak in US recreational landings occurred in 1963, and was also followed by stark declines in catch (Domeier 2001). By the 1970s Giant Sea Bass in the US were nearing extirpation largely due to fishing pressure (Domeier 2001, Baldwin and Keiser 2008, Pondella and Allen 2008). One contributing factor to the decline of Giant Sea Bass populations in the US is their formation of spawning aggregations at predictable times and places (Allen 2017, Erauskin-Extramiana et al. 2017). Species that aggregate to spawn are easily targeted once aggregation locations are found (Erauskin-Extramiana et al. 2017). At the height of Giant Sea Bass commercial and recreational fisheries, fishers in southern California heavily targeted spawning aggregations during summer months (Allen 2017). Today, Giant Sea Bass are listed as *Critically Endangered* by the International Union for Conservation of Nature (IUCN) Red List of Threatened Species (Cornish 2004).

In response to population declines, the state of California implemented regulations in 1981 that essentially closed all US Giant Sea Bass fisheries (FGC §8380, Title 14, CCR, §28.10).

Current regulations in California prohibit all recreational take of Giant Sea Bass, and allow one incidentally caught fish per trip for California commercial set gill net and trammel net fisheries (Domeier 2001, Baldwin and Keiser 2008). There are yet to be any major commercial regulations for Giant Sea Bass in Mexico (Chabot et al. 2015). The cross-border differences in management and regulation make it difficult to get a clear picture of the status of Giant Sea Bass; however, recent reports indicate that they are recovering in US waters (Pondella and Allen 2008, Allen and Andrews 2012, House et al. 2016). These reports attribute the apparent population growth of Giant Sea Bass in California waters to species-specific state fishing regulations, as well as the banning of the nearshore gill net fishery in 1994, which many believe reduced incidental commercial landings (Pondella and Allen 2008, Allen and Andrews 2012, House et al. 2016, Guerra et al. 2018).

While reports of Giant Sea Bass population growth in US waters are encouraging, the species still faces ongoing take, including the Mexican fishery, allowable commercial catch in the US, and incidental catch by US recreational fisheries. It is difficult to gather reliable data on the status of the Mexican Giant Sea Bass fishery, because much of the historic catch data reported from artisanal fisheries are aggregated based on coarse regional areas or multi-specific groupings (Erauskin-Extramiana et al. 2017). However, one study found that the combined landings of Pacific Goliath Grouper (*Epinephelus quinquefasciatus*) and Giant Sea Bass in the Magdalena-Almejas Bay lagoon complex rose steadily from approximately 5 metric tons in 2001 to 25 metric tons in 2013 (Erauskin-Extramiana et al. 2017). Furthermore, a recent study estimating Giant Sea Bass landings in Mexico from multiple data sources found that commercial landings in Mexico averaged 50.9 metric tons per year between 2000 and 2016 (Ramirez-Valdez et al. *in press*). Fishing activities in the US are also likely mediating the local recovery of this species. From 2000

to 2020, commercial fishers in the US landed an average of 2.76 metric tons of Giant Sea Bass per year (calculated from Pacific Fisheries Information Network (PacFIN) Commercial Landed Catch Species Report). Despite the ban on recreational take of the species in the US, individuals are regularly incidentally caught and released. While recreational fishers are supposed to make every effort to ensure the survival of incidentally caught Giant Sea Bass, it can be difficult to properly care for fish of their size with barotrauma, especially if captured from kayaks or larger vessels with raised decks.

The decline and subsequent indications of population growth of Giant Sea Bass can be linked to the complex history of spatial resource use and spatial management this species experienced throughout its distribution range. From fishers actively targeting areas known to be spawning aggregations (Allen 2017, Erauskin-Extramiana et al. 2017), to the apparent positive response of US Giant Sea Bass populations to spatially explicit regulations limiting fishing gear types (Pondella and Allen 2008, House et al. 2016), space appears to be an important consideration when it comes to the conservation of Giant Sea Bass. Gaining a better understanding of how this species uses space can help determine the effectiveness of current management strategies and better understand the potential risks posed by contemporary fishing activities. For example, other spatial management initiatives such as the California Marine Protected Area network, while not explicitly directed at conserving Giant Sea Bass, might provide benefits to the species by protecting important habitat or providing refuge from fisheries.

In this study we use internal acoustic tagging data to characterize Giant Sea Bass spatial ecology over a longer time scale than previously studied for the species (~three years) focusing on their movement in the La Jolla kelp forest (La Jolla, California, USA). The La Jolla kelp forest is home to at least one historic Giant Sea Bass spawning site. It is also known as one of the best areas

for divers to observe adult and young-of-the-year Giant Sea Bass (Allen et al. 2019). The kelp forest has two separate no-take marine protected areas (MPAs) as well as one of the most intensely recreationally fished areas in the San Diego region (Parnell et al. 2010). Our goals were to (1) determine whether tagged individuals are resident to La Jolla; (2) characterize the seasonality of tagged Giant Sea Bass space use; and (3) investigate how tagged individuals interact with spatial management and contemporary fishing activities that potentially influence this species.

2.2 Methods

Study Area

We conducted this study in the La Jolla kelp forest, which at ~8.25 km^2 is the second largest kelp forest in California (Parnell et al. 2005, 2006). La Jolla's kelp forest environment is marked by hard bottom with channels of sand and cobble interspersed throughout. It is bounded on the northern edge by a submerged canyon with a sandy shelf and sandy bottom habitats on the western and southern edges (Parnell et al. 2006). There are two no-take marine reserves in the area, Matlahuayl State Marine Reserve and South La Jolla State Marine Reserve (Figure 2.1). The region between these two reserves constitutes an important fishing ground for commercial sea urchin and spiny lobster fishers as well as recreational anglers from private vessels and the San Diego Commercial Passenger Fishing Vessel (CPFV) fleet, which are chartered vessels that take groups fishing (usually ~30-50 passengers) (Parnell et al. 2010).

Acoustic Tagging

We tagged seven Giant Sea Bass in the La Jolla kelp forest (Figure 2.1) from August 2018 to October 2019 using Vemco V16-4H acoustic tags with a randomized 30 to 120 s reporting

interval and 1400 d battery life. When detected by an acoustic receiver, these tags provide spatial and temporal presence information on individual fish.

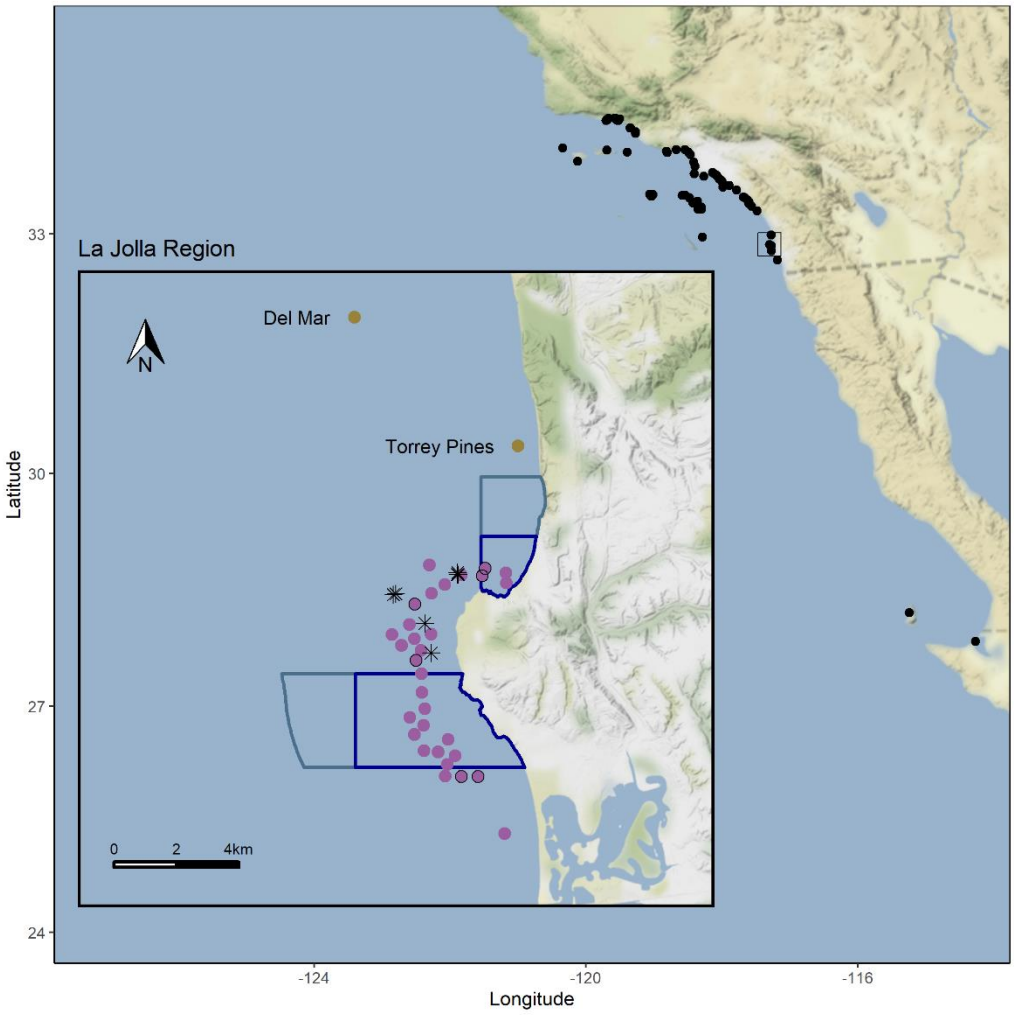

Figure 2.1. Map of the study area. The larger map depicts the broader regional receiver coverage that we checked for detections of our tagged fish. The inset map shows receivers in the La Jolla region. The dark blue polygons depict the bounds of the marine protected areas overlapping the La Jolla array, the Matlahuayl State Marine Reserve to the north and the South La Jolla State marine reserve to the south. The grey-blue polygons depict conservation areas in the region, which allow limited marine or recreational take. The purple points denote the core La Jolla array, while the green points depict other receivers adjacent to the La Jolla array. Purple points with black outlines depict the receivers where we performed range testing. The black asterisk symbols denote the locations where we captured Giant Sea Bass for tagging.

With the exception of one individual, we captured all the fish monitored in this study using hand lines equipped with 9/0 or 10/0 circle hooks and whole dead Pacific Chub Mackerel (*Scomber*

japonicus) for bait. In addition to the baited line, we also chummed the water using a combination of Shakin Bait (an Anchovy and Sardine based chum oil) and a frozen mixture of roughly chopped and/or blended Pacific Chub Mackerel, Pacific Jack Mackerel (*Trachurus symmetricus*), and/or Pacific Sardines (*Sardinops sagax*). We targeted fish at depths < 20 m and brought them to the surface at a moderate speed to minimize barotrauma while not exhausting the fish. To further address the potential negative effects of barotrauma we made every effort to reduce the amount of time each fish spent at the surface. One of the individuals we tagged was caught during Hubbs Sea World Research Institute's (HSWRI) White Seabass (*Atractoscion nobilis*) gill net survey permitted by California Department of Fish and Wildlife (CDFW) and approved by the HSWRI Institutional Animal Care and Use Committee (IACUC) protocols. After being pulled up in the gill net, we assessed this individual, found it to be in good condition, and transferred it to a holding tank before beginning tagging procedures (described below).

For all of the fish captured using hand lines, once at the surface we positioned them inside a vinyl sling mounted on the side of our vessel that restricted their movement while keeping them in the water. For the fish captured during the HSWRI survey, we kept it in an oxygenated holding tank prior to tagging, and placed it in a vinyl cradle on the deck of the vessel during surgical tagging. During tagging, we covered the fish in a wet towel and had continuous water flowing over the gills via hose and water pump. We implanted acoustic tags into each fish's gut cavity via an incision off-center of the midline and posterior to the pelvic girdle in accordance with methods outlined in previous telemetry studies (Lowerre-Barbieri et al. 2014). We used sterile antibiotic infused, dissolvable cutting sutures (PDS II violet 27" CP-1) to close the incision. We then measured each fish for total length (cm), standard length (cm), and head length (cm). We also took a small fin clip (1-2 cm) from the anal fin for later genetic and stable isotope analyses as part of

separate ongoing studies that are not reported here. We secured an external Floy tag (BFIM-96) at the base of the dorsal fin so that tagged fish could be visually identified. Finally, we positioned the fish in a dorsal side-up position to recover alongside the vessel (or within the holding tank for the HSWRI fish) before being released. In instances where fish had inflated swim bladders, we released them at depth using a descending device (SeaQuilizer). CDFW permitted our activities, and the University of California, San Diego IACUC approved our tagging protocols.

Acoustic Receiver Arrays

We used a stationary receiver array deployed in the La Jolla kelp forest to track tagged fish movements over time. This array comprised 31 Vemco VR2w single channel passive autonomous data-loggers. Each VR2w receiver logged date, time, and individual ID when a tag came within the detection range of the receiver. In addition to the 31 receivers moored in the La Jolla kelp forest, we also checked for detections of our tagged fish by other regional acoustic receiver arrays ranging from Isla de Cedros, Baja California, Mexico to Santa Barbara California, USA (Figure 2.1).

Data Analysis

We performed a detection range analysis on six of the 31 receivers in the La Jolla array based on methods used in previous acoustic telemetry research (Blincow et al. 2020) (Figure 2.1). We performed a drift starting at the coordinates of a given receiver mooring while towing a Vemco-coded transmitter tag (~ 1 to 2 m depth). We simultaneously recorded all acoustic tag transmissions (pings) during the drift using a Vemco VR100 mobile receiver unit deployed off the vessel in close proximity to the tag. Using the coordinates for each ping detection on the VR100, we calculated the distance of each ping from the VR2 receiver mooring where it was detected. We

compiled these data for all the receivers that detected the towed tag and analyzed them using a generalized linear mixed-effects model (glmm) with a logit link and a random slope effect of receiver to determine the detection probability of individual pings (binary response) and distance of the tag from the receiver (continuous covariate). With the exception of our movement rate analysis (described below), we assumed the detection range of all of our receivers to be the distance at which our model estimated we could detect tag pings with a 50% probability. We recognize that detection ranges can vary depending on environmental factors, such as diurnal noise patterns and current variability (Mathies et al. 2014, Huveneers et al. 2015); however, for the purpose of this study we made the simplifying assumption of a relatively constant detection range over time for all of our receivers.

Prior to analysis, we filtered our data to remove detections that occurred on the same day as when we tagged the fish to avoid any behavior associated with near-term recovery from tagging influencing our results (Farmer and Ault 2011). To avoid spurious detections resulting from code collisions we removed single detections that occurred in isolation on one day, and any detections from the same tag that occurred across time intervals that were less than the minimum time it takes for the tag to transmit a signal. We performed all analyses using R statistical software, version 3.6.1 (R Core Team 2019). We implemented all of our models using the lme4 package which uses a maximum likelihood approach (Bates et al. 2015). The code for our analyses can be found at https://github.com/kmblincow/GSBMovementAnalysis.

We calculated the residency of each tagged fish within the core La Jolla array by dividing the number of days the fish was at liberty by the number of days the fish was detected within the array. We calculated the mean detections per day for each tag at each receiver by dividing the total number of detections at each receiver by the total number of days each receiver was deployed. We

had one fish that left the La Jolla array and was detected consistently at the Del Mar receiver for a period of months. To confirm that this fish was active we calculated the number of detections per hour inside and outside the La Jolla array, and evaluated the results for fluctuations that would be indicative of movement.

To determine how tagged fish interacted with local MPAs we calculated the total number of detections inside and outside MPAs each day a fish was detected. Some receivers had detection ranges that crossed MPA boundaries. We classified these receivers as either inside or outside MPAs based on the position of the receiver mooring itself. We analyzed the resulting daily detection counts using a Poisson glmm (log link function) with the count of detections per day as the response variable. We included an interaction effect of month and MPA (in or out) as the explanatory variable and individual as a random intercept effect.

To investigate seasonal differences in the activity of our fish we estimated movement rates when fish transited between non-proximal receivers. We used the VTrack package (Campbell et al. 2012) to calculate the straight-line distance between receiver moorings minus a 600 m detection radius. The 600 m correction is a conservative estimate of the distance at which a receiver will have a 0% probability of detecting a tag based on our range analysis results. This was necessary to avoid overestimation of distance traveled by fish when they were occupying space between receivers with overlapping detection ranges. We divided the distance between each detection by the time between detections for each fish to calculate movement rates. The resulting movement rate data were zero-inflated, so we analyzed them using two separate models. First, we converted the movement rates to a binary variable, with 0 being a zero movement rate and 1 being a non-zero movement rate. Using this information we constructed a binomial glmm (logit link function) to calculate the probability of a positive movement rate given the explanatory variables of diel

period (dawn, day, dusk, or night) and month. Second, we filtered our data for only non-zero movement rates, and used a linear mixed-effects model to determine the effect of the explanatory variables diel period and month. We log transformed the non-zero movement rates before running the model to normalize the distribution of the data. Both models included a random intercept effect of individual.

2.3 Results

Based on our range analysis, we found that the VR2 receivers in the La Jolla array on average detect tag pings with a 50% probability at 218.3 m (Figure 2.2). When investigating receiver effects, we found that receivers that were in sandy areas on the edges of the kelp forest tended to have a larger detection radius than receivers within the kelp forest.

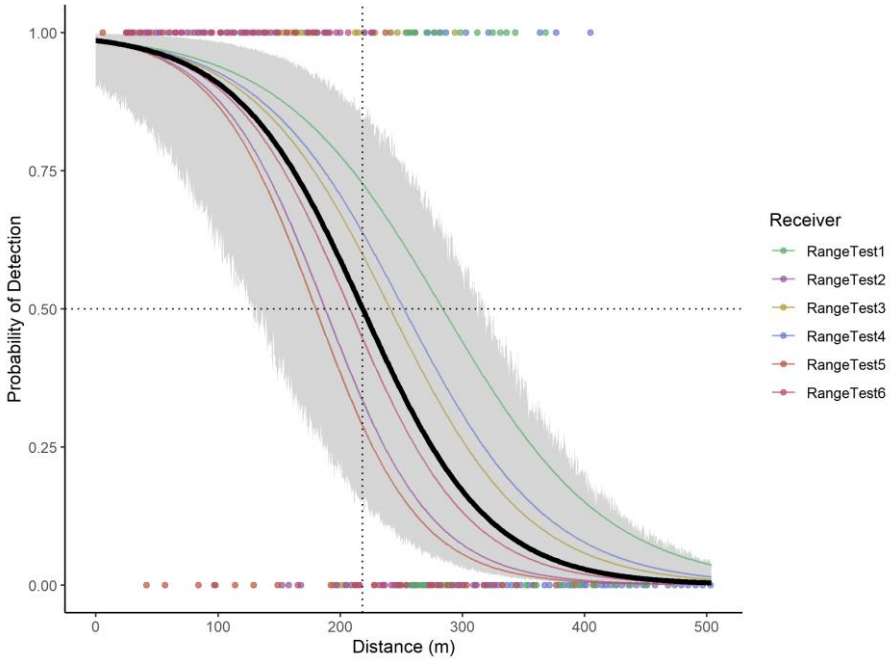

Figure 2.2. Range testing results. The colored lines depict model estimates of probability of detection with distance for each receiver, and colored points depict the binary detections of those receivers (1 for pings detected on both the VR100 and the range tested receiver or 0 for pings only detected on the VR100). The solid black line shows the global mean estimate for the probability of detection with distance of all receivers. The dotted black lines show where the global mean estimate has a 50% probability of detection (218.3m).

We tagged seven fish ranging in total length (TL) from 77 cm to 163 cm (126.14 ± 30.25; Mean ± SD) (Table 2.1). The number of days each tagged fish was at liberty ranged from 586 to 1023 (788.43 ± 169.68) (Table 2.1). The number of days each fish was detected within the La Jolla array (after data filtering) ranged from 0 to 758 (247.57 ± 265.14), and the number of receivers each fish was detected at ranged from 0 to 26 (14.43 ± 9.90) (Table 2.1). Residency within the La Jolla array ranged from 0 to 0.815 (0.288 ± 0.279) (Table 2.1). We removed two fish from subsequent analyses, because they did not have sufficient detections after filtering. Tag Number 11125 was only detected leaving the array on the day it was tagged, and thus did not have any detections following data filters to account for post-tagging behavior. Tag Number 56706 was only detected at two receivers leaving the array on the day following its tagging date.

Table 2.1. Summary data of tagged Giant Sea Bass, including tagging date, total length (TL) at tagging, and summary metrics of each fish's interaction with the La Jolla array. * These fish either had no detections after data filtering (56711) or only had detections from two receivers the day after tagging (56706), so were removed from subsequent analyses.

Tag Number	Tag Date	Fish TL (cm)	Station Count	Days At Liberty	Days Detected in Array	Array Residency
56705	8/15/2018	77	15	1023	414	0.405
56711	11/9/2018	148	26	937	179	0.191
27063	11/16/2018	117	22	930	758	0.815
56704	7/22/2019	153	16	680	202	0.297
11125*	7/23/2019	163	0	681	0	0
56706*	7/24/2019	118	2	682	1	0.001
27070	10/26/2019	107	20	586	179	0.305

We found that the spatial distribution of detections varied across fish, but that the area between the two MPAs, where we captured and released fish, recorded the most detections per day

overall (Figure 2.3). Two fish (Tag Numbers 56706 and 11125) left the La Jolla array within two days of being tagged (Table 2.1). Two fish (Tag Numbers 27063 and 56705) remained within the bounds of the La Jolla array consistently throughout their time at liberty, a period of 2.36 and 2.79 years respectively. Three fish (Tag Numbers 56711, 27070, and 56704) left the array bounds after approximately nine, eight, and six months respectively (Figure 2.3). One of these three fish traveled to the Del Mar receiver and remained there consistently for approximately five months before briefly leaving and then returning to Del Mar (Figure 2.4). Based on the fluctuations shown in the hourly detections, we are confident that this fish was active (not detections from a shed tag) following its departure from the La Jolla array. Our fish were not detected at any other receivers from the broader southern California and Baja California, Mexico regional arrays based on the most recent receiver downloads available.

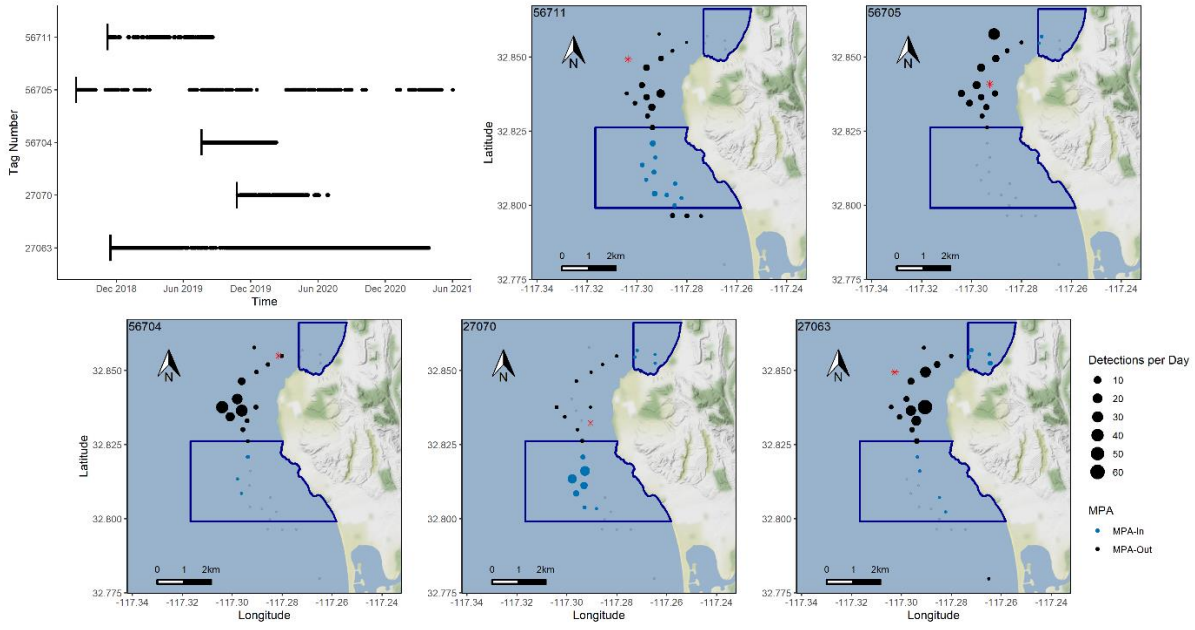

Figure 2.3. Summary of detection data for the five tagged fish used in our analysis. The first panel shows the detections within the La Jolla array across time. The other panels show the mean detections per day at each receiver in the La Jolla array for each fish (specified in the upper left corner). The size of the points on the map denotes the mean detections per day, while the color of the points denotes whether the receiver mooring occurs inside or outside a marine protected area.

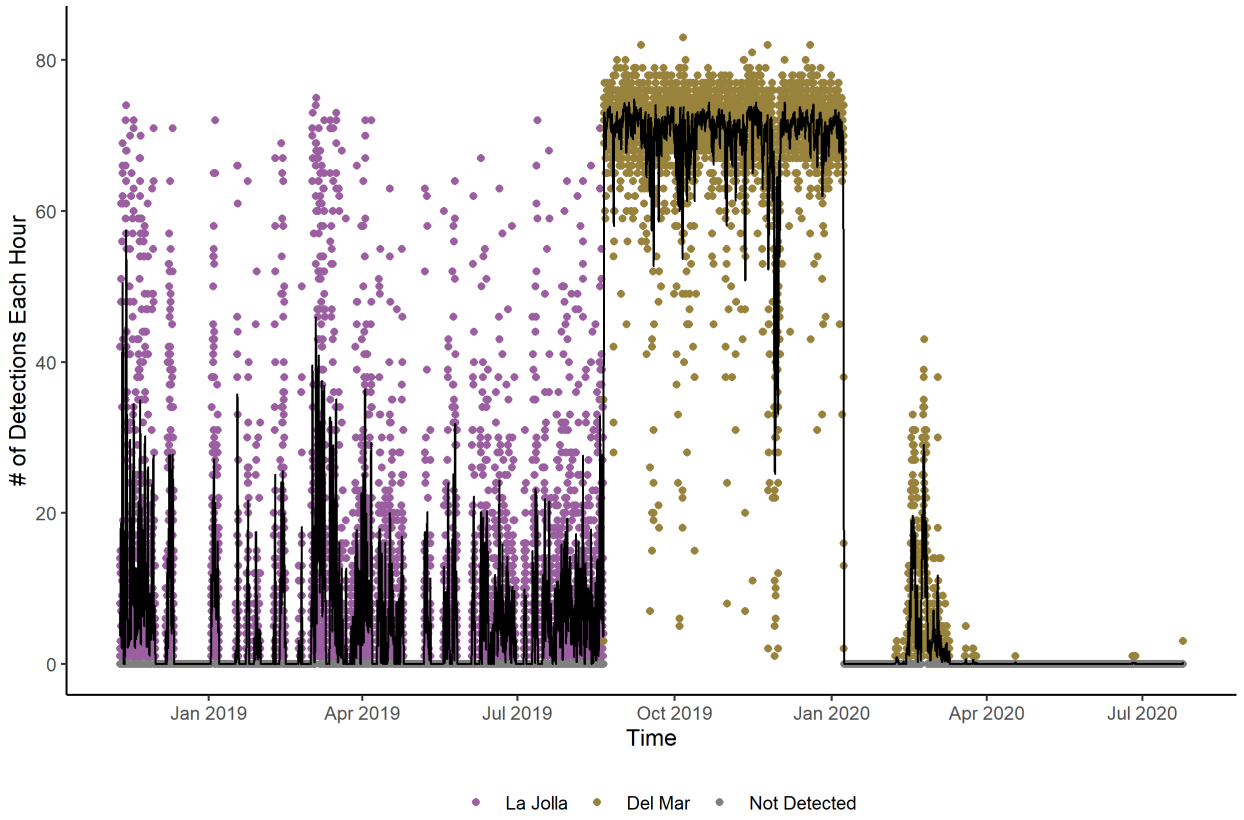

Figure 2.4. Number of detections each hour for Tag Number 56711 in the La Jolla array (purple points) and at the Del Mar Receiver (green points). The black line shows the moving average of the hourly detections across 12 hours. The fluctuations shown in this plot suggest that the fish is active despite the increased frequency of detection while at the Del Mar receiver.

Our model of daily detection count inside and outside MPAs found that fish had more detections per day outside of MPAs overall (Table 2.2; Figure 2.5 a, b). The greatest monthly difference between inside and outside MPAs occurred from August to November (Table 2.2; Figure 2.5 a, b).

Table 2.2. Summary of the Poisson generalized linear mixed-effects model of the influence of month and MPA presence on the daily detection count. The p values shown were estimated based on asymptotic Wald tests (P) (Bates et al. 2015).

Model Equation: Daily Detection Count ~ Month*MPA + (1|Tagged Individual)				
Fixed Effects				
	Estimate	**SE**	**z value**	**Pr(>|z|)**
Intercept	5.38078	0.15398	34.945	$<2e^{-16}$
MPA-Out	0.33408	0.01317	25.362	$<2e^{-16}$
Month2	-0.20623	0.01628	-12.671	$<2e^{-16}$
Month3	-0.25762	0.01552	-16.601	$<2e^{-16}$
Month4	-0.28772	0.01671	-17.214	$<2e^{-16}$
Month5	-0.45620	0.02002	-22.782	$<2e^{-16}$
Month6	-1.15353	0.03067	-37.616	$<2e^{-16}$
Month7	-1.16770	0.03159	-36.967	$<2e^{-16}$
Month8	-1.39605	0.08279	-16.863	$<2e^{-16}$
Month9	-2.35069	0.12022	-19.553	$<2e^{-16}$
Month10	-2.50720	0.08820	-28.428	$<2e^{-16}$
Month11	-1.52763	0.02750	-55.542	$<2e^{-16}$
Month12	0.25622	0.01544	16.591	$<2e^{-16}$
MPA-Out:Month2	0.25357	0.01777	14.269	$<2e^{-16}$
MPA-Out:Month3	0.43921	0.01691	25.971	$<2e^{-16}$
MPA-Out:Month4	0.47860	0.01815	26.369	$<2e^{-16}$
MPA-Out:Month5	0.12376	0.02252	5.496	$3.89e^{-08}$
MPA-Out:Month6	0.63056	0.03230	19.521	$<2e^{-16}$
MPA-Out:Month7	0.33526	0.03313	10.120	$<2e^{-16}$
MPA-Out:Month8	0.79402	0.08315	9.549	$<2e^{-16}$
MPA-Out:Month9	1.71214	0.12050	14.208	$<2e^{-16}$
MPA-Out:Month10	2.07314	0.08853	23.417	$<2e^{-16}$
MPA-Out:Month11	1.41537	0.02829	50.026	$<2e^{-16}$
MPA-Out:Month12	-0.34643	0.01687	-20.538	$<2e^{-16}$

Table 2.2. Poisson glmm, continued.

Random Effects		
	Variance	Standard Deviation
Tagged Individual (Intercept)	0.1178	0.3433

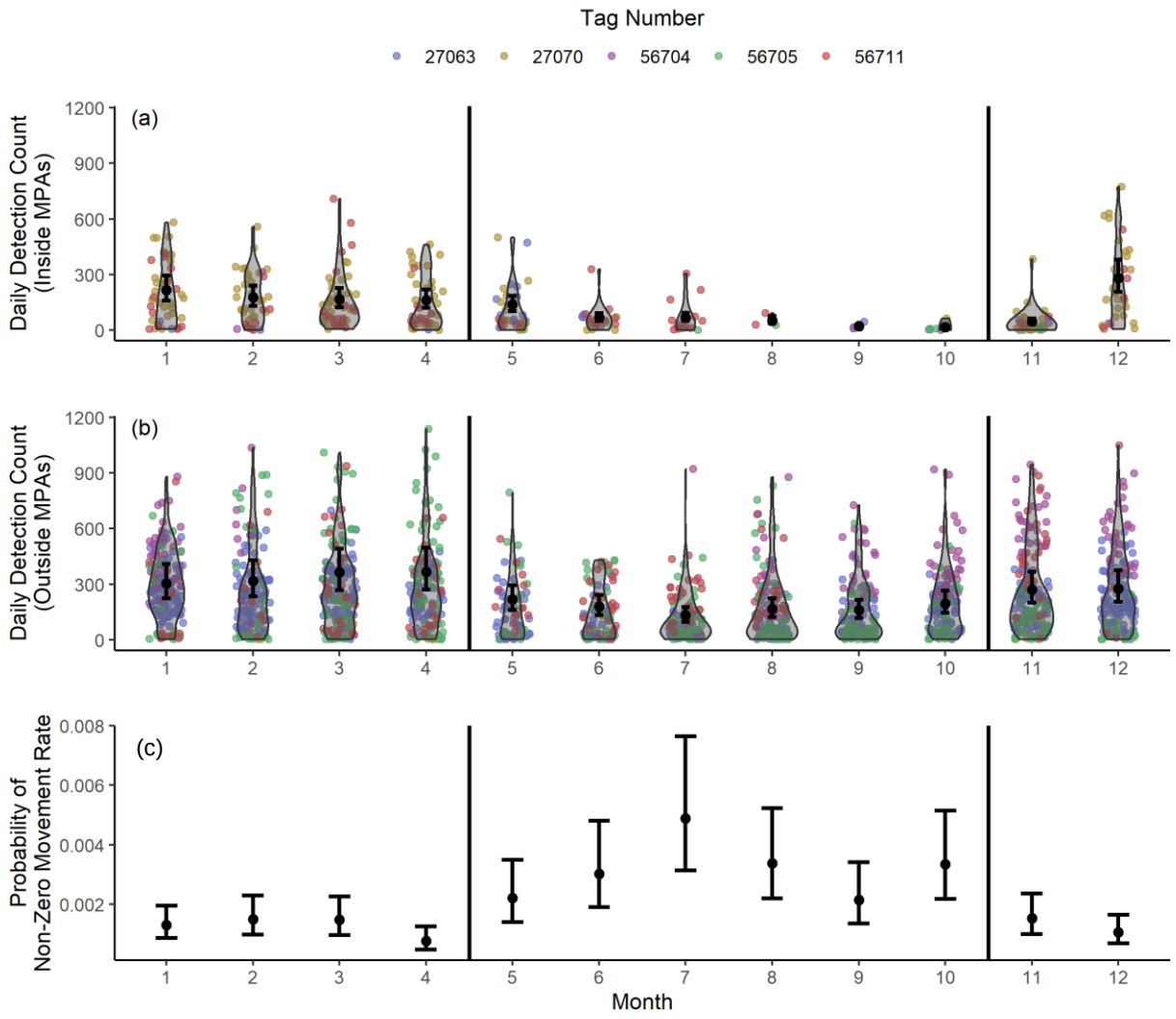

Figure 2.5. Plots of monthly daily detection counts inside (a) and outside (b) MPAs along with the monthly probability of non-zero movement rates. The color of the points in panel a and b denote the tag number, and the overlaid violin plots show the distribution of the daily detection count for each month. The black points and associated intervals denote model estimates and 90% prediction intervals of daily detection per month inside (a) and outside (b) MPAs and probability of non-zero movement rates (c). The black vertical lines in all panels show the range of spawning months reported for Giant Sea Bass.

The majority of intervals between detections did not constitute movement between non-proximal receivers. Our model of the binary response of zero movement rate or non-zero movement rate found that there were no significant differences between different diel periods (Table 2.3). Fish had a higher probability of non-zero movement during the months of May through October and a lower probability of non-zero movement during the month of April (Table 2.3, Figure 2.5c). The model of non-zero movement rates did not find any relationship with diel period. There was low variability in non-zero movement rates across months overall, but our model found that the magnitude of non-zero movement rates was smaller during May, June, and September (Table 2.4).

Table 2.3. Summary of the binomial generalized linear mixed-effects model of the influence of month and diel period on the probability of non-zero movement rates. The p values shown were estimated based on asymptotic Wald tests (P) (Bates et al. 2015).

Model Equation: Binary Movement ~ Diel Period + Month + (1|Tagged Individual)				
Fixed Effects				
	Estimate	**SE**	**z value**	**Pr(>|z|)**
Intercept	-6.59038	0.21954	-30.019	$<2e^{-16}$
Diel Period - Day	-0.03454	0.11921	-0.290	0.771995
Diel Period - Dusk	-0.23020	0.17740	-1.298	0.194428
Diel Period - Night	-0.06466	0.12588	-0.514	0.607516
Month2	-0.28772	0.12387	1.108	0.268041
Month3	-0.45620	0.12146	1.029	0.303588
Month4	-1.15353	0.16628	-3.148	0.001644
Month5	-1.16770	0.15232	3.478	0.000506
Month6	-1.39605	0.15815	5.339	$9.34e^{-08}$
Month7	-2.35069	0.14355	9.255	$<2e^{-16}$
Month8	-2.50720	0.13251	7.233	$4.73e^{-13}$
Month9	-1.52763	0.15438	3.233	0.001226
Month10	0.25622	0.12521	7.551	$4.31e^{-14}$
Month11	0.25357	0.12997	1.256	0.209161

Table 2.3 Binomial glmm, continued.

	Estimate	SE	z value	Pr(>|z|)
Month12	0.43921	0.13473	-1.535	0.124846
Random Effects				
	Variance		**Standard Deviation**	
Tagged Individual (Intercept)	0.2471		0.4971	

Table 2.4. Summary of the linear mixed-effects model of the influence of month and diel period on the non-zero movement rates. The p values shown were estimated based on asymptotic Wald tests (P) (Bates et al. 2015).

Model Equation: Non-Zero Movement Rates ~ Diel Period + Month + (1|Tagged Individual)				
Fixed Effects				
	Estimate	**SE**	**z value**	**Pr(>|z|)**
Intercept	-10.53552	0.36693	28.71267	$<2e^{-16}$
Diel Period - Day	0.00168	0.18491	0.00910	0.9927
Diel Period - Dusk	0.25430	0.27570	0.92239	0.3565
Diel Period - Night	-0.10669	0.19299	-0.55282	0.5805
Month2	-0.13921	0.18262	-0.76226	0.4461
Month3	-0.21414	0.17530	-1.22155	0.2222
Month4	0.10681	0.23552	0.45351	0.6503
Month5	-0.48130	0.21960	-2.19165	0.0286
Month6	-0.83161	0.23317	-3.56648	0.0004
Month7	-0.40127	0.21251	-1.88827	0.0593
Month8	-0.15619	0.19200	-0.81346	0.4161
Month9	-0.44481	0.22323	-1.99267	0.0466
Month10	-0.01940	0.17908	-0.10834	0.9138
Month11	-0.00214	0.18917	-0.01131	0.9910
Month12	-0.32384	0.19575	-1.65439	0.0984
Random Effects				
	Variance		**Standard Deviation**	
Tagged Individual (Intercept)	0.4213		0.6491	

2.4 Discussion

Giant Sea Bass are an ecologically and culturally important species in southern California and Baja California, Mexico. The lack of knowledge about the residency of individuals to certain areas, the seasonality of their movements, and their interaction with existing spatial management measures hinders efforts to understand the extent to which contemporary fishing activities are impacting the species. In this study, we found that some Giant Sea Bass appear to be long term residents of the La Jolla kelp forest, though residency varied among individuals. Tagged fish had the highest probability of traveling between non-proximal receivers during summer spawning months, and tended to spend more time outside of local MPAs during this same time period. Furthermore, even outside of spawning season, when fish were present in the La Jolla array, they tended to spend most of their time outside of the boundaries of local MPAs, particularly in highly trafficked recreational fishing areas.

With the exception of the two fish that left the array within two days of tagging, we found that tagged fish remained in the La Jolla area for extended periods. Two fish were consistently detected for a period of over two and a half years, while three remained in the region between six and nine months following tagging. One fish that left the array after nine months went to the vicinity of the Del Mar receiver, approximately 8 km to the north of the La Jolla array, and remained there consistently for a period of eight months with less consistent detections occurring up to almost a year after arriving at Del Mar. This apparent site fidelity agrees with the findings of previous studies on Giant Sea Bass and similar species. As part of a larger regional multi-species mark-recapture study, Hanan and Curry (2012) recaptured two out of 14 tagged Giant Sea Bass 245 and 1240 days post-tagging, one within 1 to 5 km and the other 5 to 20 km from the tagging locations. Studies on similar large predatory coastal bony fishes, Goliath Grouper (*Epinephelus*

itajara) and Giant Grouper (*Epinephelus lanceolatus*), also found site fidelity across years, in some cases with individuals being resighted in the same location up to four years after the initial record (Eklund and Schull 2001, Giglio et al. 2014, Clua et al. 2015). While our sample size is small, it is possible the large spatial extent of contiguous kelp forest habitat in La Jolla and its ability to support ample prey resources contribute to predominant model of prolonged site fidelity we observed among fish from the area (Parnell et al. 2006, Udy et al. 2019).

There is evidence of variability in site fidelity from previous work, which could account for the fish that left the La Jolla array after spending over half a year there. One of the species' congeners in the Polyprionidae family, the Hāpuku (*Polyprionidae oxygeneios*), showed variable movement patterns during a multi-year mark-recapture study with some being recaptured close to 1400 km from their tagging location and others being recaptured at the same location as tagging (Beentjes and Francis 1999). More recently, Clevenstine and Lowe (2021) used external acoustic tagging to investigate aggregation site fidelity of Giant Sea Bass on Santa Catalina Island. They found that tagged individuals tended to frequent suspected aggregation sites during the summer spawning season, and about a third of tagged individuals returned to the same aggregation site in the subsequent year (Clevenstine and Lowe 2021). They also found that while some individuals remained on the island year round, others traveled to other islands in the Channel Islands or the mainland coast of California (Burns et al. 2020, Clevenstine and Lowe 2021). We did not observe similar long distance movements in our tagged fish. There is a chance that the fish that left the La Jolla array made long excursions; however, we are unable to say for certain, because to date they have not been detected on any of the regional receivers along the southern California coast, in the Channel Islands, or Baja California, Mexico. The variability in movement patterns among individuals could be the result of demographic (e.g. sex, age, reproductive status) differentiation

in movement behavior, resource limitation and/or niche partitioning, or external environmental factors (Hertel et al. 2020). Unfortunately determining the likely cause of the individual variability observed in this and other studies is outside of the scope and scale of our work, but future research should focus on characterizing individual differences in movement behavior in Giant Sea Bass.

The fish we tagged tended to occupy areas outside of MPAs; however, we exclusively captured and tagged Giant Sea Bass outside of MPAs. It is therefore likely the case that this finding reflects strong site fidelity rather than behavioral selection for non-MPA habitat. Most of our tagged fish had the greatest detection rates on receivers near where they were captured, suggesting that they tend to occupy relatively small, defined areas. In addition, tagged fish within the La Jolla array rarely moved between non-proximal receivers. Even the fish that traveled to Del Mar, while fairly active throughout the La Jolla array during its time there, showed remarkably consistent detections (averaging over 60 detections per hour) at the Del Mar receiver for a period of five months, and was not detected at any of the other more coastal receivers just north of the Del Mar receiver. Given the persistent strong site fidelity exhibited by most of our tagged fish, we believe that the MPAs in the La Jolla kelp forest are likely sheltering individuals from contemporary fishing activities in the area in proportion to the amount their ranges overlap with protected habitat.

MPAs as management tools for Giant Sea Bass would likely be most effective if they encompassed spawning aggregation sites. Previous studies show that spatial protections of spawning aggregations can help support recovery from overfishing (Nemeth 2005, Chollett et al. 2020, Waterhouse et al. 2020). While the California MPAs were not implemented with Giant Sea Bass in mind, if their boundaries include spawning aggregation sites they could help support the species' recovery by protecting fish during a critical stage of their life history (Chollett et al. 2020). Our results suggest that there is likely a spawning aggregation in La Jolla—we detected fish year

round and found seasonal differences in movement during the presumed spawning season. Unfortunately, our results also indicate that the aggregation site may be outside of the local MPA boundaries. We found that fish were much more likely to be detected outside of MPAs during summer spawning months, and that they showed significantly higher probabilities of non-zero movement rates between non-proximal receivers during this time period. In particular, fish seemed to be most active in the northwest corner of the array, which coincides with heavily trafficked fishing grounds. Previous characterizations of spawning sites of Giant Sea Bass and similar species suggest that aggregations tend to occur near promontories and in areas with strong currents (Eklund and Schull 2001, Clevenstine and Lowe 2021); these habitat characteristics are descriptive of the northwestern La Jolla kelp forest. The La Jolla submarine canyon runs along the northwest corner of the kelp forest and is home to steep sandstone cliffs and subsurface promontories which contribute to the generation of strong currents close the edge of the kelp forest (Parnell et al. 2005, 2006, 2010). Incidentally, these same currents are responsible for attracting pelagic migratory species (e.g. Yellowtail (*Seriola lalandi*)) that are highly sought after by recreational anglers (Parnell et al. 2010).

While our sample size is small, our results provide insight into the susceptibility of La Jolla Giant Sea Bass to the three major contemporary fishing activities influencing the species: commercial catch in Mexico, incidental commercial catch in the US, and incidental recreational catch. Regarding targeted commercial catch in Mexico, while we do not have evidence of fish tagged in the US crossing the border into Mexican waters, it is not out of the realm of possibility for individuals to travel from the San Diego region to Baja California given records of fish traveling long distances in other studies (Burns et al. 2020, Clevenstine and Lowe 2021). However, based on our findings of generally high levels of regional and local site fidelity, these types of long

distance excursions are not necessarily the norm for Giant Sea Bass, and fish residing in US waters are likely to be well-protected despite the disparity in management between the US and Mexico. Similarly, incidental catch by commercial fisheries in the US does not seem to be a strong threat, at least for Giant Sea Bass in La Jolla. We did not find any evidence that fish travel beyond the scope of the 3 mile nearshore gill and trammel net ban, and the records of long distance movements from other studies indicate that when Giant Sea Bass do traverse beyond the scope of these spatial gear restrictions it is to transit relatively quickly to other coastal areas (Clevenstine and Lowe 2021). Incidental commercial landings of Giant Sea Bass are highest during the spawning months of June and July (Ramirez-Valdez et al. *in press*). It is possible that the bulk of incidental commercial landings occur at spawning aggregation sites located farther offshore or as fish are transiting to spawning aggregation sites on offshore islands, like those found on Santa Catalina Island.

The largest potential fishery-related concern for Giant Sea Bass in La Jolla appears to be incidental catch by recreational fisheries. The area where tagged fish spent most of their time is one of the most highly trafficked recreational fishing areas in San Diego (Parnell et al. 2010). As discussed above, our fish were tagged in this region, so minimally, this finding suggests that fish with ranges predominantly in this fished region are persistently exposed to incidental take. However, because tagging data suggest that this region is also used for regional spawning, the scope of impact could be much larger than just resident fish. While much of the recreational fishing community in San Diego is conscientious of regulations and efforts to support the recovery of Giant Sea Bass, fatalities do occur as a result of incidental catch. Barotrauma can occur when there is rapid change in pressure, such as when a fish is brought to the surface quickly from depth, that results in overexpansion of gases in the body of the fish, especially the swim bladder (Rummer

and Bennett 2005, Parker et al. 2006, Jarvis and Lowe 2008). One of the strongest indicators of post-release survival following barotrauma is the amount of time a fish spends at the surface between catch and release (Jarvis and Lowe 2008, Roach et al. 2011). With a species that regularly reaches over a meter in length and is often interacting with anglers on kayaks or larger chartered fishing vessels with raised decks (Parnell et al. 2010), reducing surface time is especially challenging. In the event a fish is released successfully, there is still a chance delayed mortality can occur if there is excessive damage to the swim bladder or other organs (Parker et al. 2006, Jarvis and Lowe 2008). Furthermore, sublethal effects of catch and release fishing can also negatively impact individuals by decreasing their overall fitness (Cooke and Schramm 2007, Campbell et al. 2010).

The extent to which incidental catch is a problem for Giant Sea Bass specifically is still largely unknown. Incidentally caught fish often go unreported, especially in the case of protected species. Furthermore, there are no estimates of post-release survival for Giant Sea Bass that are incidentally caught and released by recreational fishers. Future studies should attempt to quantify the effects of incidental recreational catch on Giant Sea Bass populations. Nevertheless, this study provides valuable insight that can help guide the recreational fishing community in La Jolla to minimize potential negative impacts of their activities on Giant Sea Bass. Fortunately, there is an understanding of best practices to mitigate the effects of incidental catch, chief among them quickly and efficiently releasing fish back to depth. Given that our results indicate the most likely area for a local spawning aggregation is also frequented by recreational fishers during summer months, there is an increased risk of incidental catch for Giant Sea Bass in the area during this time period. The recreational fishing community should take extra care to avoid incidental catch of Giant Sea Bass during summer months and be prepared to properly handle any individuals that are

caught. Development of tools, such as larger versions of descending devices (e.g. SeaQuilizers) often used with rockfish, can help support efforts to reduce the negative impacts of incidental catch on Giant Sea Bass.

Acknowledgements

We would like to acknowledge the funding sources that contributed to this work: the Mia Tegner Memorial Fellowship, the SIO Center for Marine Biodiversity and Conservation Mentorship Program, the Women Divers Hall of Fame Marine Conservation Scholarship sponsored by the Rachel Morrison Memorial Fund, and the Link Family Foundation (via Dr. Phil Hastings). We would like to acknowledge all of the other regional acoustic telemetry research groups that checked their databases for our tag numbers including Brian Sterling and Chris Lowe from the Lowe Lab at CSULB, Andy Nosal, Ryan Freedman and Pike Spector from the Channel Islands National Marine Sanctuary, and James Ketchum, Marc Aquino Baleytó, Mauricio Hoyos from Pelagios-Kakunjá A.C. in Baja California, Mexico. We thank the Hubbs Sea World Research Institute for allowing us to follow them during their surveys in case they caught a Giant Sea Bass. We would like to thank Phil Zerofski, Chugey Sepulveda, and Noah Ben-Aderet for helping us develop our fishing and tagging protocols. We would also like to acknowledge the *many* volunteer anglers and divers who helped with the field work for this project, especially Rich Walsh, Ross Cooper, Zach Skelton, Erica Jarvis-Mason, Shane Finnerty, Mohammad Sedarat, and Youssef Doss.

Chapter 2, in full, is currently being prepared for submission for publication and is printed here with the permission of co-author Brice X. Semmens. The dissertation author is the primary investigator and author of this paper.

Works Cited

Allen, L. G. 2017. GIANTS! Or… The Return of the Kelp Forest King. Copeia 105:10–13.

Allen, L. G., and A. H. Andrews. 2012. Bomb radiocarbon dating and estimated longevity of Giant Sea Bass (*Stereolepis gigas*). Bulletin, Southern California Academy of Sciences 111:1–14.

Allen, L. G., S. A. Benseman, and M. Couffer. 2019. Baby Giants are found at the heads of submarine canyons. Ecology 100:e02496.

Baldwin, D. S., and A. Keiser. 2008. Giant sea bass, *Stereolepis gigas*. Status of the Fisheries Report, Cal. Dept. Fish Game.

Bates, D., M. Mächler, B. Bolker, and S. Walker. 2015. Fitting Linear Mixed-Effects Models Using lme4. Journal of Statistical Software 67.

Beentjes, M. P., and M. P. Francis. 1999. Movement of hapuku (*Polyprion oxygeneios*) determined from tagging studies. New Zealand Journal of Marine and Freshwater Research 33:1–12.

Blincow, K., P. Bush, S. Heppell, C. McCoy, B. Johnson, C. Pattengill-Semmens, S. Heppell, S. Stevens-McGeever, L. Whaylen, K. Luke, and B. Semmens. 2020. Spatial ecology of Nassau grouper at home reef sites: using acoustic telemetry to track a large, long-lived epinephelid across multiple years (2005-2008). Marine Ecology Progress Series 655:199–214.

Burns, E. S., A. J. Clevenstine, R. K. Logan, and C. G. Lowe. 2020. Evidence of artificial habitat use by a recovering marine predator in southern California. Journal of Fish Biology 97:1857–1860.

Campbell, H. A., M. E. Watts, R. G. Dwyer, and C. E. Franklin. 2012. V-Track: software for analysing and visualising animal movement Detections, acoustic telemetry. Marine and Freshwater Research 63:815–820.

Campbell, M. D., R. Patino, J. Tolan, R. Strauss, and S. L. Diamond. 2010. Sublethal effects of catch-and-release fishing: Measuring capture stress, fish impairment, and predation risk using a condition index. ICES Journal of Marine Science 67:513–521.

Chabot, C. L., H. A. Hawk, and L. G. Allen. 2015. Low contemporary effective population size detected in the Critically Endangered giant sea bass, *Stereolepis gigas*, due to fisheries overexploitation. Fisheries Research 172:71–78.

Chollett, I., M. Priest, S. Fulton, and W. D. Heyman. 2020, January 1. Should we protect extirpated fish spawning aggregation sites? Elsevier Ltd.

Clevenstine, A. J., and C. G. Lowe. 2021. Aggregation site fidelity and movement patterns of the protected marine predator giant sea bass (*Stereolepis gigas*). Environmental Biology of Fishes 104:401–417.

Clua, E., C. Chauvet, J. Mourier, J. M. Werry, and J. E. Randall. 2015. Pattern of movements within a home reef in the Chesterfield Islands (Coral Sea) by the endangered Giant Grouper, *Epinephelus lanceolatus*. Aquatic Living Resources 28:53–58.

Cooke, S. J., and H. L. Schramm. 2007. Catch-and-release science and its application to conservation and management of recreational fisheries. Fisheries Management and Ecology 14:73–79.

Cornish, A. 2004. Stereolepis gigas. Page The IUCN Red List of Threatened Species.

Dayton, P. K., M. J. Tegner, P. B. Edwards, and K. L. Riser. 1998. Sliding baselines, ghosts, and reduced expectations in kelp forest communities. Ecological Applications 8:309–322.

Domeier, M. L. 2001. Giant sea bass. California's living marine resources: a status report. Calif Fish Game, Sacramento:209–211.

Eklund, A.-M., and J. Schull. 2001. A Stepwise Approach to Investigating the Movement Patterns and Habitat Utilization of Goliath Grouper, *Epinephelus itajara*, Using Conventional Tagging, Acoustic Telemetry and Satellite Tracking. Pages 189–216. Springer, Dordrecht.

Erauskin-Extramiana, M., S. Z. Herzka, G. Hinojosa-Arango, and O. Aburto-Oropeza. 2017. An interdisciplinary approach to evaluate the status of large-bodied Serranid fisheries: The case of Magdalena-Almejas Bay lagoon complex, Baja California Sur, Mexico. Ocean & Coastal Management 145:21–34.

Farmer, N. A., and J. S. Ault. 2011. Grouper and snapper movements and habitat use in Dry Tortugas, Florida. Marine Ecology Progress Series 433:169–184.

Giglio, V. J., J. Adelir-Alves, and A. A. Bertoncini. 2014. Using scars to photo-identify the goliath grouper, *Epinephelus itajara*. Marine Biodiversity Records 7.

Guerra, A. S., D. J. Madigan, M. S. Love, and D. J. McCauley. 2018. The worth of giants: The consumptive and non-consumptive use value of the giant sea bass (*Stereolepis gigas*). Aquatic Conservation: Marine and Freshwater Ecosystems 28:296–304.

Hawk, H. A., and L. G. Allen. 2014. Age and growth of the giant sea bass, *Stereolepis gigas*. CalCOFI Report 55:128–134.

Hertel, A. G., P. T. Niemelä, N. J. Dingemanse, and T. Mueller. 2020. A guide for studying among-individual behavioral variation from movement data in the wild. Movement Ecology 2020 8:1 8:1–18.

House, P. H., B. L. F. Clark, and L. G. Allen. 2016. The return of the king of the kelp forest: Distribution, abundance, and biomass of Giant sea bass (*Stereolepis gigas*) off Santa Catalina Island, California, 2014-2015. Bulletin, Southern California Academy of Sciences 115:1–14.

Huveneers, C., C. A. Simpfendorfer, S. Kim, J. M. Semmens, A. J. Hobday, H. Pederson, T. Stieglitz, R. Vallee, D. Webber, M. R. Heupel, V. Peddemors, and R. G. Harcourt. 2015. The influence of environmental parameters on the performance and detection range of acoustic receivers. Fisheries New South Wales.

Jarvis, E. T., and C. G. Lowe. 2008. The effects of barotrauma on the catch-and-release survival of southern California nearshore and shelf rockfish (Scorpaenidae, *Sebastes* spp.). Canadian Journal of Fisheries and Aquatic Sciences 65:1286–1296.

Lowerre-Barbieri, S., D. Villegas-Ríos, S. Walters, J. Bickford, W. Cooper, R. Muller, and A. Trotter. 2014. Spawning site selection and contingent behavior in common snook, *Centropomus undecimalis*. PLoS ONE 9:101809.

Mathies, N., M. Ogburn, G. McFall, and S. Fangman. 2014. Environmental interference factors affecting detection range in acoustic telemetry studies using fixed receiver arrays. Marine Ecology Progress Series 495:27–38.

Nemeth, R. S. 2005. Population characteristics of a recovering US Virgin Islands red hind spawning aggregation following protection. Marine Ecology Progress Series 286:81–97.

Parker, S. J., H. I. McElderry, P. S. Rankin, and R. W. Hannah. 2006. Buoyancy Regulation and Barotrauma in Two Species of Nearshore Rockfish. Transactions of the American Fisheries Society 135:1213–1223.

Parnell, P. E., P. K. Dayton, R. A. Fisher, C. C. Loarie, and R. D. Darrow. 2010. Spatial patterns of fishing effort off San Diego: implications for zonal management and ecosystem function. Ecological Applications 20:2203–2222.

Parnell, P. E., P. K. Dayton, C. E. Lennert-Cody, L. L. Rasmussen, and J. J. Leichter. 2006. Marine Reserve Design: Optimal Size, Habitats, Species Affinities, Diversity, And Ocean Microclimate. Ecological Applications 16:945–962.

Parnell, P., C. E. Lennert-Cody, L. Geelen, L. D. Stanley, and P. K. Dayton. 2005. Effectiveness of a small marine reserve in southern California. Marine Ecology Progress Series 296:39–52.

Pondella, D. J., and L. G. Allen. 2008. The decline and recovery of four predatory fishes from the Southern California Bight. Marine Biology 154:307–313.

R Core Team. 2019. R: A language and environment for statistical computing. R Foundation for Statistical Computing, Vienna, Austria.

Ramirez-Valdez, A., T. J. Rowell, K. E. Dale, M. Craig, L. G. Allen, J. C. Villasenor-Derbez, A. M. Cisneros-Montemayor, A. Hernandez-Velasco, J. Torre, J. Hofmeister, and B. E. Erisman. (n.d.). Asymmetry across international borders: research, fishery and management trends, and economic value of the giant sea bass (*Stereolepis gigas*). Fish and Fisheries.

Roach, J. P., K. C. Hall, and M. K. Broadhurst. 2011. Effects of barotrauma and mitigation methods on released Australian bass *Macquaria novemaculeata*. Journal of Fish Biology 79:1130–1145.

Rummer, J. L., and W. A. Bennett. 2005. Physiological Effects of Swim Bladder Overexpansion and Catastrophic Decompression on Red Snapper. Transactions of the American Fisheries Society 134:1457–1470.

Udy, J. A., S. R. Wing, S. A. O'Connell-Milne, L. M. Durante, R. M. McMullin, S. Kolodzey, and R. D. Frew. 2019. Regional differences in supply of organic matter from kelp forests drive trophodynamics of temperate reef fish. Marine Ecology Progress Series 621:19–32.

Waterhouse, L., S. A. Heppell, C. V. Pattengill-Semmens, C. McCoy, P. Bush, B. C. Johnson, and B. X. Semmens. 2020. Recovery of critically endangered Nassau grouper (*Epinephelus striatus*) in the Cayman Islands following targeted conservation actions. Proceedings of the National Academy of Sciences:201917132.

Chapter 3:

The effect of sea surface temperature on the structure and connectivity of species landings interaction networks in a multispecies recreational fishery.

Kayla M. Blincow, Brice X. Semmens

Abstract

Multispecies fisheries, particularly those that routinely adapt the timing, location, and methods of fishing to prioritize fishery targets, present a challenge to traditional single-species management approaches. Efforts to develop robust management for multispecies fisheries require an understanding of how priorities drive the network of interactions between catch of different species, especially given the added challenges presented by climate change. Using 35 years of landings data from a southern California recreational fishery, we leveraged empirical dynamic modelling methods to construct causal interaction networks among the main species targeted by the fishery. We found strong evidence for dependencies among species landings time series driven by apparent hierarchical catch preference within the fishery. In addition, by parsing the landings time series into anomalously cool, normal, and anomalously warm regimes (the latter reflecting ocean temperatures anticipated by 2040), we found that network complexity was highest during warm periods. Our findings suggest that as ocean temperatures continue to rise, so too will the risk of unintended consequences from single species management in a multispecies fishery.

3.1 Introduction

As the name suggests, a multispecies fishery is a single fishery that targets multiple species. Such fisheries, especially those that readily adapt their fishing strategy to prioritize different species targets, can create complex interactions between species landings that are difficult to account for using traditional single species assessments (Murawski 1991; Vinther et al. 2004; Thorpe et al. 2016). In recent decades, researchers and managers have developed a number of novel modelling techniques and expanded management frameworks to address some of the difficulties that can arise from applying single species tools to multispecies fisheries (e.g. Vinther et al. 2004, Ulrich et al. 2011, Plagányi et al. 2014, Thorpe et al. 2016, Nielsen et al. 2018). Despite these advances, many challenges remain when it comes to multispecies fisheries. One such challenge is the ability to quantify and describe the complex dependencies that can be created between species landings. Moreover, given the influence of climate change on ocean ecosystems, efforts to understand how future ocean conditions will mediate such dependencies is an important part of planning for resilient fisheries.

Climate change presents a formidable challenge across disciplines and sectors globally, impacting everything from crop yields (Campbell et al. 2016; Kukal and Irmak 2018), to the frequency of disease outbreaks (Wu et al. 2016; Caminade et al. 2019), to fisheries yields (Weatherdon et al. 2016; Free et al. 2019). The impact of climate change on social-ecological systems, or systems in which humans and nature interact (e.g., fisheries), can be especially difficult to predict as they constitute a complex network of social, environmental, and economic interactions (Folke 2006; Miller et al. 2010; Garmestani et al. 2019). Yet, understanding and predicting climate induced shifts in social-ecological systems, including fisheries, is a critical part of efforts to maintain productivity and protect livelihoods.

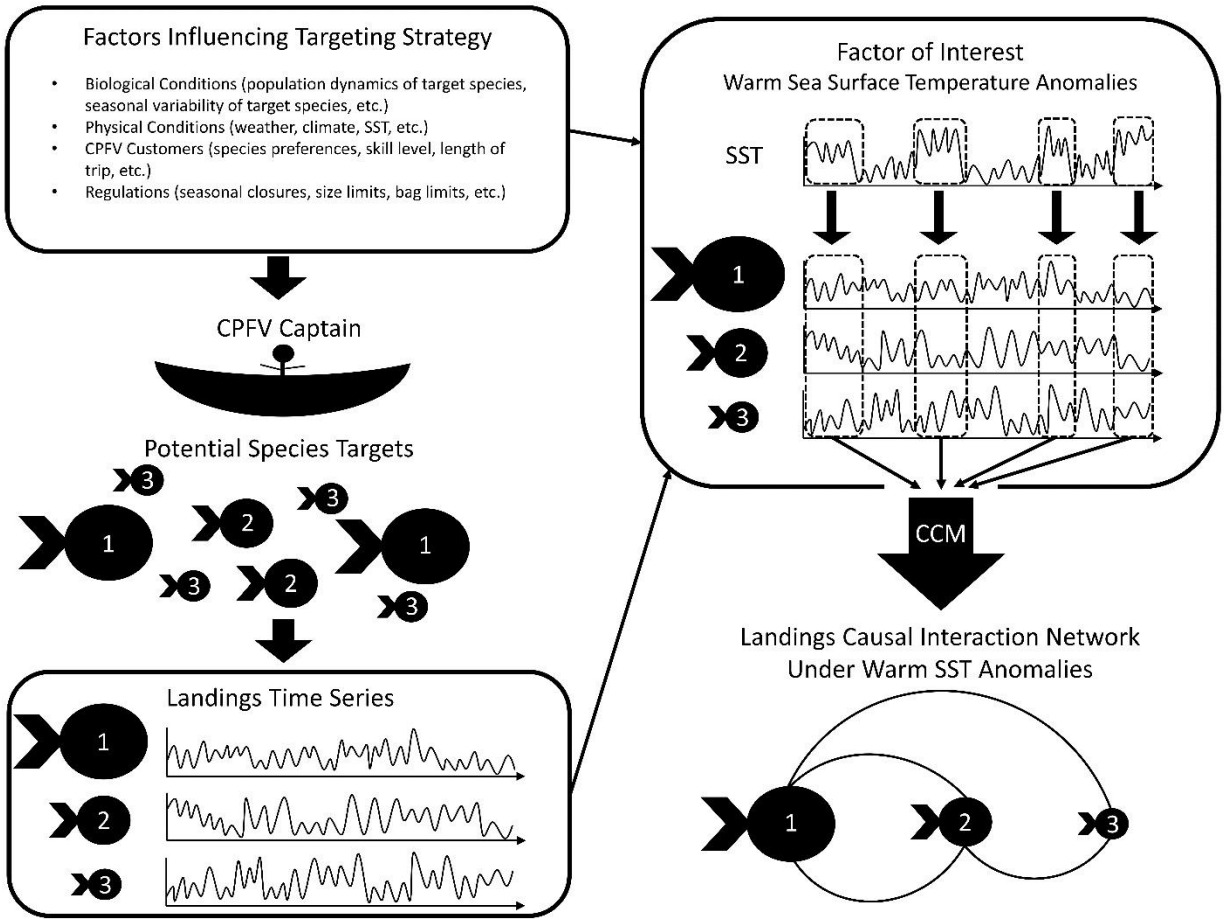

Figure 3.1. Visualization of the conceptual framework of our analysis. Landings time series from a fishery are the result of a combination of interacting factors which influence how CPFV captains choose to target different species. These factors can be environmental, social, or regulatory. To identify how a specific factor, warm SST, influences the causal interaction network of species landings, we filtered our landings time series based on that factor of interest. We then used convergent cross mapping to identify causal relationships between those filtered species landings and construct the interaction network. By comparing interaction networks under different SST conditions, we can gain insight into how SST influences the underlying landings connectivity in this fishery.

One of the hallmark effects of anthropogenic climate change is a global increase in sea surface temperature (SST) (Rayner et al. 2003; Weatherdon et al. 2016). In this study we used catch data from a multispecies fishery to construct causal networks of species landings under different SST conditions to better understand differences in landings network structure and complexity under different ocean temperature scenarios. A visual representation of the conceptual framework of our

analysis is provided in Figure 3.1. The basis of our approach lies in the understanding that by identifying relationships between the landings of different species targeted by the same fishery, we can gain insight into the extent to which shifts in the landings of one species can influence the landings of other species. We can compile these relationships to build networks of causal interactions between landings of species targeted by the same fishery. This is useful, because fisheries landings data are a representation of all of the upstream processes that influence species-specific catch including, but not limited to, fisher preference, regulations, population dynamics, and environmental variability. By grouping landings based on an upstream process of interest, regional SST in our case, it is possible to see how that process influences the causal landings network, which in turn provides insight into the responses of the fishery as a whole to that process. If the underlying landings network responds to regional SST changes by becoming more complex and connected, processes that influence the landings of a single species, such as regulatory changes, are more likely to have unintended effects on other species targeted by the same fishery.

To identify causal relationships between landings time series we employed empirical dynamic modelling (EDM), a nonlinear time series analysis method. This approach draws from Takens' theorem, which posits that you can reconstruct the manifold of a chaotic dynamical system by lagging a time series of a variable from that system across the appropriate dimensions (Takens 1981; Deyle and Sugihara 2011). Convergent cross mapping (CCM) uses this theorem as a basis to test for causal relationships between variables from the same system by determining the extent to which the time series of one variable can estimate states of the other (Sugihara et al. 2012). By applying CCM to catch time series, we were able to explicitly describe the underlying structure of a multispecies fishery by constructing networks of causal interactions between the landings of different fishery species.

We chose to investigate the southern California Commercial Passenger Fishing Vessel (CPFV) fishery as our case study. This is a multispecies recreational fishery that constitutes an important part of the economy and culture of southern California (Weber and Heneman 2000; Schroeder and Love 2002; Jarvis et al. 2004; Bellquist and Semmens 2016; Bellquist et al. 2017). It is important to note that since this is a recreational fishery and fishers are not selling their catch, the relative perceived value (hereafter referred to as "value") of different species is based on the collective preferences of the recreational angling community. The CPFV fleet is made up of charter sport fishing vessels which typically take groups of 30-50 anglers on fishing trips in the inshore and offshore waters of southern California and northern Baja California, Mexico (Parnell et al. 2010; Bellquist et al. 2017). CPFV captains take into account the desires and skill level of their patrons, environmental variables, and sport fishing regulations to decide which species are the best targets for any given trip. As a consequence of these decisions, species that are not necessarily biologically or ecologically connected become linked through their fishery landings. For example, the seasonal emergence of warm water species in summer months and regulation changes limiting harvest of one or more species have resulted in shifting species targets and ultimately, shifts in landings (Dotson & Charter 2003, Bellquist & Semmens 2016). It seems reasonable to conjecture that climate driven shifts in SST would similarly reorganize the landings interaction network of the southern California CPFV fishery.

California's Fourth Climate Change Assessment states that, based on climate model predictions, SST in the region of our case study will increase ~0.5 to 1.5˚C by 2040 and 2 to 4˚C by 2100 (Sievanen et al. 2018). CPFVs are known to show seasonal variation in species landings, in part due to changes in SST that mediate the presence of transient, often high value species, such as Tuna spp. (Dotson and Charter 2003; Parnell et al. 2010). However, it is less clear how sustained

(cross season) SST changes resulting from climate change will influence the interactions between species landings. To isolate how the complexity of such landings interaction networks might change under different SST regimes, we built our networks after first grouping the landings time series into cool, normal, and warm regimes based on past regional SST anomalies. We reasoned that the dynamics present during anomalously warm periods, in particular, would provide insight into what we might expect from future CPFV species landings interactions given climate change. The networks we created inherently account for the complex dynamics associated with management action, fisher behavior, environmental variability, and every other factor influencing the fishery, because they rely on landings data that are influenced by all of these things. Using these species landings networks, we identified and highlighted potential challenges to the resilience and management of the southern California CPFV fishery.

3.2 Methods

Data

We used California Department of Fish and Wildlife (CDFW) CPFV logbook data for this analysis. These data constitute daily trip records from CPFVs, including information on the date of fishing, trip length, port code or town of landing, and the CDFW fishing blocks fished (10-minute latitude by 10-minute longitude). Landings are recorded as the number of fish kept by species per trip. It should be noted that the logbook data do not necessarily represent a census of landings from the CPFV fishery due to log non-compliance by captains; however, logbook landings are consistent with other catch reports from this fishery, including reports to newspapers for advertising purposes, and the logbook data are frequently used as the primary source of data

for investigating trends in the CPFV fishery (Hill and Barnes 1998; Dotson and Charter 2003; Bellquist et al. 2017). While CPFV logbook data were available from 1980 to 2017, to perform our analysis it was necessary to limit our time series to the extent of our available SST data (1983-2017).

The species frequently targeted by CPFVs vary across the California coast (Dotson and Charter 2003). To account for this, we filtered the logbook data based on regional classifications of the CPFV fleet made in Dotson and Charter (2003) to only include ports south of San Clemente (Zone A). By limiting our analysis to this region, we were able to limit the number of species groups targeted by the fleet. Based on our region of interest, we selected six species and species complexes for our analysis: Rockfish spp. (*Sebastes sp.*, Sebastidae), Kelp Bass (*Paralabrax clathratus*, Serranidae), Barred Sand Bass (*Paralabrax nebulifer*, Serranidae), Yellowtail (*Seriola lalandi*, Carangidae), Pacific Bonito (*Sarda leniolata*, Scombridae), and Tuna spp. (*Thunnus sp.*, Scombridae). We selected Barred Sand Bass and Kelp Bass because they are the most important recreational species in the region based on the number of fish taken and the relative importance placed on them by the CPFV fleet (Dotson and Charter 2003; Jarvis et al. 2014; Bellquist et al. 2017). Pacific Bonito and Rockfish spp. account for the second and third largest percentages of total landings respectively, after bass species (Dotson and Charter 2003). We selected Tuna spp. and Yellowtail because, based on weight, they are among the largest recreational harvests in California, and are especially important in the southern-most region (Dotson and Charter 2003). For the Rockfish group, we compiled the landings of all *Sebastes* sp. represented in the data. For the Tuna group, we compiled landings of the three most commonly caught Tuna species in southern California: Albacore (*Thunnus alalunga*, Scombridae), Yellowfin Tuna (*Thunnus albacares*, Scombridae), and Pacific Bluefin Tuna (*Thunnus orientalis*, Scombridae).

Different vessels in the CPFV fleet have different strategies for targeting fish (Bellquist et al. 2017). Some vessels only target high value species typically found farther offshore, while others exclusively fish nearshore (Bellquist et al. 2017). To avoid potential biases associated with different targeting strategies, we filtered the data to include only those vessels that interact with the full suite of species groups we identified by targeting both nearshore and offshore species. To identify which vessels targeted both nearshore and offshore species we determined the top 10 most-landed species for each vessel and evaluated them for the presence of our species groups. We then determined whether nearshore and offshore CDFW fishing blocks accounted for the bulk of each vessel's landings to confirm that the vessel was interacting with areas associated with each of our species groups. Nearshore fishing blocks included all blocks that touched the mainland coast. With the exception of the blocks along the coast of offshore islands, the rest of the fishing blocks were classified as offshore. We evaluated vessels that frequently targeted fishing blocks associated with offshore islands on a case by case basis as captains will often opportunistically target high value offshore species while transiting to the islands to target more nearshore associated species. If a vessel did not chiefly target members of our species groups, solely targeted nearshore, or solely targeted offshore fishing blocks, we did not include them in the analysis. This resulted in a total of 270 vessels out of a possible 428 from our selected region. After selecting vessels, we summed the landings of our six species groups from these vessels and created a daily landings time series for each group spanning from 1983 to 2017 (Figure 3.2). For the species complexes, Rockfish spp. and Tuna spp., we pooled the landings for the species included in those groups (group composition specified above). For the construction of the interaction networks, we limited our time series to the main fishing season of March through October. Note that our EDM analysis methods are robust to time gaps (described below).

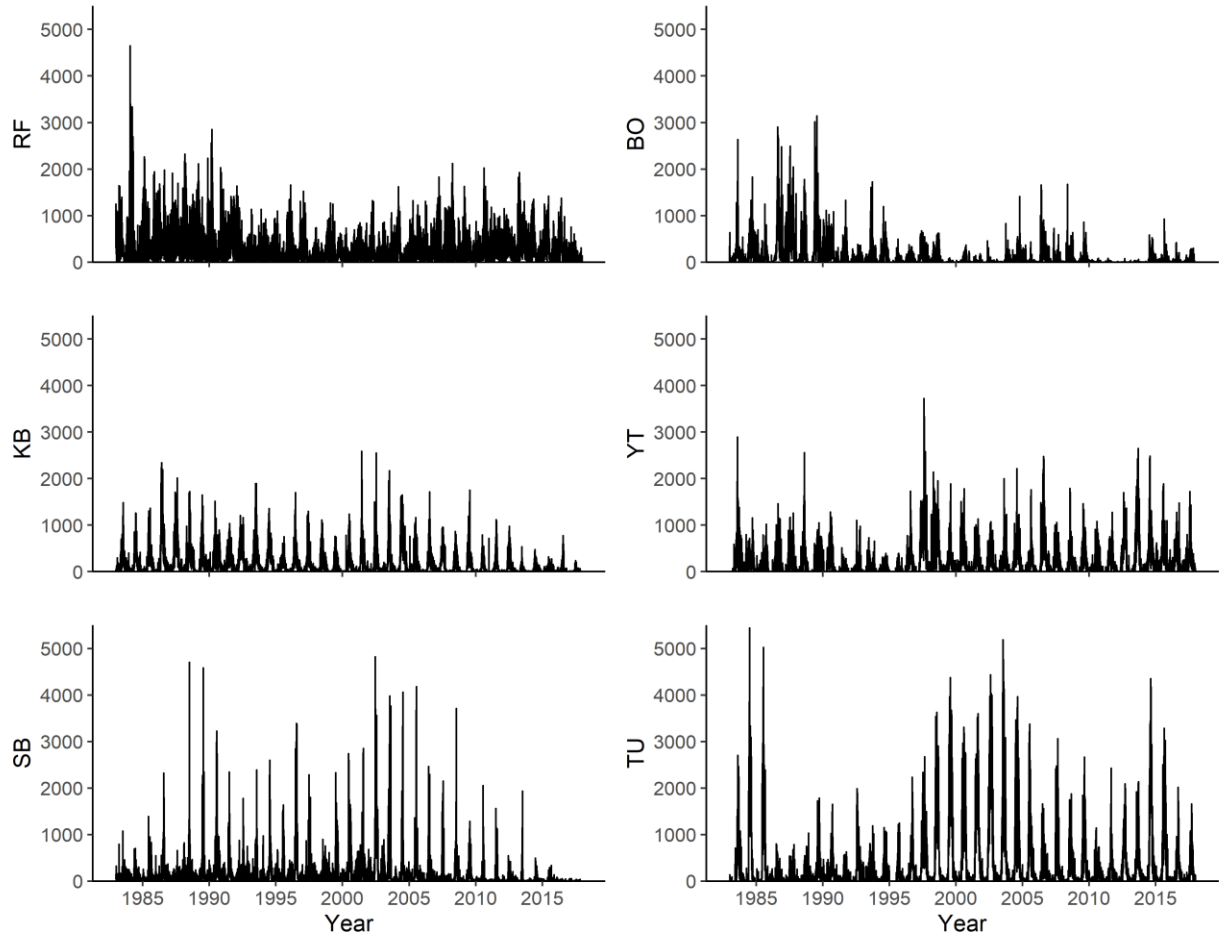

Figure 3.2. Landings time series (1983 – 2017) for each species group: RF = Rockfish spp., KB = Kelp Bass, SB = Barred Sand Bass, BO = Pacific Bonito, YT = Yellowtail, TU = Tuna spp.

We used the National Oceanic and Atmospheric Administration's (NOAA) Optimum Interpolation Sea Surface Temperature (OISST) data to classify the years in the CPFV landings time series based on SST. These data interpolate observations from satellites, ships, buoys, and Argo floats to create a map of daily SST at a resolution of 1/4°, and were provided by the NOAA/Ocean and Atmospheric Research/Earth System Research Laboratories Physical Sciences Laboratory (NOAA/OAR/ESRL PSL), Boulder, Colorado, USA from their website at https://psl.noaa.gov/ (Reynolds et al. 2007). For this analysis, we selected SST data from a grid of

the Southern California Bight ranging from Point Conception, California, USA to Punta Colonet, Baja California, Mexico. We classified each year from our time series as “anomalously warm”, “anomalously cool”, or “normal”. To do so, we first removed seasonal temperature effects by standardizing our SST data by calculating monthly temperature anomalies, such that the mean and standard deviation of SST for each month was 0 and 1, respectively. We then calculated a three month rolling mean of the daily SST anomalies across the temperature time series. We classified any year that had a three month rolling mean that exceeded one standard deviation from the mean at any point during the year as “anomalously warm” in the positive direction and “anomalously cool” in the negative direction (Figure 3.3). We classified the remaining years as “normal”. We explored other SST classification methods, such as classifying years based on recorded El Nino Southern Oscillation (ENSO) events, and found that our results were generally robust to different methods of classification. We ultimately chose to classify years using the methods described, because they more accurately represented regional SST anomalies in our southern California study area than other commonly used classifications.

We performed all analyses using R statistical software, version 3.6.1 (R Core Team 2019). The code for our analyses can be found at https://github.com/kmblincow/CPFVs_CCMandSST.

Convergent Cross Mapping

We tested for causal relationships between the landings of each of our species groups using CCM. CCM is a non-parametric method for identifying causal relationships in nonlinear dynamic systems (Sugihara et al. 2012). Given two time series, X and Y, CCM tests for causation by determining the extent to which the historical record of the values of Y, the predictor variable, can reliably estimate corresponding time points of X, the target variable (Sugihara et al. 2012). If X causally influences Y, it is possible to reconstruct system states of X from Y, because Y is

inherently dependent on the dynamics of X (Sugihara et al. 2012; Ye et al. 2015). It is important to note that causal networks built from multiple time series can be transitive; if X causes Y and Y causes Z, it follows that X and Z will also display a causal relationship (Sugihara et al. 2012). CCM detects these types of transitive causal relationships as well. For a more in depth explanation and discussion of how CCM is able to distinguish causal relationships from correlative ones, see Sugihara et al. (2012).

We used the rEDM package (version 0.7.5) to carry out our CCM analyses (Ye et al. 2021). After classifying each year based on SST, we subset and grouped the species landings time series based on these classifications. We performed CCM on every possible pairing of our species groups using daily landings time series from the main fishing season for all the years within each SST classification. CCM allows for specification of non-consecutive time series when constructing manifolds, allowing us to build networks representing the main fishing season for all the years in each SST classification despite the fact they did not constitute a continuous time series. To lower computing time, we scaled our time series such that the landings ranged from 0 to 1 by dividing each observation by the maximum landings observation. For each cross map we used Simplex projection to identify the optimal embedding dimension, and tested for non-linearity using S-map forecasting (Sugihara et al. 2012). We used Pearson's correlation coefficient (ρ) to measure relative cross map strength, or the relative strength of the causal effect between the two cross-mapped landings time series (Sugihara et al. 2012).

Due to the seasonal nature of the landings time series, it is critical to distinguish between seasonal correlation effects and true causal effects. To test the significance of the causal relationships we observed, we used a seasonal surrogate test (Deyle et al. 2016). To perform this test, we cross mapped every predictor time series (each species landings time series within each

SST classification) against 500 surrogate time series that preserved the seasonality of the original target time series but with randomized anomalies by computing the mean seasonal trend over the specified time period then shuffling the residuals. If the cross-map prediction was greater than the 95^{th} percentile for the true target time series than the surrogate time series ($p < 0.05$), then we concluded that there was a causal interaction between the two landings time series in question. We subsequently constructed interaction networks between species landings for each SST classification based on the relationships we identified as significant.

Network Analysis

Networks are often visualized using nodes (depictions of unit of interest) and edges (visualizations of the relationship connecting the nodes) (Proulx et al. 2005). In our case our nodes are our landings time series for each species group and our edges are the causal relationships we found between the landings time series using CCM. Networks can also be directed or undirected (Proulx et al. 2005). A directed network has edges which incorporate directionality depicting which node is influencing the other in any given relationship in the network (Proulx et al. 2005). Our network is directed, because our causal relationships display directionality. Additionally, network edges can be weighted, meaning the relationships between nodes can carry some value (Opsahl et al. 2010). In our case, our edges are weighted by the strength of the causal relationship detected by the CCM analysis (ρ). There are mathematical tools and techniques (i.e. network analysis tools) that are used to describe the structure and connectivity of relationships between the nodes and edges of a network (Proulx et al. 2005).

We used two network analysis metrics, network density and degree centrality, to quantitatively characterize the structure of the interaction networks that resulted from the CCM analysis. Network density is the ratio of the number of direct connections in a network to the total

number of direct connections possible, and indicates the overall complexity of causal interactions in the network. Degree centrality is a metric that classifies nodes of a network based on how connected they are relative to other nodes. High degree centrality indicates greater connectivity of a node, or network, when considering centrality of all nodes. As a result, networks with higher overall degree centrality are generally more complex. We used the degree centrality metric for directed and weighted networks put forth in Opsahl (2010), which accounts for the number of connections (i.e. edges) a node has, as well as the weights associated with those connections (in our case the strength of the causal interaction):

(1) $$C_{D-in}^{w\alpha}(i) = k_i^{in} \times \left(\frac{s_i^{in}}{k_i^{in}}\right)^{\alpha}$$

(2) $$C_{D-out}^{w\alpha}(i) = k_i^{out} \times \left(\frac{s_i^{out}}{k_i^{out}}\right)^{\alpha}$$

Where degree centrality in (Equation 1) or out (Equation 2) of a node (i) is $C_D^{w\alpha}$, k_i is the number of edges in or out of node (i), s_i is the total weight of the edges in or out of node (i), and α is a tuning parameter which denotes the relative influence of k and s. We set α to 0.5, which gives equal weight to the number and weight of edges at a node (Opsahl et al. 2010).

3.3 Results

Based on our standardization of monthly SST anomalies, we classified 11 years as anomalously cool, nine years as anomalously warm, and 15 years as normal (Figure 3.3). Each SST classification was comprised of years spread throughout the time series.

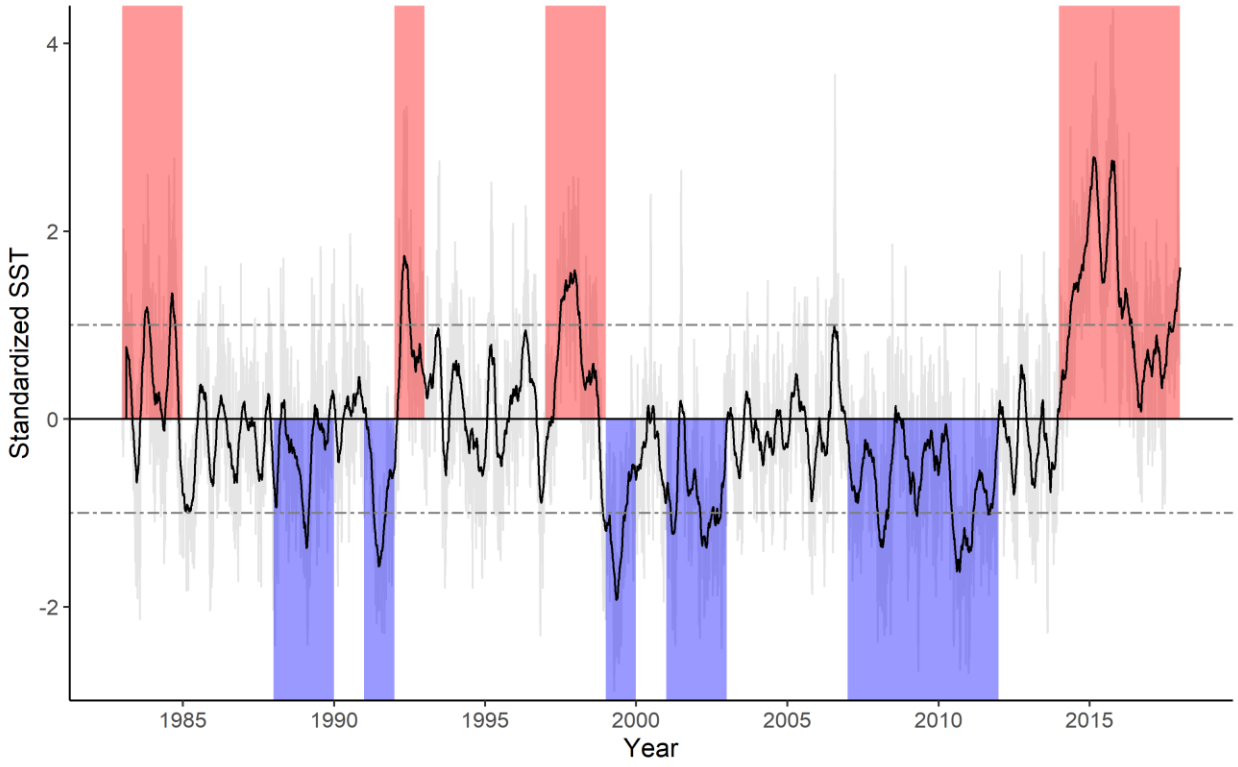

Figure 3.3. SST time series (1983 – 2017) standardized to depict monthly anomalies. Light gray lines depict the daily SST monthly anomalies. The solid black line depicts the three month rolling mean of the daily SST monthly anomalies. The dashed horizontal lines depict one standard deviation above and below the mean. We classified years as anomalously cool if the three month rolling mean exceeded one standard deviation below the mean at any point during the year (marked with blue rectangles), and as anomalously warm if the three month rolling mean exceeded one standard deviation above the mean (marked with red rectangles). All other years are classified as normal.

We found significant causal interactions between species landings under each SST classification ($p < 0.05$). Often these were bi-directional interactions, in which the two species landings causally influenced each other. The interaction networks varied in structure and strength of connections under each SST classification, and increased in complexity with increasing temperature (Figure 3.4). Many of the relationships we found are likely a result of transitive causation (X causes Y, Y causes Z, therefore X also causes Z) (Sugihara et al. 2012), making it difficult to disentangle each species to species relationship.

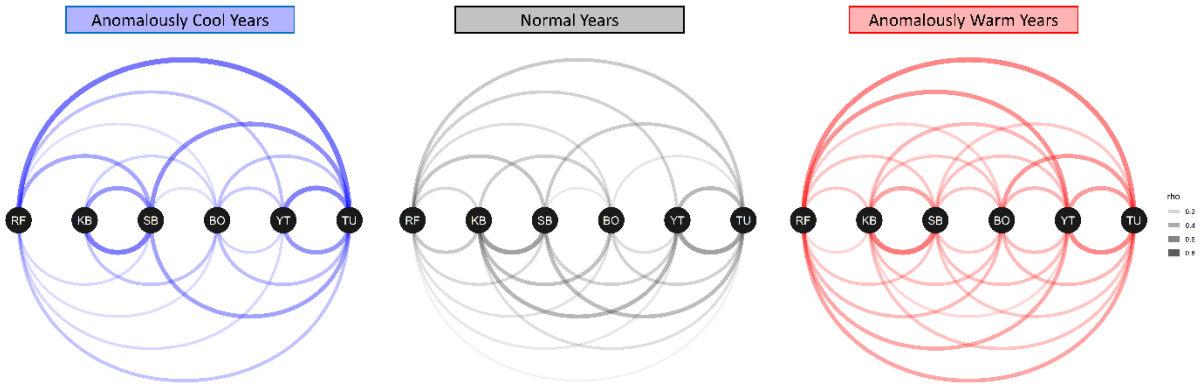

Figure 3.4. Species landings interaction networks for each SST classification. The network for anomalously cool years is shown in blue, the network for normal years is shown in gray, and the network for anomalously warm years is shown in red. For all networks the black circles (nodes) denote the species groups: RF = Rockfish spp., KB = Kelp Bass, SB = Barred Sand Bass, BO = Pacific Bonito, YT = Yellowtail, TU = Tuna spp. The direction and strength of the causal interaction between landings of species groups is shown by the lines connecting the species nodes. Links above the central plane of the nodes indicate causal relationships going from left to right, while links below the central plane denote causal relationships from right to left. The width and transparency of the link indicates the strength of the causal interaction, measured by Pearson's correlation coefficient (rho).

The anomalously warm network had the highest density (0.967), followed by the normal (0.800), and then the anomalously cool networks (0.700). The degree centrality of the nodes varied between the different SST classifications (Figure 3.5). The anomalously warm network showed the highest degree centrality overall with all outgoing and incoming nodes having a degree centrality greater than 2.0 (Figure 3.5). The spread of the degree centrality across nodes was greatest for the anomalously cool (1.08 – 2.61, 1.85 ± 0.45; Range, Mean ± SD) and normal networks (1.00 – 2.71, 1.93 ± 0.56), showing higher variability in the connectedness of nodes than the anomalously warm network (2.04 – 2.92, 2.60 ± 0.22).

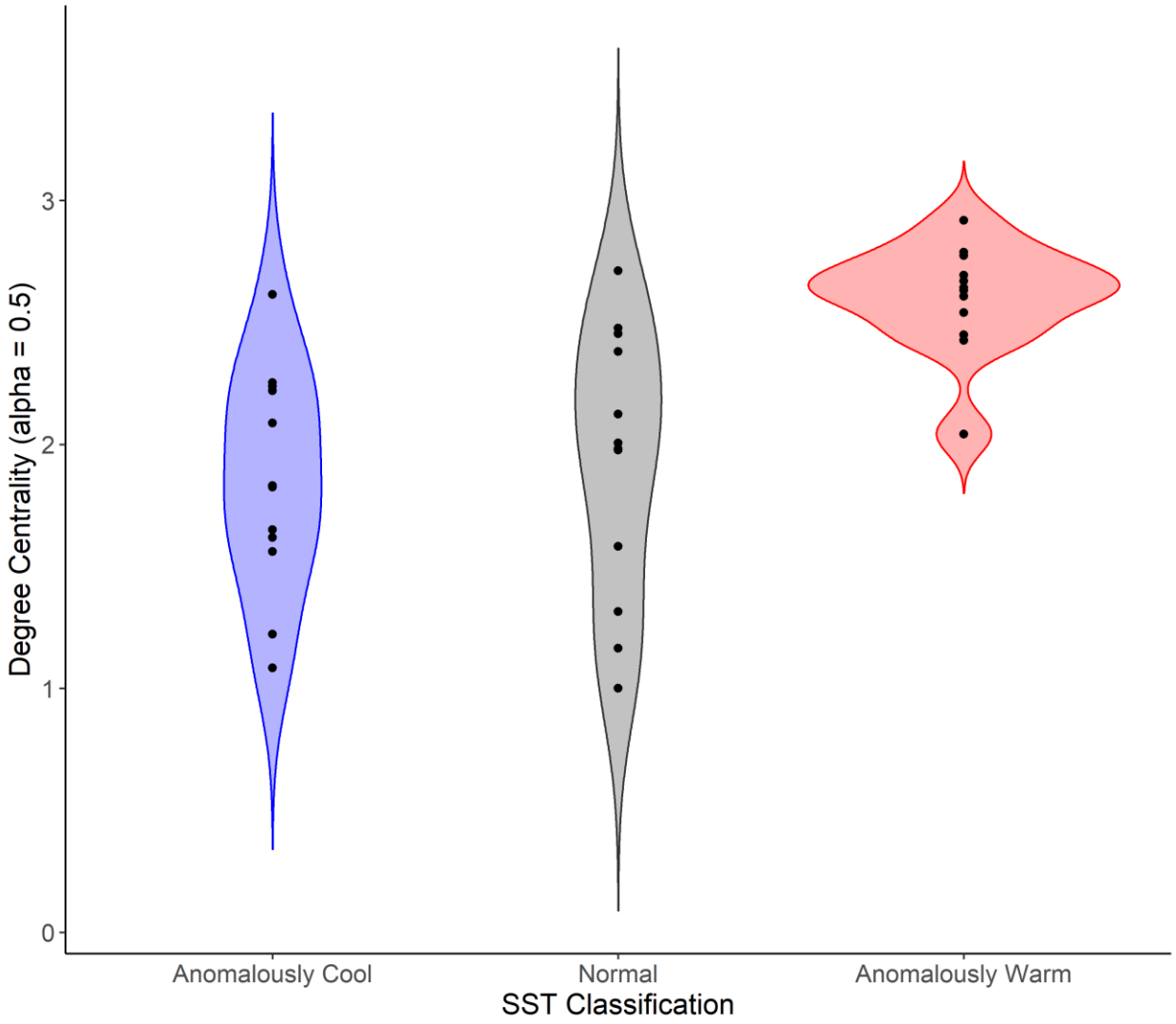

Figure 3.5. Violin plot showing the distribution of the degree centrality of all incoming and outgoing nodes in the networks for each of the SST classifications, where the width of the violin corresponds to the distribution of degree centrality values of all nodes. Raw degree centrality values are shown by the black points.

We found that the proportions of total landings made up by each species group varied between SST classifications (Figure 3.6). Yellowtail and Tuna spp. made up a larger proportion of total landings with increased SST. Others made up a larger proportion of total landings with decreased SST, such as Rockfish spp.

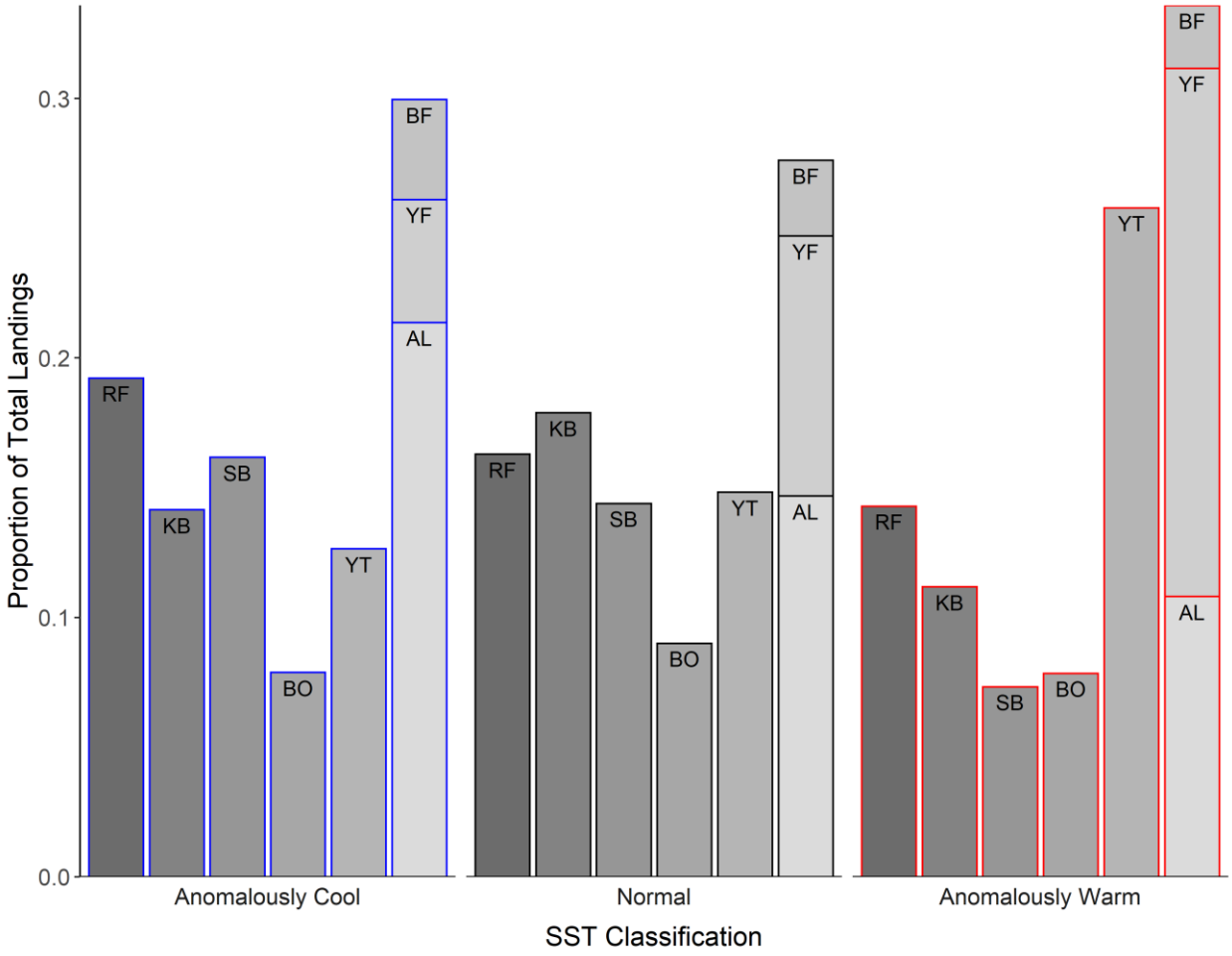

Figure 3.6. Proportion of total landings made up by each species group for the different SST classifications for years across the time series (1983 – 2017). Species groups are shown by different shades of gray: RF = Rockfish spp., KB = Kelp Bass, SB = Barred Sand Bass, BO = Pacific Bonito, YT = Yellowtail. The tuna group is split into a stacked bar of the three species comprising the species group: AL = Albacore, YF = Yellowfin Tuna, BF = Bluefin Tuna.

3.4 Discussion

Multispecies fisheries constitute complex social-ecological systems that can be difficult to manage, especially given the added challenges associated with climate change. Climate change is causing the world's oceans to warm, and predictions suggest that marine environments will experience a greater frequency of warm SST anomalies in the future (Cai et al. 2014, 2015;

Sievanen et al. 2018). This warming impacts fisheries, but the extent and nature of these impacts is not well understood, particularly within multispecies fisheries (Perry et al. 2010; Pörtner and Peck 2010; Cheung et al. 2013; Weatherdon et al. 2016). We used a retrospective analysis to describe underlying causal interaction networks of species landings in a multispecies fishery under different SST scenarios. While many of the individual relationships we found could be deduced based on anecdotal knowledge of our case study fishery, others were more difficult to account for, likely due to being a result of transitive causation. The focus of our study was to use CCM to quantify the structure of the entire network as a function of SST, allowing us to draw conclusions about how the system, as a whole, responds to warming. It is important to note that our "system" is limited to the vessels which we selected for in the CPFV fleet, namely those southern California vessels which target the full suite of our species of interest. Vessels that choose to solely target nearshore or solely target offshore species are likely subject to different underlying landings network conditions. We found causal dependencies between species landings under all SST scenarios, but warmer temperatures were associated with more connected causal interaction networks as shown by higher network density and degree centrality values. Notably, the anomalously warm SST conditions from our analysis mirror regional climate model predictions for the year 2040 (increase of ~0.5 to 1.5˚C) (Sievanen et al. 2018). The increased connectivity of the species landing interaction network under future warm SST conditions will likely increase the risk of unintended consequences from single species management, as changing the landings of one species will have stronger and more complex cascading effects throughout the landings network. Robust fisheries management in a future warm ocean thus demands the continued development of tools which can account for multispecies interactions.

Studies investigating the response of fisheries to climate change tend to focus on the biological system rather than the human dimensions (Field and Francis 2006; Haynie and Pfeiffer 2012). In this study, we chose to use landings data as the basis of our CCM networks, because these data implicitly capture both the ecological dynamics of this fishery and the economic, institutional, and management dynamics. This is especially important in the CPFV social-ecological system, because the multispecies nature of this fishery creates linkages between species that would not otherwise be connected in a purely ecological context (Dotson and Charter 2003). For example, we found significant causal interactions between Rockfish spp. and Tuna spp. under every SST scenario. These species occupy different habitats, have different life history strategies, and would only interact in the natural environment under the rarest of circumstances. Nevertheless, their landings are linked because they are targeted by the same fishery. One strength of CCM is that it does not necessitate parsing apart the myriad potential drivers of the dynamics of CPFV landings (Sugihara et al. 2012). Because this method allows the data as a whole to direct the results, the networks we constructed are inherently influenced by all the factors that influence the landings themselves.

By splitting our time series based on SST anomalies, we were able to isolate how temperature influences this system, while still allowing for the other socio-ecological dynamics to operate. One concern with this approach is that filtering our data by SST could be confounded by other major shifts in the system, such as technological advances, that occur at the same time, which would result in our spuriously attributing the changes we saw to SST when in fact they were the result of unknown drivers. This is unlikely in our analysis, because the years included in each of the SST classifications are dispersed throughout the landings time series and there are no coincident major shifts in the management, environment, or functioning of the CPFV fishery that

occurred across all of the years represented in each of the SST scenarios. For example, in 2013 CDFW enacted new regulations on the bass species complex (*Paralabrax sp.*) which raised the size limit from 12 to 14 inches and reduced the bag limit from 10 to 5 individuals (California Code of Regulations Title 14, Section 28.30). While our time series encompasses these changes in regulation, they did not influence our SST network comparisons, because our SST classifications include sufficient time periods before and after these changes.

Based on knowledge of the fishery, we believe that an underlying hierarchical valuation of species targeted by the CPFV fleet is driving the dependencies we observed in our networks. Generally, pelagic species like Tuna spp. and Yellowtail are more highly valued by the recreational community than other commonly encountered nearshore species such as Rockfish spp. (Dotson and Charter 2003; Parnell et al. 2010). Despite the fact that nearshore species are generally more consistent targets, CPFV captains will often opt to invest resources in traveling farther if there are reports of Tuna or Yellowtail, especially off San Diego in southern California (Dotson and Charter 2003; Parnell et al. 2010). During anomalously warm years higher value species such as Yellowtail become more prevalent (Dotson & Charter 2003). We believe this increased presence of highly valued species accounts for the more complex landings network constructed from anomalously warm years (as shown by the physical structure of the network, higher network density, and higher degree centrality values), because CPFV captains are more regularly making the choice to target these species over more consistent nearshore targets. Anomalously cool and normal years likely have less complex networks, because only a subset of the species groups are readily available. This assertion is further reinforced by the greater proportion of landings made up by high value, transient species in anomalously warm years. Our analysis quantitatively confirms anecdotal and

previously published evidence of the hierarchy of target species among southern California CPFVs (Dotson and Charter 2003; Parnell et al. 2010; Bellquist et al. 2017).

One major concern in predicting fishery responses to climate change is determining the ability of fishery systems to adapt to the unforeseen consequences of a changing ocean (Perry et al. 2010; Chavez et al. 2017; Fuller et al. 2017). Social-ecological resilience can be defined as the ability of a social-ecological system to withstand disturbances while preserving the same basic function (Folke 2006; Craig 2017; Garmestani et al. 2019). The less adaptable a fishery system is, the more vulnerable it is thought to be to perturbation, and therefore the less resilient it is (Chavez et al. 2017; Fuller et al. 2017; Gaines et al. 2018). By explicitly describing the underlying structure of species landings networks under different SST scenarios, our analysis provides an avenue for assessing the resilience of the CPFV fleet to warming ocean conditions. The marked differences in network density and degree centrality between the different SST networks suggests that the CPFV vessels we studied are well-equipped to adapt to changing conditions brought on by different SST scenarios. The structural differences in landings networks we observed are likely due to the fact that the CPFV fishery is able to readily adjust to changes in species availability brought on by SST changes. Indeed, the CPFV fleet has a long history of proving themselves adaptable to system disturbances (Dotson and Charter 2003). This is in large part due to the flexibility in target species afforded to CPFVs; they are able to alter their target strategy relatively quickly in response to system changes. For example, in 2001, in apparent response to regulations limiting the catch of Rockfish spp., the fleet began targeting alternative species like Sanddab (*Citharichthys sp.*, Paralichthyidae) (Dotson and Charter 2003). Given the perseverance captains have shown in the past, and our demonstration that the underlying species landings network can

and will shift under different SST conditions, it is likely the southern California CPFVs can rise to the challenges posed by climate change.

It is difficult to make broad generalizations about the effect of warming SST and climate change on multispecies fisheries; however, our analysis demonstrates that quantifying causal interactions between species landings can be a helpful tool in characterizing fishery-level responses to climate change. A key determinant of changes in network structure and connectivity in our case study was the increased presence of high value transient species during anomalously warm years. Numerous studies have documented fishery species range shifts driven by climate change (e.g. Booth, Bond, & Macreadie, 2011; Gaines et al., 2018; Rogers et al., 2019). Many other multispecies fisheries target species whose presence are mediated by factors affected by climate change, and it is likely that many will experience landings network reorganization in the future as a result. Our findings suggest that the nature of the reorganization will be fishery dependent, based on species-level responses to climate impacts, the underlying preference structure for target species, and the ability of the fishery to adapt to changing conditions. Gaining an understanding of the structure of species landings networks and how the dependencies therein change as a function of climate impacts provides valuable insight into the often unseen interactions in multispecies fisheries that can influence the effectiveness of fisheries management measures.

The CPFV fleet is an important part of the economy, ecosystem, and culture of the southern California region (Schroeder and Love 2002; Dotson and Charter 2003; Jarvis et al. 2004; Bellquist and Semmens 2016). While not comprehensive in its analysis of the potential impacts of climate change, this study provides some guidance as to what can be expected as the CPFV fishery confronts the challenges of a warming ocean. We have shown that years with anomalously warm SST akin to what we can expect as a result of near-term climate change are characterized by more

complex and connected networks of species landings. Increased dependencies between species landings are ill-suited for single species management, because management actions meant to regulate the landings of one species can have unforeseen impacts on the landings of other species throughout the network. To support the continued success of the southern California CPFV fleet and multispecies fisheries more broadly in the face of a warming ocean, management agencies need to continue making strides toward implementing multispecies and ecosystem-based approaches.

Acknowledgements

We would like to thank CDFW for providing access to the CPFV logbook dataset, and for providing valuable feedback on this manuscript before submission. We would like to thank NOAA/OAR/ESRL PSL for providing open access SST data. We would also like to acknowledge Chase James, Erica Mason, Noah Ben-Aderet, and Lyall Bellquist for providing insight, critical comments, and suggestions during the analysis and manuscript development process.

Chapter 3, in full, has been submitted for publication and is printed here with the permission of co-author Brice X. Semmens. The dissertation author is the primary investigator and author of this paper.

Works Cited

Bellquist, L., Semmens, B., Stohs, S., and Siddall, A. 2017. Impacts of recently implemented recreational fisheries regulations on the Commercial Passenger Fishing Vessel fishery for Paralabrax sp. in California. Mar. Policy 86: 134–143. Elsevier.

Bellquist, L., and Semmens, B.X. 2016. Temporal and spatial dynamics of 'trophy'-sized demersal fishes off the California (USA) coast, 1966 to 2013. Mar. Ecol. Prog. Ser. 547: 1–18.

Booth, D.J., Bond, N., and Macreadie, P. 2011. Detecting range shifts among Australian fishes in response to climate change. Mar. Freshw. Res. 62(9): 1027–1042. Available from https://doi.org/10.1071/MF10270.

Cai, W., Borlace, S., Lengaigne, M., Van Rensch, P., Collins, M., Vecchi, G., Timmermann, A., Santoso, A., McPhaden, M.J., and Wu, L. 2014. Increasing frequency of extreme El Niño events due to greenhouse warming. Nat. Clim. Chang. 4(2): 111–116. Nature Publishing Group.

Cai, W., Wang, G., Santoso, A., McPhaden, M.J., Wu, L., Jin, F.-F., Timmermann, A., Collins, M., Vecchi, G., and Lengaigne, M. 2015. Increased frequency of extreme La Niña events under greenhouse warming. Nat. Clim. Chang. 5(2): 132–137. Nature Publishing Group.

Caminade, C., McIntyre, K.M., and Jones, A.E. 2019. Impact of recent and future climate change on vector-borne diseases. Ann. N. Y. Acad. Sci. 1436(1): 157–173. John Wiley and Sons Inc. doi:10.1111/nyas.13950.

Campbell, B.M., Vermeulen, S.J., Aggarwal, P.K., Corner-Dolloff, C., Girvetz, E., Loboguerrero, A.M., Ramirez-Villegas, J., Rosenstock, T., Sebastian, L., Thornton, P.K., and Wollenberg, E. 2016. Reducing risks to food security from climate change. Glob. Food Sec. 11: 34–43. doi:https://doi.org/10.1016/j.gfs.2016.06.002.

Chavez, F.P., Costello, C., Aseltine-Neilson, D., Doremus, H., Field, J.C., Gaines, S.D., Hall-Arber, M., Mantua, N.J., McCovey, B., Pomeroy, C., Sievanen, L., Sydeman, W., and Weeler, S.A. 2017. Readying California Fisheries for Climate Change. Oakland, California, USA. Available from https://www.oceansciencetrust.org/wp-content/uploads/2016/06/Climate-and-Fisheries_GuidanceDoc.pdf.

Cheung, W.W.L., Watson, R., and Pauly, D. 2013. Signature of ocean warming in global fisheries catch. Nature 497(7449): 365–368. Nature Publishing Group. doi:10.1038/nature12156.

Craig, R.K. 2017. Putting Resilience Theory into Practice: The Example of Fisheries Management. Nat. Resour. Environ. 31(3): 3–7. Available from

https://heinonline.org/HOL/P?h=hein.journals/nre31&i=141.

Deyle, E.R., Maher, M.C., Hernandez, R.D., Basu, S., and Sugihara, G. 2016. Global environmental drivers of influenza. Proc. Natl. Acad. Sci. U. S. A. 113(46): 13081–13086. National Academy of Sciences. doi:10.1073/pnas.1607747113.

Deyle, E.R., and Sugihara, G. 2011. Generalized Theorems for Nonlinear State Space Reconstruction. PLoS One 6(3): e18295. Public Library of Science. Available from https://doi.org/10.1371/journal.pone.0018295.

Dotson, R., and Charter, R. 2003. Trends in the Southern California sport fishery. Calif. Coop. Ocean. Fish. Investig. Rep.: 94–106. California Cooperative Oceanic Fisheries Investigations.

Field, J.C., and Francis, R.C. 2006. Considering ecosystem-based fisheries management in the California Current. Mar. Policy 30(5): 552–569. Pergamon. doi:10.1016/j.marpol.2005.07.004.

Folke, C. 2006. Resilience: The emergence of a perspective for social-ecological systems analyses. Glob. Environ. Chang. 16: 253–267. doi:10.1016/j.gloenvcha.2006.04.002.

Free, C.M., Thorson, J.T., Pinsky, M.L., Oken, K.L., Wiedenmann, J., and Jensen, O.P. 2019. Impacts of historical warming on marine fisheries production. Science (80-.). 363(6430): 979 LP – 983. doi:10.1126/science.aau1758.

Fuller, E.C., Samhouri, J.F., Stoll, J.S., Levin, S.A., and Watson, J.R. 2017. Characterizing fisheries connectivity in marine social–ecological systems. ICES J. Mar. Sci. 74(8): 2087–2096. Oxford University Press.

Gaines, S.D., Costello, C., Owashi, B., Mangin, T., Bone, J., Molinos, J.G., Burden, M., Dennis, H., Halpern, B.S., Kappel, C. V, Kleisner, K.M., and Ovando, D. 2018. Improved fisheries management could offset many negative effects of climate change. Sci. Adv. 4(8): eaao1378. doi:10.1126/sciadv.aao1378.

Garmestani, A., Craig, R.K., Gilissen, H.K., McDonald, J., Soininen, N., van Doorn-Hoekveld, W.J., and van Rijswick, H.F.M.W. 2019. The Role of Social-Ecological Resilience in Coastal Zone Management: A Comparative Law Approach to Three Coastal Nations . Available from https://www.frontiersin.org/article/10.3389/fevo.2019.00410.

Haynie, A.C., and Pfeiffer, L. 2012. Why economics matters for understanding the effects of climate change on fisheries. ICES J. Mar. Sci. 69(7): 1160–1167. doi:10.1093/icesjms/fss021.

Hill, K.T., and Barnes, J.T. 1998. Historical catch data from California's commercial passenger

fishing vessel fleet: status and comparison of two sources. California Department of Fish and Game, Marine Region Technical Report Number 60.

Jarvis, E.T., Allen, M.J., and Smith, R.W. 2004. Comparison of recreational fish catch trends to environment-species relationships and fishery-independent data in the southern California bight, 1980-2000. Calfornia Coop. Ocean. Fish. Investig. Rep. 45: 167. California Cooperative Oceanic Fisheries Investigations.

Jarvis, E.T., Gliniak, H.L., and Valle, C.F. 2014. Effects of fishing and the environment on the long-term sustainability of the recreational saltwater bass fishery in southern California. Calif. Fish Game 100(2): 234–259.

Kukal, M.S., and Irmak, S. 2018. Climate-Driven Crop Yield and Yield Variability and Climate Change Impacts on the U.S. Great Plains Agricultural Production. Sci. Rep. 8(1): 3450. doi:10.1038/s41598-018-21848-2.

Miller, K., Charles, A., Barange, M., Brander, K., Gallucci, V.F., Gasalla, M.A., Khan, A., Munro, G., Murtugudde, R., Ommer, R.E., and Perry, R.I. 2010. Climate change, uncertainty, and resilient fisheries: Institutional responses through integrative science. Prog. Oceanogr. 87(1): 338–346. doi:https://doi.org/10.1016/j.pocean.2010.09.014.

Murawski, S.A. 1991. Can We Manage Our Multispecies Fisheries? Fisheries 16(5): 5–13. John Wiley & Sons, Ltd. doi:https://doi.org/10.1577/1548-8446(1991)016<0005:CWMOMF>2.0.CO;2.

Nielsen, J.R., Thunberg, E., Holland, D.S., Schmidt, J.O., Fulton, E.A., Bastardie, F., Punt, A.E., Allen, I., Bartelings, H., Bertignac, M., Bethke, E., Bossier, S., Buckworth, R., Carpenter, G., Christensen, A., Christensen, V., Da-Rocha, J.M., Deng, R., Dichmont, C., Doering, R., Esteban, A., Fernandes, J.A., Frost, H., Garcia, D., Gasche, L., Gascuel, D., Gourguet, S., Groeneveld, R.A., Guillén, J., Guyader, O., Hamon, K.G., Hoff, A., Horbowy, J., Hutton, T., Lehuta, S., Little, L.R., Lleonart, J., Macher, C., Mackinson, S., Mahevas, S., Marchal, P., Mato-Amboage, R., Mapstone, B., Maynou, F., Merzéréaud, M., Palacz, A., Pascoe, S., Paulrud, A., Plaganyi, E., Prellezo, R., van Putten, E.I., Quaas, M., Ravn-Jonsen, L., Sanchez, S., Simons, S., Thébaud, O., Tomczak, M.T., Ulrich, C., van Dijk, D., Vermard, Y., Voss, R., and Waldo, S. 2018. Integrated ecological–economic fisheries models—Evaluation, review and challenges for implementation. Fish Fish. 19(1): 1–29. John Wiley & Sons, Ltd. doi:https://doi.org/10.1111/faf.12232.

Opsahl, T., Agneessens, F., and Skvoretz, J. 2010. Node centrality in weighted networks: Generalizing degree and shortest paths. Soc. Networks 32: 245–251. doi:10.1016/j.socnet.2010.03.006.

Parnell, P.E., Dayton, P.K., Fisher, R.A., Loarie, C.C., and Darrow, R.D. 2010. Spatial patterns of fishing effort off San Diego: implications for zonal management and ecosystem function.

Ecol. Appl. 20(8): 2203–2222. John Wiley & Sons, Ltd. doi:10.1890/09-1543.1.

Perry, R.I., Ommer, R.E., Allison, E.H., Badjeck, M.-C., Barange, M., Hamilton, L., Jarre, A., Quinones, R.A., and Sumaila, U.R. 2010. Interactions between changes in marine ecosystems and human communities. Mar. Ecosyst. Glob. Chang.: 221–252. Oxford University Press, Oxford, UK.

Plagányi, É.E., Punt, A.E., Hillary, R., Morello, E.B., Thébaud, O., Hutton, T., Pillans, R.D., Thorson, J.T., Fulton, E.A., Smith, A.D.M., Smith, F., Bayliss, P., Haywood, M., Lyne, V., and Rothlisberg, P.C. 2014. Multispecies fisheries management and conservation: tactical applications using models of intermediate complexity. Fish Fish. 15(1): 1–22. John Wiley & Sons, Ltd. doi:10.1111/j.1467-2979.2012.00488.x.

Pörtner, H.O., and Peck, M.A. 2010. Climate change effects on fishes and fisheries: towards a cause-and-effect understanding. J. Fish Biol. 77(8): 1745–1779. John Wiley & Sons, Ltd. doi:10.1111/j.1095-8649.2010.02783.x.

Proulx, S.R., Promislow, D.E.L., and Phillips, P.C. 2005. Network thinking in ecology and evolution. Trends Ecol. Evol. 20(6): 345–353. doi:https://doi.org/10.1016/j.tree.2005.04.004.

R Core Team. 2019. R: A language and environment for statistical computing. R Foundation for Statistical Computing, Vienna, Austria. Available from https://ww.r-project.org/.

Rayner, N.A.A., Parker, D.E., Horton, E.B., Folland, C.K., Alexander, L. V, Rowell, D.P., Kent, E.C., and Kaplan, A. 2003. Global analyses of sea surface temperature, sea ice, and night marine air temperature since the late nineteenth century. J. Geophys. Res. Atmos. 108(D14). Wiley Online Library.

Reynolds, R.W., Smith, T.M., Liu, C., Chelton, D.B., Casey, K.S., and Schlax, M.G. 2007. Daily High-Resolution-Blended Analyses for Sea Surface Temperature. J. Clim. 20(22): 5473–5496. American Meteorological Society, Boston MA, USA. doi:10.1175/2007JCLI1824.1.

Rogers, L.A., Griffin, R., Young, T., Fuller, E., Martin, K.S., and Pinsky, M.L. 2019. Shifting habitats expose fishing communities to risk under climate change. Nat. Clim. Chang. 9(7): 512–516. Nature Publishing Group.

Schroeder, D.M., and Love, M.S. 2002. Recreational fishing and marine fish populations in California. Calif. Coop. Ocean. Fish. Investig. Rep.: 182–190. California Cooperative Oceanic Fisheries Investigations.

Sievanen, L., Phillips, J., Colgan, C., Griggs, G., Finzi Hart, J., Hartge, E., Hill, T., Kudela, R., Mantua, N., Nielsen, K., and Whiteman, L. 2018. California's Coast and Ocean Summary Report. California's Fourth Clim. Chang. Assessment.

Sugihara, G., May, R., Ye, H., Hsieh, C., Deyle, E., Fogarty, M., and Munch, S. 2012. Detecting Causality in Complex Ecosystems. Science (80-.). 338(6106): 496 LP – 500. doi:10.1126/science.1227079.

Takens, F. 1981. Detecting strange attractors in turbulence. *In* Symposium on Dynamical Systems and Turbulence. *Edited by* D. Rand and L. Young. Springer Verlag, Berlin. pp. 366–381.

Thorpe, R.B., Dolder, P.J., Reeves, S., Robinson, P., and Jennings, S. 2016. Assessing fishery and ecological consequences of alternate management options for multispecies fisheries. ICES J. Mar. Sci. 73(6): 1503–1512. doi:10.1093/icesjms/fsw028.

Ulrich, C., Reeves, S.A., Vermard, Y., Holmes, S.J., and Vanhee, W. 2011. Reconciling single-species TACs in the North Sea demersal fisheries using the Fcube mixed-fisheries advice framework. ICES J. Mar. Sci. 68(7): 1535–1547. doi:10.1093/icesjms/fsr060.

Vinther, M., Reeves, S.A., and Patterson, K.R. 2004. From single-species advice to mixed-species management: taking the next step. ICES J. Mar. Sci. 61(8): 1398–1409. doi:10.1016/j.icesjms.2004.08.018.

Weatherdon, L. V, Magnan, A.K., Rogers, A.D., Sumaila, U.R., and Cheung, W.W.L. 2016. Observed and Projected Impacts of Climate Change on Marine Fisheries, Aquaculture, Coastal Tourism, and Human Health: An Update . Available from https://www.frontiersin.org/article/10.3389/fmars.2016.00048.

Weber, M.L., and Heneman, B. 2000. Guide to California's Marine Life Management Act. Common Knowledge Press Bolinas, California.

Wu, X., Lu, Y., Zhou, S., Chen, L., and Xu, B. 2016. Impact of climate change on human infectious diseases: Empirical evidence and human adaptation. Environ. Int. 86: 14–23. doi:https://doi.org/10.1016/j.envint.2015.09.007.

Ye, H., Clark, A., Deyle, E., and Munch, S. 2021. rEDM: Applications of Empirical Dynamic Modeling from Time Series. Available from https://ha0ye.github.io/rEDM.

Ye, H., Deyle, E.R., Gilarranz, L.J., and Sugihara, G. 2015. Distinguishing time-delayed causal interactions using convergent cross mapping. Sci. Rep. 5: 14750. Nature Publishing Group.

Chapter 4:

Reconciling differences in management and sustainability of seafood consumption and production globally.

Kayla M. Blincow, Alan C. Haynie, Brice X. Semmens

Abstract

Ensuring the sustainability of seafood is increasingly important for supporting food security and stable livelihoods in the face of a growing human population. Previous work has demonstrated that, on a country-by-country basis, fisheries management intensity is positively correlated with the sustainability of seafood production. However, because seafood consumption sustainability depends on seafood sourcing, even countries with intensively managed fisheries may largely consume (and economically support) seafood from less intensively managed sources. Here we combined three disparate datasets to relate global seafood trade dynamics to fisheries management to estimate the disparity between management of seafood production and consumption across countries. We found that countries that have intensively managed fisheries had comparatively lower levels of management intensity associated with their consumption. In the context of seafood sustainability, countries with the highest production sustainability, on average, consumed less sustainable seafood products than what they produced. On the other hand, many countries with less intensive fisheries management consumed more sustainable seafood than they produced. These disparities appeared to be related to wealth, with higher GDP countries having a greater disparity between sustainability of seafood consumption and production. We assert that the globalization of seafood trade and trends in the flow of seafood products contribute to the disparities in the sustainability of seafood consumption and production in the context of management. To support the sustainability of seafood consumption we need better mechanisms for tracing the fate of seafood products from their point of capture to their final point of consumption.

4.1. Introduction

Freshwater and marine products sourced from wild capture and aquaculture fisheries, referred to from here onward as seafood, play a critical role in global food systems. In 2017, approximately 3.3 billion people derived 20% of their animal protein intake from fish, with this percentage being even higher for many developing and small island nations (FAO 2020a). In addition to providing sustenance, seafood and fishing industries are an important source of jobs and income for many people around the world, supporting the livelihoods of more than 10% of the global population (Teh and Sumaila 2013, FAO 2020a). As demand for fisheries as a source of food and livelihoods increases through time, so do potential negative environmental impacts stemming from unsustainable fishing (e.g. loss of biodiversity, fisheries-induced evolution, and altered trophic dynamics; Smith et al. 2010, Heino et al. 2015, Ortuño Crespo and Dunn 2017). In recognition of the importance of marine and aquatic resources, such as fisheries, to global development the United Nations included them in their Sustainable Development Goals for 2030, calling on the global community to "conserve and sustainably use the oceans, seas, and marine resources for sustainable development" (UN General Assembly 2015, Ovando et al. 2021).

Sustainable fisheries can be defined in many ways. On a fishery-by-fishery basis in wild capture fisheries, managers often rely on the development of standard indicators to assess and regulate sustainable production, such as maximum sustainable yield (MSY) abundance (B/B_{MSY}) or fishing mortality (U/U_{MSY}) (FAO 2019, Hilborn et al. 2020). The effectiveness of these indicators (and thus fisheries management) is dependent on the quality of data available, the sophistication of modeling methods, and ultimately, the successful application of regulatory efforts (Ovando et al. 2021). As such, one measure of fisheries sustainability on the scale of countries is the relative level of fisheries management and enforcement. Increased fisheries management

intensity is associated with more sustainable fisheries production (Costello et al. 2016, Melnychuk et al. 2017, 2021, Hilborn et al. 2020). That is, countries that are better equipped to establish strong fisheries management, particularly in reference to enforcement, fishing regulations, and capacity to conduct stock assessments (Melnychuk et al. 2017), have relatively few overfished stocks. Similarly, within aquaculture, countries that have the stability and capacity to support strong property rights and establish regulatory oversight of the industry have more strongly managed and sustainable aquaculture production (Anderson 2015). While countries with stronger capacity to manage their fisheries generally produce sustainable seafood, the sustainability of their consumption is the product of both locally produced seafood and imports from other countries—the latter operating outside the bounds of local fisheries management.

Trade of seafood products is increasingly globalized (Swartz et al. 2010, Asche et al. 2015, Gephart and Pace 2015). As some of the most traded food commodities in the world, 78% of seafood products experience competition from international trade and 38% of all fisheries production enters international trade markets (FAO 2020a). The globalization of seafood markets means that countries are not just consuming seafood products that they produce themselves, but rather are a part of a vast network of international seafood trade that derives products from many different sources. This creates potential for a mismatch between seafood production and seafood consumption sustainability (Guillen et al. 2018).

In this study, we adapted a metric of country-specific management intensity to account for consumption sustainability based on both production and trade, and compared it to previous estimates of production-only sustainability. To do so, we combined different sources of fisheries trade data to link management intensity (as a metric for sustainability), seafood production, and seafood consumption. In particular, we used the FAO Food Balance Sheet of fish and fishery

products (FAO 2020b) and a highly resolved international trade dataset, the HIS MarkIT Global Trade Atlas (GTA). By contrasting production versus consumption sustainability on a country-by-country basis, we highlight those countries with broad disparities between the two, and discuss the economics and information gaps that may be causing such disparities.

4.2. Methods

We used three main sources of data in our analysis: the FAO Food Balance Sheet of fish and fishery products (FAO 2020b), the GTA dataset (data compiled by the Alaska Fisheries Information Network in GTA_TRADE_DATA_V), and the Fishery Management Index (FMI) (Melnychuk et al. 2017, Ocean Health Index 2019). We used information from these sources and various assumptions (defined below) regarding the nature of trade of seafood products and consumption to estimate the management intensity of seafood products that are consumed within a country. Using these values we explored the relationship between management of seafood products consumed and produced across countries globally. We performed all of our analyses using R Statistical Software, version 3.6.1 (R Core Team 2019). The corresponding code can be found at https://github.com/kmblincow/GlobalSeafoodTrade.

Data

The FAO Food Balance Sheet includes information on the production, imports, exports, and total food supply of seafood products associated with countries grouped by coarse product types and year (FAO 2020b). The product types in the FAO data are derived from the International Standard Statistical Classification of Aquatic Animals and Plants (ISSCAAP) and include: Freshwater and Diadromous Fish, Pelagic Fish, Demersal Fish, Marine Fish Not Elsewhere

Indicated (NEI), Crustaceans, Cephalopods, Molluscs Excluding Cephalopods, and Aquatic Animals NEI. We relied chiefly on the FAO dataset as the core of our analysis due to it being the standard data used in these types of analysis and a lack of a better alternative including estimates of the components of seafood consumption across a wide array of countries.

The GTA data include information on the quantity of imports and exports of seafood products (Harmonized System Codes (HS) -03, -16) between trade partners. We will refer to countries that report to the dataset as "reporters" and their associated trade partners as "partners". We used this dataset to define which trade partners contributed to the imports of reporters recorded in the FAO Food Balance Sheet. We filtered out products that are not intended for human food consumption as defined by the FAO Food Balance Sheet metadata, including ornamentals, oils, feed, and capsules. We also filtered out trade relationships that did not apply to our analysis, for example, some countries reported trade that occurred between regions within their national boundaries. Additionally, we filtered out reporters that were grouped or were duplicates of other reporters (e.g. European Union reporters that were aggregates of member countries). The GTA data on imports and exports are recorded in product weight, while the FAO data is recorded in live weight. To combine information from both datasets we converted the product weights to live weights in the GTA data. We used the suggested conversion factors (CF) from the FAO Coordinating Working Party on Fishery Statistics (CWP) Handbook of Fishery Statistical Standards detailed in Annex I.1 (FAO 2004). In cases where products did not have a direct FAO CF, we used the most closely taxonomically related CF available. There were some cases (0.2% of total imports) that did not have a close equivalent FAO CF (e.g. caviar and shark fins) or did not have information regarding the product (e.g. confidential product trade). In these cases we used the best available CF from other sources or assigned a CF of 1. In particular, we chose to assign a

CF of 1 to product groups with no information, such as confidential trade, as we did not have a basis for determining what an appropriate CF would be other than the product weight itself. Additionally, we classified all GTA products into the FAO ISSCAAP product groupings used in the FAO Food Balance Sheet data.

The FMI data constitute estimates of the management intensity of wild capture fisheries in different countries. Originally created by Melnychuk et al. (2017), FMI is a metric ranging from 0 to 1 that uses information from surveys of fisheries experts to assess research, management, enforcement, and socioeconomics of fisheries management across 28 different countries that account for > 80% of global catch. Melnychuk et al. later expanded the FMI to include additional countries and fisheries stocks (Melnychuk et al. 2020, Hilborn et al. 2020). The Ocean Health Index (OHI) estimated FMI for additional countries/territories in order to incorporate it into their resilience estimates of coastal countries for their 2019 Ocean Health Index global assessment (Halpern et al. 2012, Ocean Health Index 2019). To do so, they used linear models to determine which variables best predicted FMI from an original set of 40 countries from Melnychuk et al., including various measures of gross domestic product (GDP), governance, and region. They found that the Social Progress Index (SPI) and United Nations geo-regions were the best predictors of FMI. SPI is an index that measures how well countries support basic human needs, foundations of wellbeing, and opportunity for their citizens (Stern et al. 2018). After fitting a linear model using these explanatory variables, they used it to fill gaps in the FMI dataset to include 80 additional countries/territories (Ocean Health Index 2019). There were a total of 324 different trade partners reported in the GTA dataset, some of which represented smaller territories within countries or groupings of multiple countries. For trade partners that constituted groups of countries (e.g. European Union) or unrecognized territories we determined FMI by either calculating the mean

FMI of the group of countries or finding the most closely related country or territory associated with the unaccounted for trade partner. For the remaining countries (n = 44), we used the OHI gap filling model to further expand the FMI dataset. We should note that FMI was created as a measure of management intensity for wild capture fisheries, but we applied it to both wild capture and aquaculture seafood products as the trade datasets do not specify the method of production. We believe this is a safe assumption considering many of the country-level factors influencing management intensity of wild capture seafood products (e.g. enforcement capacity) have similar influences on the management of aquaculture seafood products (Anderson 2015). For the purposes of our analysis we are referring to the FMI data of country-level management intensity as FMI_P, or the FMI associated with a country's production. The data also formed the basis for our calculation of FMI_I, or the management intensity of a country's imports of seafood products, and FMI_C, or the management intensity of a country's consumption of seafood products (see below).

Calculating FMI_C

We combined the three datasets described above to determine the FMI associated with consumption (FMI_C) for each reporter present in both the GTA and FAO datasets. The GTA data did not have high resolution trade information for all reporters prior to 2012, and the FAO dataset only included data up to 2017. For these reasons we limited our analysis to the years 2012-2017.

We used the same equation for calculating consumption that underpins the FAO Food Balance Sheet calculation of total food supply to serve as the basis for our calculations (Equation 1). This equation states that the product that is available for human consumption is what is left over after accounting for inputs of product from domestic production and imports from other countries, and outputs of product associated with exports:

(1) $$C = P + I - E$$

Where for any given reporter and product group, C is consumption of the seafood product, P is domestic production of the product, I is imports of the product from other countries, and E is exports of the product to other countries. Building from this fundamental relationship we generated an equation for calculating FMI_C (Equation 2):

(2) $$FMI_{C_r} = \left(p_{P_{Cr}} \times FMI_{P_r}\right) + \left(p_{I_{Cr}} \times FMI_{I_r}\right)$$

Where for reporting country *r*, $p_{P_{Cr}}$ is the proportion of consumption of a product associated with domestic production, $p_{I_{Cr}}$ is the proportion of consumption associated with imports from other countries, FMI_{P_r} is the production FMI for the reporting country, and FMI_{I_r} is the FMI associated with the trade partners supplying imports of the product scaled based on their contribution to total imports to country *r*. We calculated FMI_{I_r} as follows (Equation 3):

(3) $$FMI_{I_r} = \sum_{j=Partner1}^{n} \left(\left(p_{P_{Ej}} \times p_{I_{rj}} \times FMI_{P_j}\right) + \left(p_{I_{Ej}} \times p_{I_{rj}} \times FMI_{glbl}\right)\right)$$

Where $p_{P_{Ej}}$ is the proportion of exports of a product by trade partner *j* associated with their domestic production, $p_{I_{Ej}}$is the proportion of exports by trade partner *j* associated with their imports, $p_{I_{rj}}$ is the proportion of imports of the reporting country *r* associated with trade partner *j*, FMI_{P_j} is the production FMI for trade partner *j*, and FMI_{glbl} is a global estimate of the FMI for a given product scaled based on the relative production by countries (Equation 4):

(4) $$FMI_{glbl} = \sum_{k=country1}^{n} \left(p_{Pglbl_k} \times FMI_{P_k}\right)$$

Where p_{Pglbl_k} is the proportion of global production of a product associated with country *k*, and FMI_{P_k} is the production FMI associated with country *k*.

Assumptions and Sensitivity of Unknown Parameters

In the equations above, there are 3 key unknowns that we were unable to estimate with the data in hand: 1) the proportion of consumption of a product that is associated with domestic production ($p_{P_{Cr}}$), 2) the proportion of exports of a product that is associated with domestic production ($p_{P_{Ej}}$), and 3) country of origin for any re-exported seafood products. Each of these unknowns are the result of a common, and poorly documented practice: re-exporting and/or re-importing products. While some countries do report re-exports, the recognized definition of re-exports within global trade only includes products that are imported and re-exported in the same form. Products that are imported and undergo processing get reported as new products originating from the point of processing. For example, if country A imports whole fish from country B, then processes and re-exports that product as canned fish, that fish becomes a new product attributed to country A. As a result, tracing the origin of seafood products that undergo processing in countries separate from where they are harvested is currently not possible with the data we have. For the purposes of this study we will refer to this challenge as the issue of re-exports. Since our goal was to trace the origin of seafood products from their original point of raw production, we were forced to make assumptions regarding these values. To address these unknowns, we either made regularizing assumptions, or conducted a parameter sensitivity analysis based on prior parameter estimates in the literature.

Regarding the proportion of consumed seafood products that are domestic in origin, we used a range of parameters, including a naïve assumption and two values derived from the literature. First, we calculated FMI_C under the assumption that, for all countries and products, consumption that was domestic in origin was proportional to the amount of domestic production of that product. For example, if a country produced 50 tons of fish and imported 10 tons of fish,

we assumed the total food supply available for consumption associated with domestic production versus imports was 5:1 ($p_{P_{Cr}}$: $p_{I_{Cr}}$). We refer to this FMI_C estimate as the proportional derivation. Second, we relied on an estimate of the proportion of consumption associated with domestic production made in Gephart et al. (2019). They estimated that 35-38% of seafood consumption in the United States is produced domestically, accounting as best as possible for the issue of re-exports. We applied a $p_{P_{Cr}}$of 0.365 to all countries for our second estimate of FMI_C, which we refer to as the Gephart derivation. Given that it is not necessarily reasonable to assume all countries would operate under similar circumstances to the United States in regards to seafood trade dynamics, we applied one additional estimate. We used a value from Guillen et al. (2018) that used a Multi-Region Input-Output model (MRIO) to characterize global seafood consumption and estimated that approximately 74% of final consumption of seafood products is from domestic supply globally. Their MRIO model did not directly account for the issue of re-exports, and assumed products originated from the country of export. We applied a $p_{P_{Cr}}$of 0.74 to all countries for our third estimate of FMI_C, which we refer to as the Guillen derivation.

Regarding the proportion of exports of a product from trade partners that are domestic in origin (Equation 3), we used the naïve assumption that both $p_{P_{Ej}}$ and $p_{I_{Ej}}$ were equal to 0.5. For most countries, this is likely an underestimate of the amount of exports associated with domestic production. However, by making this assumption it allows us to simultaneously leverage the power of the highly resolved binational trade flows present in the GTA data while still allowing our results to correct for the issue of re-exports by attributing a conservative proportion of exports to a global mean FMI (described below).

Finally, regarding the country of origin for any re-exported seafood products, we made the regularizing assumption that re-exported products had an FMI equivalent to the global average of

the FMI for all product groups and countries. We scaled this global estimate based on the level of production of each product by each country (Equation 4).

Analysis

We calculated all of the equations above based on the FAO product groups, and aggregated the final FMI_C estimates based on the relative proportion of total seafood consumption associated with each product. All of the assorted FMI_P values were drawn from the FMI dataset. The GTA data provided the relative contribution of different trade partners to each reporter's imports. The FAO data provided information on the total food supply and relative proportions of different product groups to the total food supply for each reporter. We compared the total live weight of imports by country from the GTA dataset against the FAO dataset to determine how much they differed, and found that the FAO data had lower estimates, in some cases substantially so (see Figure A4.1). Despite the disparities in the magnitude of trade reported by the different datasets, we assumed that the relative contribution of trade partners derived from the GTA data was the same for the FAO data.

We analyzed our resulting estimates of FMI_C using linear modelling techniques. We used simple linear models to determine the direct relationship between FMI_P and our estimates of FMI_C. We tested for differences in the disparity of FMI_P and the mean of our FMI_C estimates (FMI_{Cmean}) using a multiple linear regression with FMI_P-FMI_{Cmean} as the response variable and region and per capita GDP as the explanatory variables. We further explored the trade relationships associated with the largest importers and exporters globally by looking at the relative contributions and differences in FMI_P among their trade partners.

4.3. Results

We found that while all countries had an FMI_C that differed from their FMI_P (Figure 4.1), the direction and magnitude of the difference depended on their FMI_P. Countries on the lower end of the FMI_P spectrum tended to have FMI_C values greater than their FMI_P, while countries on the higher end of the FMI_P spectrum tended to have FMI_C values lower than their FMI_P (Figure 4.1).

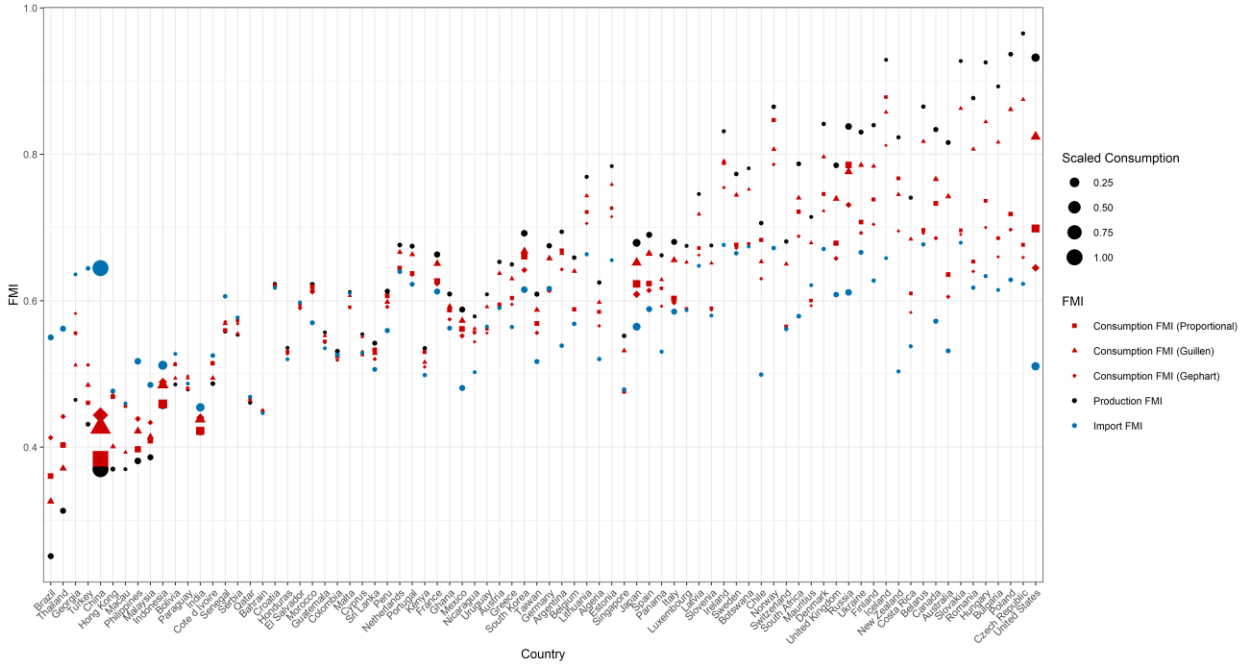

Figure 4.1. Results of the FMI calculations for all countries. Countries along the x axis are ordered based on the magnitude of the difference between FMI_P and FMI_{Cmean} across all products. The color and shape of the points are indicative of the FMI calculation, with red points of different shapes denoting FMI_C derivations, blue points denoting FMI_I, and black points denoting FMI_P. The size of the points is the consumption of each country (Total Food Supply from FAO data) scaled by dividing by the maximum consumption estimate (China).

We found that overall FMI_C had a significant positive linear relationship with FMI_P, which was expected given the FMI_C calculations were dependent on FMI_P. The estimates of the linear coefficients varied across the different FMI_C derivations (Figure 4.2). The Guillen FMI_C derivation had the highest slope estimate and was the closest to a 1:1 relationship between FMI_P and FMI_C ($FMI_C = 0.797 \times FMI_P + 0.112$, $R^2 = 0.99$), followed by the proportional estimate ($FMI_C = 0.602$

x FMI_P + 0.210, R^2 = 0.85), then the Gephart estimate (FMI_C = 0.511 x FMI_P + 0.287, R^2 = 0.87) (Figure 4.2). Countries with FMI_P values at the extreme ends of the spectrum differed the most from the 1:1 relationship (Figure 4.2).

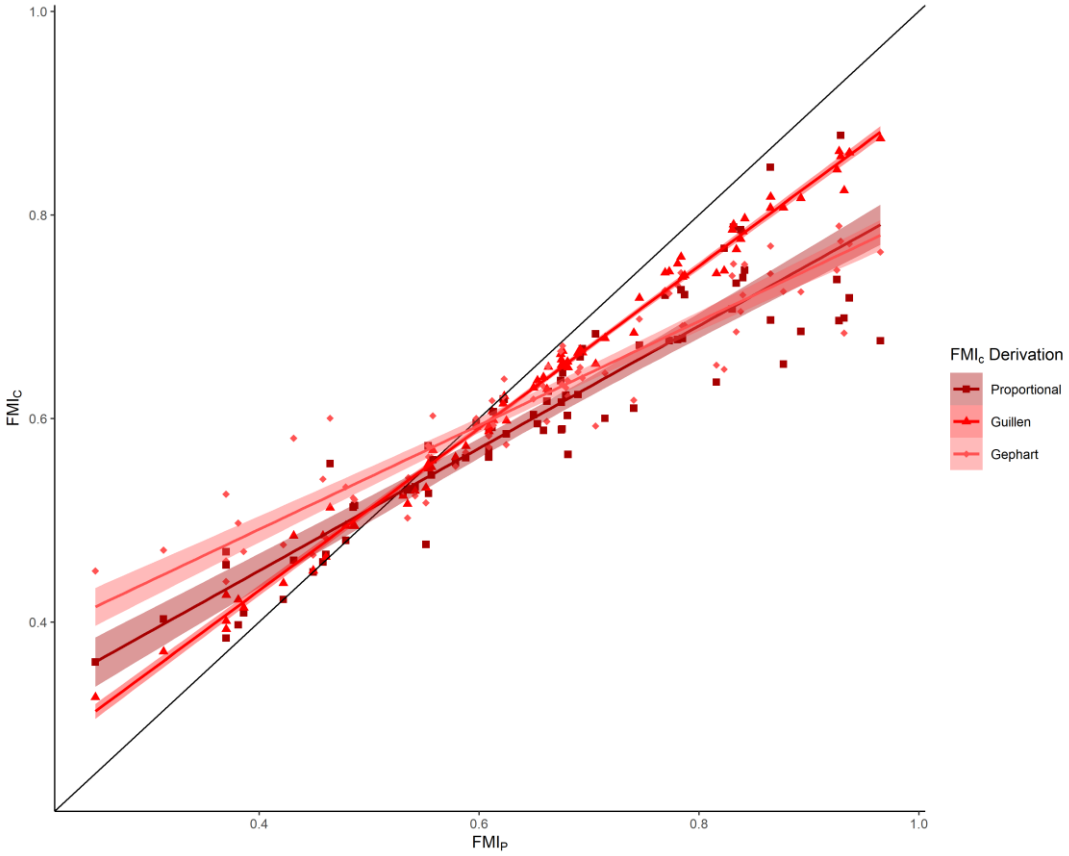

Figure 4.2. Plot comparing FMI_P to the different FMI_C derivations. The points depict the raw data (countries), while the lines show the linear model results. The shaded areas around the lines denote the 95% confidence intervals for the linear model fit. The different colors denote the different FMI_C derivations. The black line shows the hypothetical direct 1:1 relationship between the two variables for comparison.

We found significant differences in the disparity between FMI_P and FMI_{Cmean} with region and per capita GDP (R^2 = 0.67, F(13,65) = 13.24, p = $1.19e^{-13}$). There was a significant positive effect of per capita GDP (p = 0.001) (Figure 4.3a). There were significant differences among regions, with Eastern Europe (p = $2.29e^{-5}$), Australia and New Zealand (p = 0.034), and Northern America (p = .007) differentiating from the intercept region of Southern Asia (Figure 4.3b). All of

these regions showed model estimates well above zero, indicating their FMI_P is likely to be greater than their FMI_C. The model estimates for Asian regions were chiefly less than zero, indicating their FMI_P is likely to be less than their FMI_C.

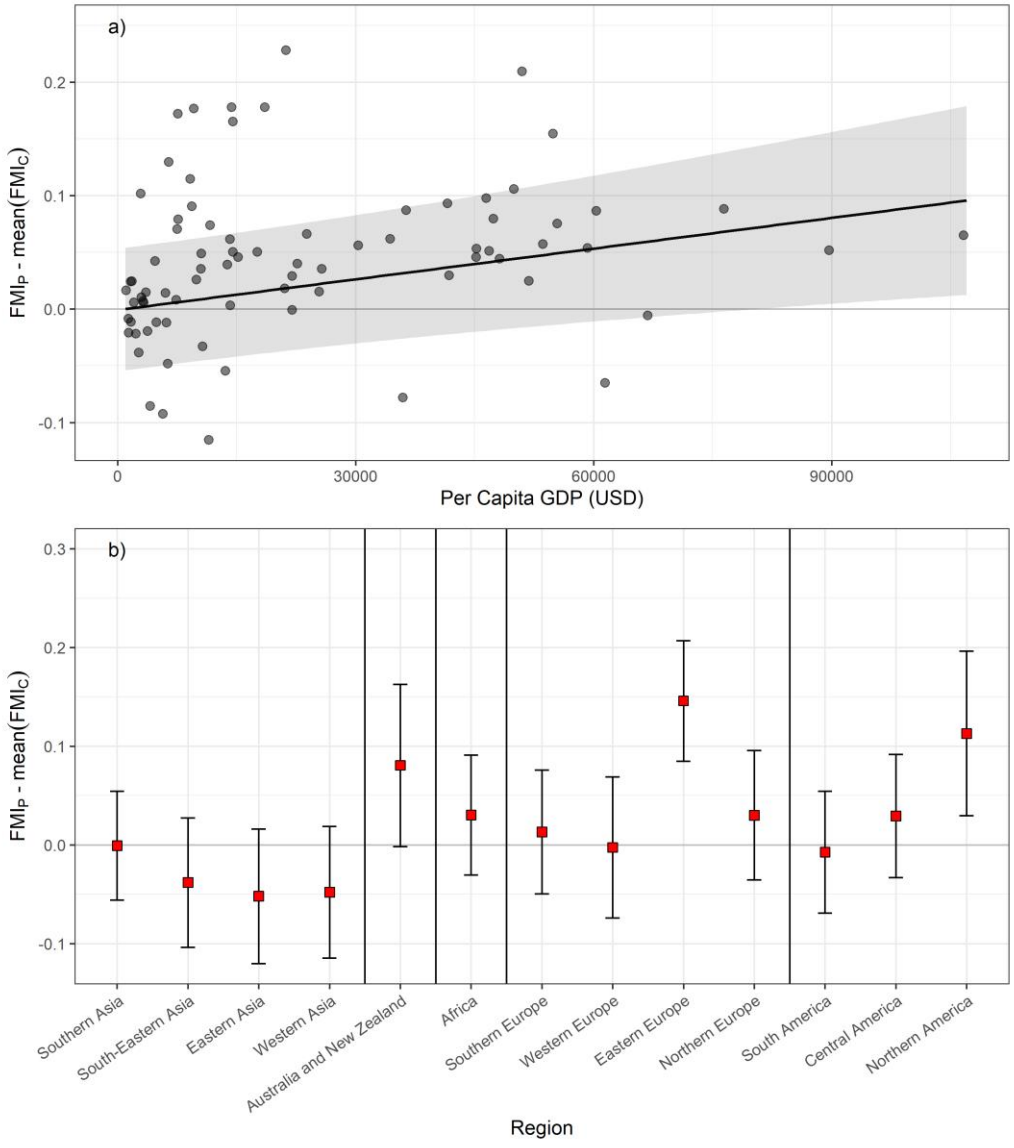

Figure 4.3. Multiple linear regression results showing the effect of region and per capita GDP on the disparity between FMI_P and FMI_{Cmean}. The top panel (a) shows the relationship with GDP with the points indicating the raw data, the line the model estimate, and the shaded area the 95% confidence interval. The lower panel (b) shows the model estimates of the disparity by region. The point estimates for each region are shown by the red squares, and the intervals denote the 95% confidence intervals.

The top five exporters by volume across 2012 to 2017 in descending order were China, Norway, Thailand, Russia, and the United States (Figure 4.4a). The top five importers in descending order were the United States, China, Japan, Spain, and France (Figure 4.4b). The highest exporters tended to trade with more partners than the highest importers.

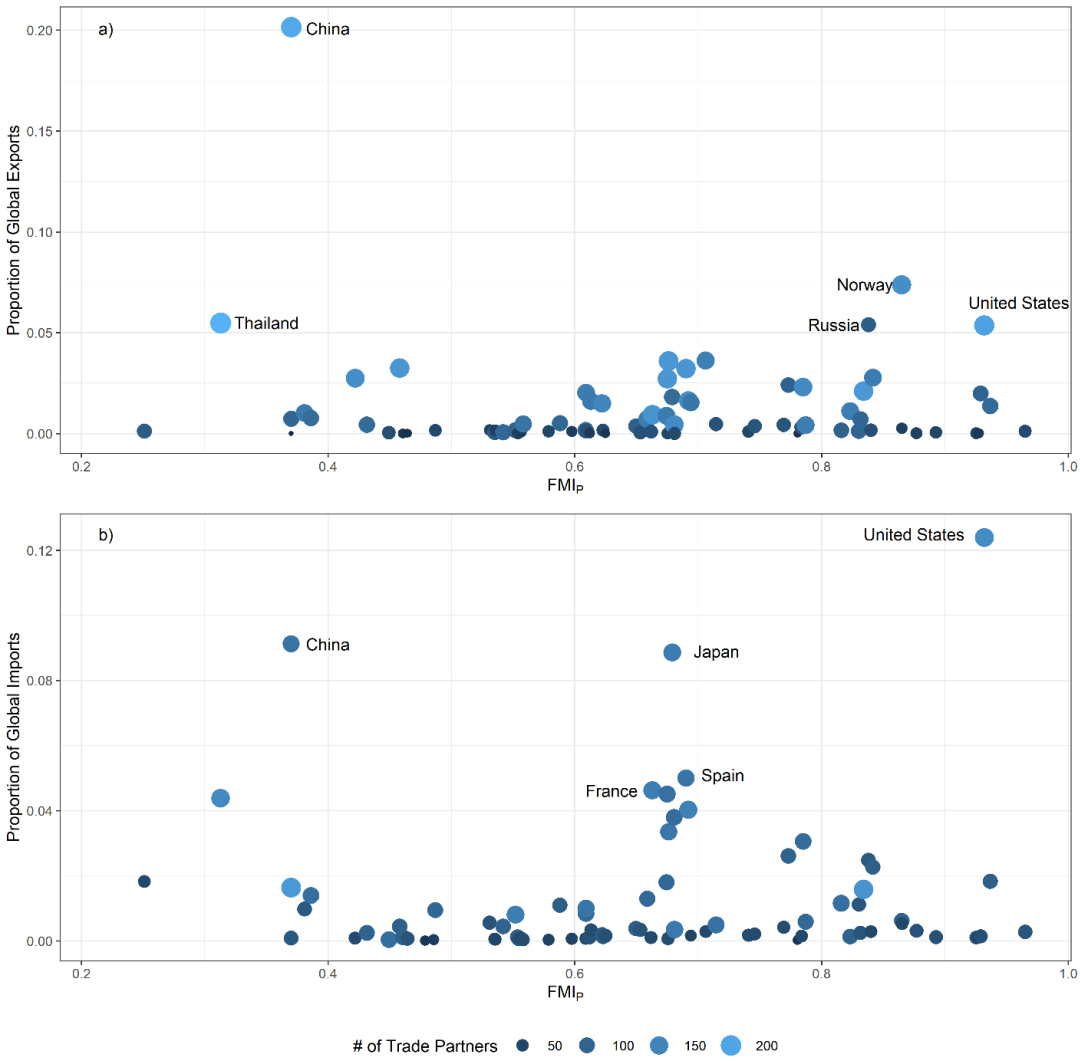

Figure 4.4. The proportion of global exports (a) and imports (b) from 2012-2017 by FMI_P. The size and color of the points shows the number of trade partners for each country (note difference in scale of y-axis). The top five exporters and importers are labeled in each panel.

China and the United states contributed most to global exports and imports, respectively. China's exports are traded globally, with the largest proportions of its exports going to Japan

(17.9%), South Korea (15.1%), and the United States (14.6%) (Figure 4.5). A majority of China's major trade partners had higher FMI_P values than China itself (0.370; Figure 4.5). The United States traded largely with countries that have lower FMI_P values (Figure 4.6). The majority of imports coming into the United States were from Asian countries (>57% of total imports), with the largest contributions from the region coming from China (24.8%), Vietnam (9.4%), Thailand (6.7%), and Indonesia (6.3%) (Figure 4.6). The second largest country contributing to the United States' imports after China was Canada (13.9%) (Figure 4.6).

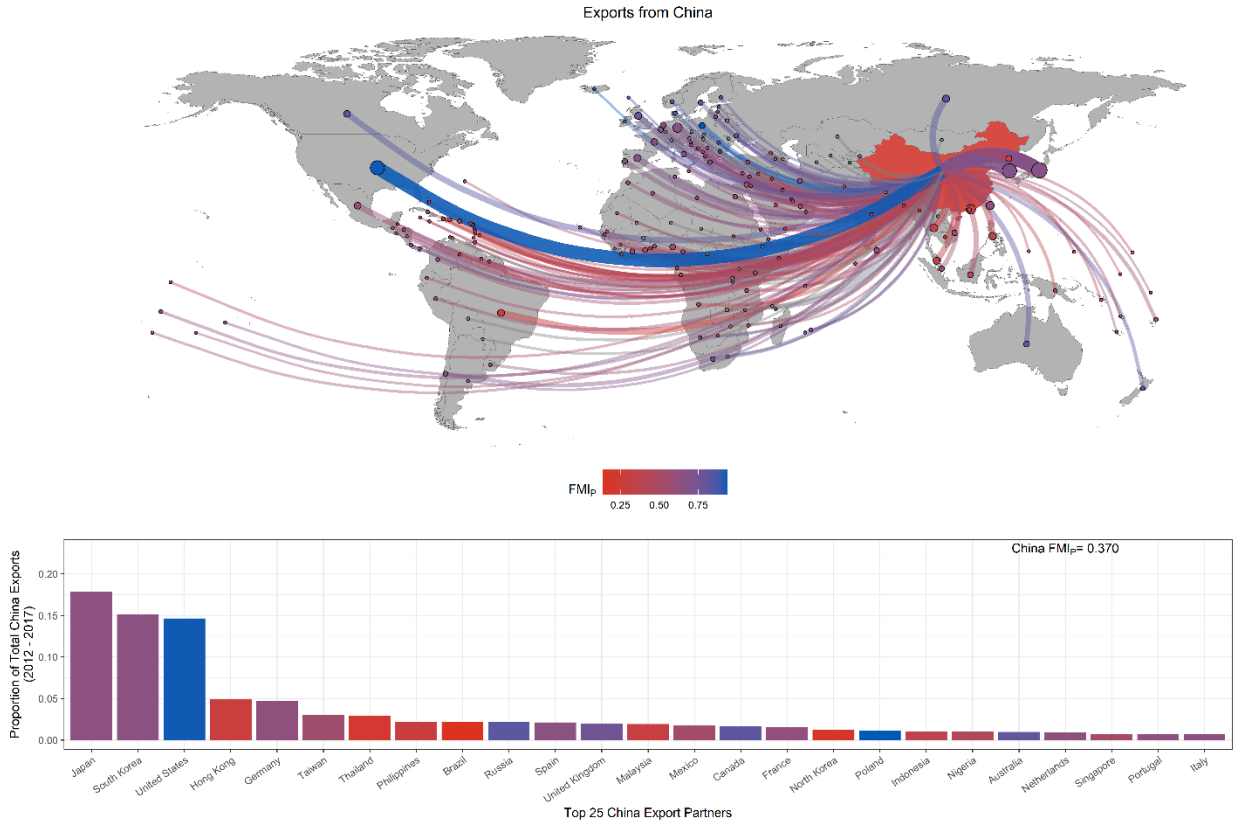

Figure 4.5. Figure depicting China's global exports 2012-2017. In the top panel, China is shaded based on its own FMI_P. The lines and points show the destination of exports from China, with the color denoting the FMI_P of the export trade partner. The thickness and darkness of the lines and points are scaled to the magnitude of the trade going to each country. The bottom panel shows the top 25 trade partners receiving China's exports and the proportion of China's total exports attributable to each partner. The bars are shaded based on the trade partner's FMI_P.

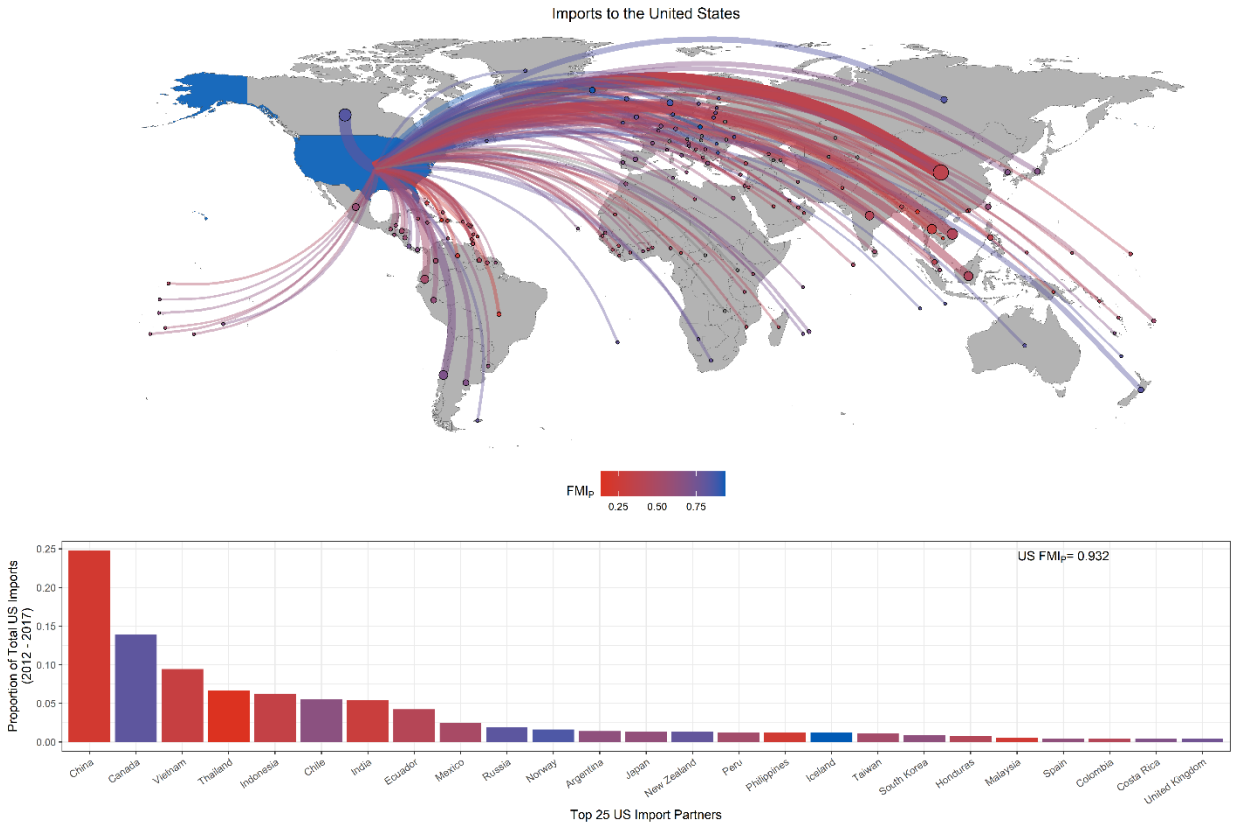

Figure 4.6. Figure depicting the origin of the United States' imports 2012-2017. In the top panel, the United States is shaded based on its own FMI_P. The lines and points show the origin of imports to the United States, with the color denoting the FMI_P of the import trade partner. The thickness and darkness of the lines and points of origin are scaled to the magnitude of the trade coming from each country. The bottom panel shows the top 25 trade partners contributing to the United States' imports and the proportion of the United Sates' total imports attributable to each partner. The bars are shaded based on the trade partner's FMI_P.

4.4. Discussion

Most efforts to assess national seafood sustainability have focused on the quality of fisheries management and enforcement of seafood harvest domestically (Costello et al. 2016, Melnychuk et al. 2017, Hilborn et al. 2020). However, seafood is one of the most traded food commodities in the world, with most countries relying on international trade to some extent to support their seafood consumption (Swartz et al. 2010, Asche et al. 2015, FAO 2020a). As this global trade gains complexity, it is increasingly clear that assessments of national seafood

sustainability must also account for the sustainability of imported seafood products. Here, we generated estimates of the management intensity associated with country-specific seafood consumption (FMI_C), accounting both for production and imports, and assessed disparities between this metric and the management intensity of country-specific seafood production (FMI_P). We then related these estimates of management intensity to sustainability of production and consumption based on the understanding that more intensely managed fisheries tend to be more sustainable (Costello et al. 2016, Melnychuk et al. 2017, 2021, Hilborn et al. 2020). Overall we found that countries that have intensively managed fisheries (higher FMI_P) tend to have relatively lower FMI_C than countries with less intensively managed fisheries (lower FMI_P). That is, countries associated with sustainable seafood production, on average, consumed seafood products at much lower sustainability levels than what they produced. On the other hand, many countries with low FMI_P actually consumed more sustainable seafood than they produced. In general, these disparities appear to be at least partially mediated by wealth; as GDP increases, so does the disparity between the sustainability of consumption and production.

While directly calculating sustainability of seafood consumption is fraught with uncertainty, the general patterns we observed appear robust to the different parameter estimates we considered. The reciprocal pattern we found in the relationship between FMI_P and its difference with FMI_C highlights the overall disparity in management intensity globally. This pattern held, regardless of the assumptions we made concerning the proportion of national seafood consumption stemming from domestic production versus imports. It makes sense given the nature of the globalization of seafood trade that countries at the upper end of the FMI_P spectrum, which are known for producing well-managed, sustainable seafood (Macpherson 2018, Gephart et al. 2019), will almost always see decreases in the level of management associated with their seafood

consumption the more they rely on imports from other countries. Alternately, countries with less intensive fisheries management occupying space at the lower end of the FMI_P spectrum will almost always see an increase in the level of management associated with their seafood consumption the more they rely on imports. We cannot definitively determine the magnitude of the disparity between the management intensity of seafood production and consumption without knowledge of the relative proportions of seafood consumption attributable to domestic production. However, we can feel confident that there is in fact a disparity for most countries because most countries rely at least in part on imports to supply their seafood consumption.

The globalization of seafood trade means that domestic fisheries management practices have international influence, and guarantees that countries will see differences in the level of management in seafood they produce versus seafood they consume. We found that the countries responsible for the most global exports of seafood tended to export to a large number of trade partners. China ($FMI_P = 0.370$) as the largest exporter across the time period we studied, exported seafood products with remarkably broad global reach (Figure 4.5). Because of this, the sustainability of fishery management practices in China are a part of the seafood consumption sustainability budget of most countries across the globe. Many countries, especially in the developed world, are net importers of seafood, meaning they consume more than they produce (Bellmann et al. 2016, Watson et al. 2016, West et al. 2019). It follows that the level of fisheries management associated with their seafood consumption will shift principally based on the countries from which they import. In general, developed countries, or countries that have developed economies based on United Nations assessments, tend to import most of their seafood products from developing countries, or countries that have less developed economies according to the United Nations (Asche et al. 2015, Ye and Gutierrez 2017, Watson et al. 2017). Developed

countries have had decreased fisheries production in recent years, and responded in part by increasing reliance on seafood imports (Ye and Gutierrez 2017). An increase in the production and export of high quality seafood from the developing world has largely met this demand (Asche et al. 2015, Watson et al. 2016, 2017, Ye and Gutierrez 2017). Fisheries management and governance in the developing world is generally lower than in the developed world (Smith et al. 2010, Asche et al. 2015, Ye and Gutierrez 2017), meaning this flow of exports from developing countries to developed countries contributes to a mismatch in the overall sustainability of seafood consumption in developed countries compared to their seafood production.

The impact of the disparity in management practices associated with fisheries production and imports in the developed world is highlighted by our examination of the United States, the largest importer of seafood globally across the time period we studied. The United States is estimated to rely on imports for 62-65% of their seafood consumption (Gephart et al. 2019). Every trade partner in the top 25 sources of imports to the United States from 2012-2017 had a lower FMI_P than the United States ($FMI_P = 0.932$), and the majority of United States imports by volume had origins from countries with $FMI_P < 0.5$. It is clear the United States is largely consuming seafood that is held to different management and sustainability standards than what they produce. One interpretation of this is that countries in the developed world with intensive management practices, such as the United States, are diverting the costs of their intensively managed production of luxury seafood products to developing nations that forego the costs of more intensive management in favor of short-term economic development supported by the income derived from exporting seafood (Ye and Gutierrez 2017).

Many seafood products traverse complex global processing and supply chains before they reach their final destination (Bellmann et al. 2016, Blaha and Katafono 2020). When products are

imported, processed, and exported as entirely new products they get attributed to the country that did the processing, not the country that initially harvested them from the environment (Pramod et al. 2014, Watson et al. 2016, Gephart et al. 2019). As a result of these trade dynamics we, like many other accounts of global seafood consumption (e.g. Watson et al. 2016, Gephart et al. 2019), were unable to directly estimate the proportion of a country's consumption and exports associated with their own production versus imports. This issue of re-exports is just one in a list of challenges facing seafood traceability. Fisheries reporting largely fails to capture transshipment, or offloading of catch to refrigerated vessels far from port masking original catch locations (Miller et al. 2018). There are also issues of mislabeling (Watson et al. 2016), high seas fishing, and private fisheries agreements that result in products being attributed to countries separate from where they are harvested (Ye and Gutierrez 2017, Watson et al. 2017). In addition, there is poor accounting for illegal, unreported, and unregulated (IUU) fishing practices (Agnew et al. 2009, Pramod et al. 2014, Watson et al. 2016). By not having a reliable means to track products from their source to the final point of consumption, it is challenging to accurately estimate the sustainability of seafood consumption (Watson et al. 2016, Gephart et al. 2019). Given the increasing global trade in seafood products, this lapse in the accounting of seafood traceability makes efforts to promote sustainability difficult (Watson et al. 2016, Gephart et al. 2019). Furthermore, the inability to determine the origin of products shields less sustainable products from economic disincentives to production, and thus indirectly promotes unsustainable fisheries.

What can be done to improve seafood traceability, particularly as it relates to the issue of re-exports? Some non-profit groups have begun establishing consumer-facing traceability certifications that attempt to inform consumers of the origin of seafood products that meet their certification criteria (Bailey et al. 2016). These programs allow consumers to choose between

certified products that have some degree of traceability to their point of capture over uncertified/untraceable products (Bailey et al. 2016). While such programs are a step in the right direction, they are also wide-ranging in terms of their scope and efficacy, especially given that most products are not traceable to their point of origin (Bailey et al. 2016). Chan et al. (2015) provide some suggestions for improving customs accounting of wildlife trade products, including seafood. For example, they suggest extending the international standardized system of names and codes for trade classification (HS) to include 10 digits that would allow for more specificity in product reporting (Chan et al. 2015). While increased specificity in customs product reporting would certainly help decrease the uncertainty in tracing supply chains of seafood products, there is still a need for a mechanism to track seafood from the point of capture to the point of consumption. Emerging technologies such as blockchain provide one avenue for addressing this need. Blockchain in the context of fisheries would essentially provide a definitive, immutable digital record of the path of a seafood product. Blockchain works by creating a unique digital link between points of the seafood supply chain, with new data added at each point the product is transformed or traded (Blaha and Katafono 2020). For example, when a fish is caught it can be given a unique, immutable digital identifier containing information on the point of capture. When it is subsequently sent to a processing facility, it will be given a new unique digital identifier that is directly linked to the original one containing information on the point of capture. This happens at each point of the supply chain. If at any point the data is changed or the chain is broken, all participants in the blockchain network are notified helping to avoid fraudulent activity. By chaining these identifiers together, it is possible to track the movement of an individual product from the point of capture to the point of consumption. This type of technology is not without barriers to implementation including regulatory uncertainty, limited interoperability, costs

associated with developing blockchain solutions or relying on third party services to implement them, lack of centralized management, and risks associated with inaccurate data reporting at any point of the chain (Blaha and Katafono 2020, Howson 2020). Nevertheless, if blockchain technology continues to develop and improve it could help address one of the biggest challenges in seafood traceability and consumption accounting.

It is well documented that improved fisheries management supports more sustainable fisheries (Costello et al. 2016, Ye and Gutierrez 2017, Melnychuk et al. 2021). In particular, supporting the development of multi-faceted approaches to management that include rebuilding plans for overfished stocks and are catered to the individual capacity of countries to implement and sustain management is likely to have to greatest positive impact on sustainability (Costello et al. 2020, Melnychuk et al. 2021). These types of changes to fisheries management systems can be costly and difficult to implement in developing countries, but previous work has shown that the long term benefits of establishing effective fisheries management systems outweigh the short term costs (Mangin et al. 2018). Mechanisms such as trade agreements or tariffs have the potential to incentivize developing countries to prioritize improving fisheries management practices if implemented with that goal in mind (Bellmann et al. 2016, Watson et al. 2017). Additionally, consumers have the power to promote improved fisheries management practices through the choices they make regarding their seafood purchases (Vázquez-Rowe et al. 2013, McClenachan et al. 2016). This consumer purchasing power is further aided by attempts from non-profits to reduce the ambiguity in seafood traceability and sustainability via certification systems, such as those created by the Marine Stewardship Council (McClenachan et al. 2016, Bailey et al. 2018). Though we should note these programs are not without their pitfalls including increased consumer confusion is some cases (largely due to the complex nature and varying definitions associated with

classifying seafood as sustainable) and barriers to access for small-scale and developing country fisheries that do not have the capacity or infrastructure to meet certification standards (Bellmann et al. 2016, McClenachan et al. 2016, Bailey et al. 2018). All of these strategies for supporting increased fisheries management in developing countries need to be considered carefully as each carries a risk of increasing the disparity between developed and developing nations if financial, infrastructural, or capacity barriers are not addressed (Bailey et al. 2016, 2018, Bellmann et al. 2016).

Developed countries that have the capacity to do so have largely implemented intensive fisheries management that supports sustainable seafood production. Increasingly, however, a country's seafood consumption is the result of a complex network of global production and trade, and we have demonstrated that even countries with the best fisheries management are heavily contributing to the economic drivers behind the fishing practices of countries with less intensive fisheries management via seafood consumption. Thus, any assessment of national seafood sustainability that does not account for the sustainability of seafood products consumed will continue to paint a skewed picture of seafood sustainability that is particularly rosy for the wealthiest countries. As the global community strives to meet the United Nations Sustainable Development Goals for 2030, the nature of the globalization of seafood trade and consumption, and the challenges we face in accounting for global seafood trade, will be critical to determining which steps need to be taken to ensure the sustainability of seafood globally.

Acknowledgements

We would like to acknowledge the Edna Bailey Sussman Fund Graduate Environmental Internship for supporting this work. We thank Camille Kohler for her support in accessing the GTA data. We thank Brian Garber-Yonts, Ben Fissel, and Mike Dalton at NOAA's Alaska Fisheries Science Center for their insight and access to the GTA data. We would also like to acknowledge the NOAA Fisheries Office of Science and Technology Economics Program who funded our access to the GTA data. Thank you to Alex Israel for his insight in the development of this project, and enduring and contributing to many conversations about the best way to navigate this analysis.

Chapter 4, in full, is currently being prepared for submission for publication and is printed here with the permission of co-authors Alan C. Haynie and Brice X. Semmens. The dissertation author is the primary investigator and author of this paper.

Appendix

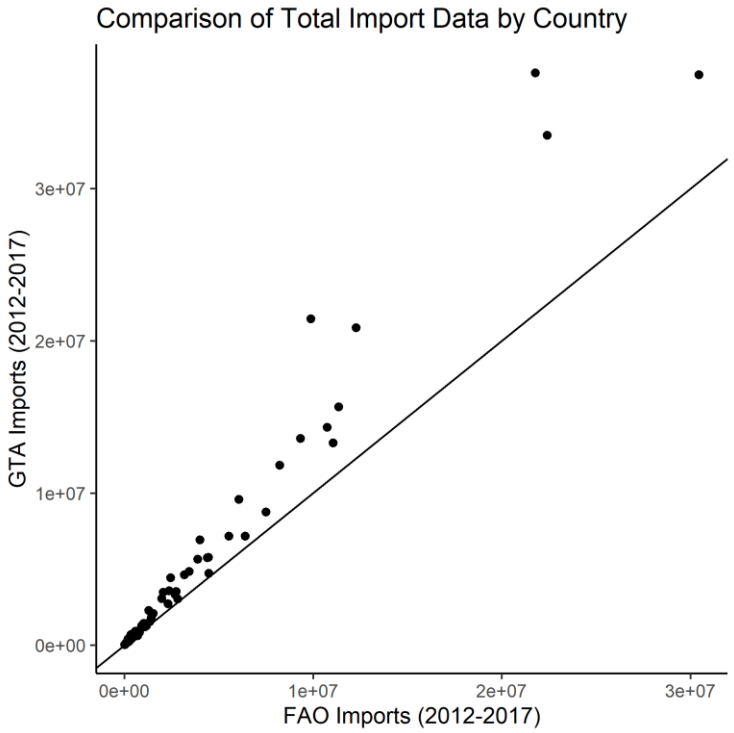

Figure A4.1. Comparison of total imports by country between FAO and GTA datasets. The 1:1 line indicating an exact match between the data is shown in the solid black line.

Works Cited

Agnew, D. J., J. Pearce, G. Pramod, T. Peatman, R. Watson, J. R. Beddington, and T. J. Pitcher. 2009. Estimating the Worldwide Extent of Illegal Fishing. PLOS ONE 4:e4570.

Anderson, J. L. 2015. Aquaculture and the Future: Why Fisheries Economists Should Care. Marine Resource Economics 17:133–151.

Asche, F., M. F. Bellemare, C. Roheim, M. D. Smith, and S. Tveteras. 2015. Fair Enough? Food Security and the International Trade of Seafood. World Development 67:151–160.

Bailey, M., S. R. Bush, A. Miller, and M. Kochen. 2016. The role of traceability in transforming seafood governance in the global South. Current Opinion in Environmental Sustainability 18:25–32.

Bailey, M., H. Packer, L. Schiller, M. Tlusty, and W. Swartz. 2018. The role of corporate social responsibility in creating a Seussian world of seafood sustainability. Fish and Fisheries 19:782–790.

Bellmann, C., A. Tipping, and U. R. Sumaila. 2016. Global trade in fish and fishery products: An overview. Marine Policy 69:181–188.

Blaha, F., and K. Katafono. 2020. Blockchain Application in Seafood Value Chains. FAO Fisheries and Aquaculture Circular:1-43,I,IV.

Chan, H.-K., H. Zhang, F. Yang, and G. Fischer. 2015. Improve customs systems to monitor global wildlife trade. Science 348:291 LP – 292.

Costello, C., L. Cao, S. Gelcich, M. Á. Cisneros-Mata, C. M. Free, H. E. Froehlich, C. D. Golden, G. Ishimura, J. Maier, I. Macadam-Somer, T. Mangin, M. C. Melnychuk, M. Miyahara, C. L. de Moor, R. Naylor, L. Nøstbakken, E. Ojea, E. O'Reilly, A. M. Parma, A. J. Plantinga, S. H. Thilsted, and J. Lubchenco. 2020. The future of food from the sea. Nature 2020 588:7836 588:95–100.

Costello, C., D. Ovando, T. Clavelle, C. K. Strauss, R. Hilborn, M. C. Melnychuk, T. A. Branch, S. D. Gaines, C. S. Szuwalski, R. B. Cabral, D. N. Rader, and A. Leland. 2016. Global fishery

prospects under contrasting management regimes. Proceedings of the National Academy of Sciences 113:5125–5129.

FAO. 2004. Handbook of fishery statistical standards. Coordinating Working Party on Fishery Statistics.

FAO. 2019. International Symposium on Fisheries Sustainability: Strengthening the science-policy nexus. Rome.

FAO. 2020a. The State of World Fisheries and Aquaculture 2020. Sustainability in Action.

FAO. 2020b. Fishery and Aquaculture Statistics. Food balance sheets of fish and fishery products 1961-2017 (FishstatJ). FAO Fisheries Division [online].

Gephart, J. A., H. E. Froehlich, and T. A. Branch. 2019. To create sustainable seafood industries, the United States needs a better accounting of imports and exports. Proceedings of the National Academy of Sciences 116:9142–9146.

Gephart, J. A., and M. L. Pace. 2015. Structure and evolution of the global seafood trade network. Environmental Research Letters 10:125014.

Guillen, J., F. Natale, N. Carvalho, J. Casey, J. Hofherr, J.-N. Druon, G. Fiore, M. Gibin, A. Zanzi, and J. T. Martinsohn. 2018. Global seafood consumption footprint. Ambio 2018 48:2 48:111–122.

Halpern, B. S., C. Longo, D. Hardy, K. L. McLeod, J. F. Samhouri, S. K. Katona, K. Kleisner, S. E. Lester, J. O'Leary, M. Ranelletti, A. A. Rosenberg, C. Scarborough, E. R. Selig, B. D. Best, D. R. Brumbaugh, F. S. Chapin, L. B. Crowder, K. L. Daly, S. C. Doney, C. Elfes, M. J. Fogarty, S. D. Gaines, K. I. Jacobsen, L. B. Karrer, H. M. Leslie, E. Neeley, D. Pauly, S. Polasky, B. Ris, K. S. Martin, G. S. Stone, U. R. Sumaila, and D. Zeller. 2012. An index to assess the health and benefits of the global ocean. Nature 2012 488:7413 488:615–620.

Heino, M., B. D. Pauli, and U. Dieckmann. 2015. Fisheries-induced evolution. Annual review of ecology, evolution, and systematics 46.

Hilborn, R., R. O. Amoroso, C. M. Anderson, J. K. Baum, T. A. Branch, C. Costello, C. L. de Moor, A. Faraj, D. Hively, O. P. Jensen, H. Kurota, L. R. Little, P. Mace, T. McClanahan, M. C. Melnychuk, C. Minto, G. C. Osio, A. M. Parma, M. Pons, S. Segurado, C. S. Szuwalski, J. R. Wilson, and Y. Ye. 2020. Effective fisheries management instrumental in improving fish stock status. Proceedings of the National Academy of Sciences 117:2218–2224.

Howson, P. 2020. Building trust and equity in marine conservation and fisheries supply chain management with blockchain. Marine Policy 115:103873.

Macpherson, M. 2018. In Pursuit of "Optimum" Forty Years of Federal Fisheries Management Under the Magnuson-Stevens Fishery Conservation and Management Act. Tulane Environmental Law Journal 31:209–277.

Mangin, T., C. Costello, J. Anderson, R. Arnason, M. Elliott, S. D. Gaines, R. Hilborn, E. Peterson, and R. Sumaila. 2018. Are fishery management upgrades worth the cost? PLOS ONE 13:e0204258.

McClenachan, L., S. T. M. Dissanayake, and X. Chen. 2016. Fair trade fish: consumer support for broader seafood sustainability. Fish and Fisheries 17:825–838.

Melnychuk, M. C., N. Baker, D. Hively, K. Mistry, M. Pons, C. E. Ashbrook, C. Minto, R. Hilborn, and Y. Ye. 2020. Global trends in status and management of assessed stocks: achieving sustainable fisheries through effective management. Food & Agriculture Org.

Melnychuk, M. C., H. Kurota, P. M. Mace, M. Pons, C. Minto, G. C. Osio, O. P. Jensen, C. L. de Moor, A. M. Parma, L. R. Little, D. Hively, C. E. Ashbrook, N. Baker, R. O. Amoroso, T. A. Branch, C. M. Anderson, C. S. Szuwalski, J. K. Baum, T. R. McClanahan, Y. Ye, A. Ligas, J. Bensbai, G. G. Thompson, J. DeVore, A. Magnusson, B. Bogstad, E. Wort, J. Rice, and R. Hilborn. 2021. Identifying management actions that promote sustainable fisheries. Nature Sustainability 2021 4:5 4:440–449.

Melnychuk, M. C., E. Peterson, M. Elliott, and R. Hilborn. 2017. Fisheries management impacts on target species status. Proceedings of the National Academy of Sciences 114:178–183.

Miller, N. A., A. Roan, T. Hochberg, J. Amos, and D. A. Kroodsma. 2018. Identifying Global Patterns of Transshipment Behavior. Frontiers in Marine Science 0:240.

Ocean Health Index. 2019. ohiprep version: Prepareation of data for global scenarios of the Ocean Health Index, 7/19/2021. National Center for Ecological Analysis and Synthesis, Univeristy of California, Santa Barbara.

Ortuño Crespo, G., and D. C. Dunn. 2017. A review of the impacts of fisheries on open-ocean ecosystems. ICES Journal of Marine Science 74:2283–2297.

Ovando, D., R. Hilborn, C. Monnahan, M. Rudd, R. Sharma, J. T. Thorson, Y. Rousseau, and Y. Ye. 2021. Improving estimates of the state of global fisheries depends on better data. Fish and Fisheries:faf.12593.

Pramod, G., K. Nakamura, T. J. Pitcher, and L. Delagran. 2014. Estimates of illegal and unreported fish in seafood imports to the USA. Marine Policy 48:102–113.

R Core Team. 2019. R: A language and environment for statistical computing. R Foundation for Statistical Computing, Vienna, Austria.

Smith, M. D., C. A. Roheim, L. B. Crowder, B. S. Halpern, M. Turnipseed, J. L. Anderson, F. Asche, L. Bourillón, A. G. Guttormsen, A. Khan, L. A. Liguori, A. McNevin, M. I. O;Connor, D. Squires, P. Tyedmers, C. Brownstein, K. Carden, D. H. Klinger, R. Sagarin, and K. A. Selkoe. 2010. Sustainability and Global Seafood. Science 327:784 LP – 786.

Stern, S., A. Wares, and T. Epner. 2018. Social Progress Index: 2018 Methodology Report.

Swartz, W., U. Rashid Sumaila, R. Watson, and D. Pauly. 2010. Sourcing seafood for the three major markets: The EU, Japan and the USA. Marine Policy 34:1366–1373.

Teh, L. C. L., and U. R. Sumaila. 2013. Contribution of marine fisheries to worldwide employment. Fish and Fisheries 14:77–88.

UN General Assembly. 2015. Transforming our world: the 2030 Agenda for Sustainable Development.

Vázquez-Rowe, I., P. Villanueva-Rey, M. T. Moreira, and G. Feijoo. 2013. The role of consumer purchase and post-purchase decision-making in sustainable seafood consumption. A Spanish

case study using carbon footprinting. Food Policy 41:94–102.

Watson, R. A., B. S. Green, S. R. Tracey, A. Farmery, and T. J. Pitcher. 2016. Provenance of global seafood. Fish and Fisheries 17:585–595.

Watson, R. A., R. Nichols, V. W. Y. Lam, and U. R. Sumaila. 2017. Global seafood trade flows and developing economies: Insights from linking trade and production. Marine Policy 82:41–49.

West, C. D., E. Hobbs, S. A. Croft, J. M. H. Green, S. Y. Schmidt, and R. Wood. 2019. Improving consumption based accounting for global capture fisheries. Journal of Cleaner Production 212:1396–1408.

Ye, Y., and N. L. Gutierrez. 2017. Ending fishery overexploitation by expanding from local successes to globalized solutions. Nature Ecology & Evolution 2017 1:7 1:1–5.